Regulation of Ciz1 by Cyclin A-Cyclin Dependent Kinase 2 (CDK2) Mediated Phosphorylation

By Diana Baxter (BSc (Hons))

October 2015

Thesis submitted for the degree of MSc (by Research)

Lancaster University

Division of Biomedical and Life Sciences

ABSTRACT

The progression of the cell cycle is a tightly regulated process, regulated by the activities of cyclin dependent kinases. Phosphorylation of target proteins regulates key transitions in the cell cycle contributing to accurate DNA replication and cell division. Here we evaluate the regulation of the protein Ciz1 by cyclin A-CDK2.

Ciz1 promotes localisation of cyclin A-CDK2 to chromatin sites at the G_1/S phase transition and this ternary complex promotes initiation of DNA replication. However, the mechanisms by which Ciz1 is regulated are not fully understood. Here, Ciz1 protein levels are shown to be reduced after inhibition of CDK activity, suggesting that CDK-mediated phosphorylation of Ciz1 could contribute to increased protein stability.

As Ciz1 is known to be a substrate of cyclin A-CDK2, enzyme kinetic studies were performed to evaluate whether there is preferential phosphorylation at specific sites within Ciz1. We characterise new phospho-specific antibodies that will be of benefit in future in *in vivo* studies evaluating the role of phosphorylation at specific sites in regulation of Ciz1 function.

Using His-ubiquitin, we show that Ciz1 is covalently linked to ubiquitin. These complexes are stabilised after inhibition of the proteasome, consistent with degradation by the proteasomal. Further evidence presented demonstrates that an E3 ligase (Cdh1) interacts with Ciz1 via a conserved destruction box in the N-terminus. Taken together, the data presented here suggest that Ciz1 is regulated at multiple levels post-transitionally that contribute to ensuring it accumulates precisely at the G_1/S phase transition. This may have important implications for its role as a driver mutation in cancer biology.

ACKNOWLEDGEMENTS

I would like to thank my supervisor Dr Nikki Copeland for providing all the support required and for giving me the opportunity to work on this project in the first place.

I would also like to thank Urvi Thacker who was always there to help out and give her insight on planned experiments.

There are many other people in the department who also helped out in many different ways, making my time in the lab easier by sharing their own experiences and even lab materials!

Finally, I would like to thank my family who have continuously supported me throughout my studies.

DECLARATION

All data presented in this thesis was obtained by the candidate and has not been submitted in any form other than in this thesis.

TABLE OF CONTENTS

LIST OF FIGURES

1. INTRODUCTION

1.1 AN INTRODUCTION TO THE CELL CYCLE

The cell cycle consists of four major phases and is strictly regulated by a large number of factors such as fibroblast growth factors (Dailey et al., 2005). Failure in the control of this process can have drastic consequences; such as uncontrolled cell proliferation, leading to cancer (Welcker and Clurman, 2008). The cell cycle is divided into four phases: the G_1, S, G_2 and M phases (Cho et al., 1998). However, there is an additional stage that describes the non-replicative state that over 95% of cells enter between cell cycle divisions that is referred to as G_0 or quiescence (Pardee, 1974, Cheung and Rando, 2013). A cell must commit to entering the cell cycle after mitosis or quiescence; the specific occurrence of which is known as the restriction point (R), first defined as the stage in the cell cycle at which nutrition levels in the cell are optimum to allow the cell cycle to progress (Pardee, 1974). Many different factors including growth factors lead to the activation of downstream pathways. One protein activated in this process is Ras, which sends signals further along down several different pathways (Goodsell, 1999). One such pathway results in the expression of cyclin D1 and suppression of the CDK inhibitor $p27^{Kip1}$ (Aktas et al., 1997). In this way, cells can progress through the G_1 phase due to the presence of cyclin D1 and the removal of the inhibition of CDKs by $p27^{Kip1}$. The primary factors that drive cell cycle progression are two protein families known as cyclins and cyclin-dependent kinases (CDKs) (Murray, 2004, Sánchez and Dynlacht, 2005).

There are four main cyclins that regulate cell cycle progression. Each cyclin binds to its appropriate cognate partner, leading to the activation of its kinase activity and phosphorylation of its target substrates (Jeffrey et al., 1995, Obaya and Sedivy, 2002). A diagram of the cell cycle showing the four stages together with the accompanying cyclin-CDK complexes is shown in Figure 1.

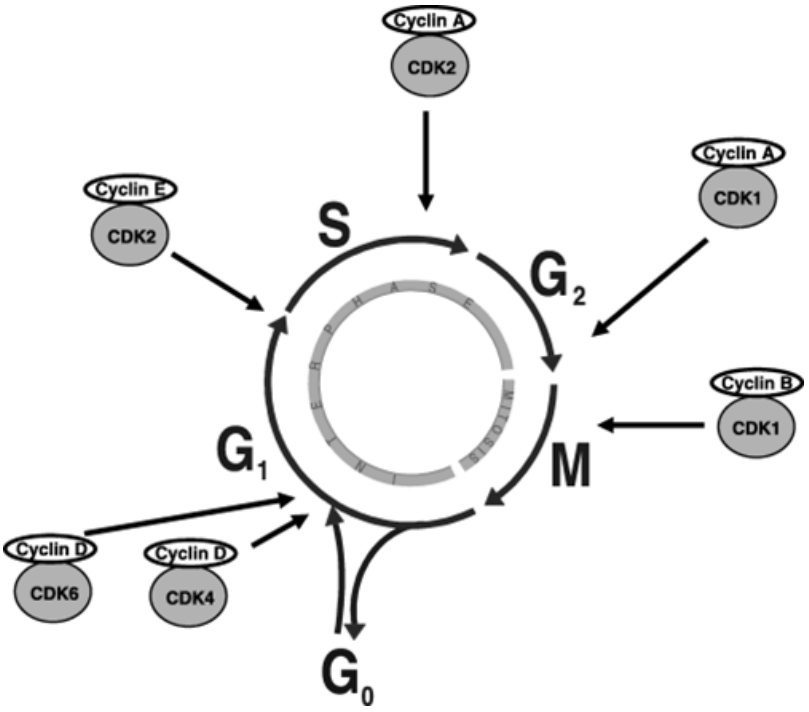

Figure 1: Regulation of the cell cycle by cyclin-CDK complexes
Each stage of the cell cycle is tightly regulated by a specific CDK molecule complexed with its partnering cyclin. These complexes ensure that each stage of the cell cycle progresses smoothly and is complete before the cell is allowed to enter the next stage (Vermeulen et al., 2003).

As indicated by their name, CDKs phosphorylate multiple substrates leading to a number of consequences including both activation and inactivation of proteins; the consequences of which cause the progression of the cell cycle and also ensure that the cell does not revert back to an earlier stage (Bloom and Cross, 2007). This forward only direction of the cell cycle is in part aided by the removal of proteins once their functions are no longer required by the cell. Many proteins are degraded by the ubiquitin proteasome system, with ubiquitin ligases targeting specific substrates only. This ensures that the correct proteins are removed from the system at the correct time (Lecker et al., 2006).

After mitosis has occurred, cells enter either quiescence (G_0) or the G_1 phase during which the cell prepares to enter the next stage known as the S phase. There are two main G_1 phase cyclins, each of which bind to distinct CDKs and perform different

functions. These are cyclin D, which binds to CDK4 or CDK6 and is largely responsible for progression through the G_1 phase (Meyerson and Harlow, 1994) and cyclin E, which binds CDK2 and is active later in the G_1 phase as it is responsible for transitioning to the S phase (Ohtsubo et al., 1995).

Cyclin D binds to either CDK4 or CDK6 and is involved in promoting the progression through the R point, requiring sustained extracellular signal regulated kinase (ERK) activity, which can be induced in Chinese hamster embryo fibroblasts by the presence of platelet-derived growth factor (PDGF) (Foster et al., 2010, Weber et al., 1997). Cyclin E binds to CDK2 and commits the cell to DNA replication by removing suppression of the transcription factor E2F, which is responsible for the expression of several genes required for the cell to enter the S phase (Foster et al., 2010). Once this stage has been passed, the cell can no longer return to G_1. The main suppressor of E2F is the retinoblastoma protein (pRb) family that consists of the pocket proteins p105, p107 and p130 containing A and B subdomains, separated by a highly conserved spacer region that allows these subdomains to assemble into a pocket-like structure (Giordano et al., 2007). As the cell cycle progresses through the G_1 phase, pRb is phosphorylated by cyclin D-CDK4/6, removing suppression of E2F (Baker et al., 2005) and then cyclin E-CDK2 forming a positive feedback loop (Giacinti and Giordano, 2006). In this way, pRb limits cell cycle progression until cyclin D-CDK4/6 activity is high enough. This activity is determined by levels of mitogenic signalling (Carpenter and Cohen, 1990, Massagué et al., 2000, Aktas et al., 1997).

Both cyclin E and cyclin A are required for S phase entry and activity, unlike other cyclins. This was first shown in *Xenopus* egg extracts where DNA replication ability was assessed in the presence and absence of cyclin-CDK complexes (Strausfeld et al., 1996). Cyclin A binds CDK2 during the S phase and is required for DNA replication

as it is responsible for activating the replication complexes assembled on DNA (Coverley et al., 2002). Part of this activation occurs when cyclin A-CDK2 phosphorylates Cdc6, a member of the pre-replication complex. This phosphorylation causes Cdc6 to re-localise to the cytoplasm, suggesting that this also contributes to prevention of re-replication (Petersen et al., 1999). However, more recently, cyclin A has also been found to bind CDK1, with levels of cyclin A bound to CDK1 or CDK2 rising during S phase and continuing until almost the end of the G_2 phase. These complexes are required for DNA replication as well as preparing the cell for mitosis such as organisation of centrosomes (Hochegger et al., 2008, De Boer et al., 2008).

High CDK activity during DNA replication also functions to prevent re-replication. This is achieved by phosphorylation of pre-replication complex components, thus inhibiting their assembly onto DNA, preventing the formation of new sites on DNA where replication can be initiated (Arias and Walter, 2007). Cyclin A-CDK2 is responsible for activating cyclin B-CDK1 associated with centrosomes and for translocating other pools of cyclin B-CDK1 to the nucleus. In this way, cyclin A-CDK2 regulates the timing of entry into the M phase (De Boer et al., 2008). Duplication of centrosomes has also been shown to require cyclin-CDK2 activity although the exact mechanism for this process is not understood (Lacey et al., 1999, Matsumoto et al., 1999, Tsou and Stearns, 2006).

During the G_2 phase, re-replication of DNA continues to be inhibited by cyclin B-CDK1 in several ways including down-regulating Cdc6 activity (Nguyen et al., 2001) and the cell prepares to enter the M phase where mitosis occurs. Entry into the M phase requires activation of $p34^{cdc2}$ (Nurse, 1990). Shortly before this stage is reached; levels of cyclin B bound to CDK1 rise; with complexes initially located at the centrosomes (Jackman et al., 2003). Activation of these complexes results in the

centrosomes being separated and the cyclin B-CDK1 complexes themselves are translocated to the nucleus where mitosis initiates with the degradation of the nuclear envelope and the condensing of the chromosomes (Takizawa and Morgan, 2000). The mitotic spindles are also formed; completing the events of metaphase. Once these events have occurred, the cyclin B-CDK1 complexes are degraded by the anaphase promoting complex/cyclosome (APC/C) E3 ubiquitin ligase during anaphase (Hochegger et al., 2008), resulting in low levels of CDK activity. Mitosis then concludes with new daughter cells formed; at which stage the cells can either enter quiescence (G_0) or enter the cell cycle (G_1) once again.

Re-entry into G_1 requires continued mitogenic signalling which leads to production of increased CDK activity to avoid entry into a quiescent state (Spencer et al., 2013). Cyclin expression is dependent on the stage of the cell cycle which is determined by the activity of the cyclin expressed previously except for cyclin D expression, which is dependent on mitogenic signalling. CDKs are relatively stable and are generally constitutively expressed. However, their activity is limited by cyclin expression. This means that between the degradation of cyclin B at the end of mitosis and the expression of cyclin D at the beginning of G_1, CDK activity is very low (Obaya and Sedivy, 2002). Levels of cyclin proteins are also determined by their degradation.

Exit from mitosis requires inactivation of mitotic cyclins. This has been shown to require Cdc14 phosphatase activity, which among other functions, is thought to be responsible for dephosphorylating Cdh1, an activator protein that forms part of the E3 ligase APC/C complex and is responsible for mitotic cyclin degradation. Cdc14 is also responsible for dephosphorylating Sic1, a CDK inhibitor, resulting in this protein no longer being marked for degradation (Visintin et al., 1998). The APC/C is also

responsible for the degradation of cyclin A when the cell first enters mitosis (Geley et al., 2001).

The G_1 phase involves assembling all the machinery required for DNA replication; the pre-replication complex followed by the pre-initiation complex which bind to DNA and contain the proteins required for DNA replication (Diffley and Labib, 2002, Blow, 2001). This occurs during the S phase; with the G_1/S checkpoint forming a control that ensures all components are present and correctly assembled before the cell is allowed to enter the replicative phase. One protein that forms part of this checkpoint is Cdc25A phosphatase. This is responsible for removing the inhibitory phosphorylations of CDK2, thus allowing increased CDK activity. However, if the DNA is damaged, the ATM pathway is activated, leading to reduced Cdc25A activity. As a result, the inhibition of CDK2 is not removed and the cell cycle cannot progress (Donzelli and Draetta, 2003).

The pre-replication complex is formed on DNA where origin recognition complexes (ORC) are located (Evrin et al., 2009). It consists of a replicative DNA helicase composed of six members of the MCM (minichromosome maintenance) protein family (MCM2-7) (Bochman and Schwacha, 2008), MCM9, Cdt1, which is required for loading of the MCM2-7 complex (Lutzmann and Mechali, 2008, Rialland et al., 2002)and Cdc6 (Sacco et al., 2012). Activation of this complex leads to the formation of the pre-initiation complex, consisting of other proteins including Cdc45 and the GINS complex (Walter and Newport, 2000, Sacco et al., 2012). This ultimately leads to recruitment of DNA polymerases and the formation of the replication fork (Waga and Stillman, 1998, Heller et al., 2011, Leman and Noguchi, 2013). All activation steps require CDK activity (Bochman and Schwacha, 2009, Liu et al., 2004, Lei and Tye, 2001).

1.2 THE UBIQUITIN-PROTEASOME SYSTEM (UPS)

The ubiquitin proteasome system is composed of a large network of proteins that work together to degrade proteins. This serves a number of purposes including protein homeostasis and regulation of transitions in the cell cycle (Lecker et al., 2006, Nakayama and Nakayama, 2006). As this system is irreversible, it must be tightly regulated to ensure that a correct balance exists between degradation and synthesis and that specific proteins are only degraded when required (Lecker et al., 2006).

Proteasome substrates are marked with multiple ubiquitin chains that are conjugated to target protein that mark them for degradation. Ubiquitin is a highly conserved protein found in eukaryotes that covalently attaches to other proteins using the glycine residue at the C terminus in ubiquitin and a lysine residue in the target protein (Hershko et al., 1984, Chau et al., 1989, Kerscher et al., 2006). However, binding of further ubiquitin monomers can occur at distinct lysine residues. Depending on which of these residues is used to form poly-ubiquitin chains; the purpose of this chain varies (Pickart, 2001). Early studies performed in the 1980's using β-galactosidase, a protein known to be ubiquitylated, revealed that binding of the first ubiquitin monomer to the substrate only occurs at certain specific lysine residues. In addition, the poly-ubiquitin chain that targeted the substrate to the 26S proteasome was formed by bonds between the residues glycine 76 and lysine 48 between individual ubiquitin monomers (Hershko et al., 1984, Chau et al., 1989). However, if poly-ubiquitin chains are formed using the lysine 63 residue instead, the function of this lysine 63-linked chain seems not to be to target the substrate to the 26S proteasome but as something different such as to act as a signalling mechanism (Pickart, 2001, Li and Ye, 2008). More recently, other lysine linkages have been observed (Fig. 3) (Dikic et al., 2009). Three classes of enzymes are involved in the ubiquitylation process: the E1, E2 and E3 enzymes

(Scheffner et al., 1995). Ubiquitin molecules are attached to E1 activating enzymes before being transferred to E2 conjugating enzymes. The activated ubiquitin is then transferred to the substrate by the E3 ligase (Fig. 2).

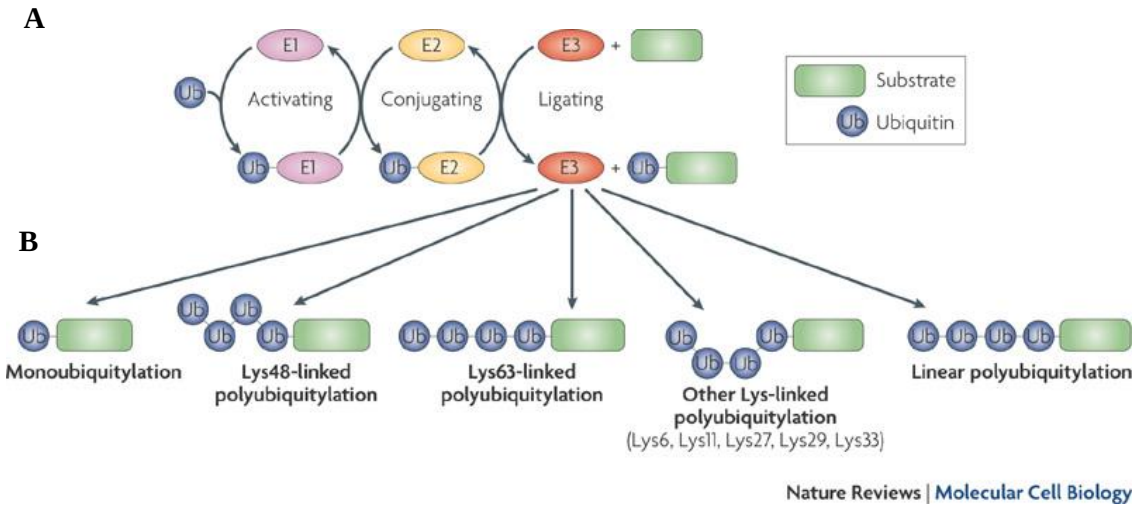

Figure 2: The enzyme cascade resulting in substrate ubiquitylation (Dikic et al., 2009)
(A) The activation of ubiquitin monomers and their transfer to the substrate. **(B)** Ubiquitin monomers can form chains using different linkages. This can act as a signalling system in itself to denote a function.

Eight E1 enzymes that are known to initiate conjugation of ubiquitin or ubiquitin like proteins have been identified in humans. Activation of ubiquitin occurs in two steps. E1 first catalyses acyl-adenylation of the C-terminus of ubiquitin before this structure is attacked by a catalytic cysteine residue within E1 that causes the formation of the activated ubiquitin complexed with the E1 by a thioester bond (Haas et al., 1982) ('Activating', Fig. 2A). This process requires ATP. The activated ubiquitin protein can then be transferred to an E2 conjugating enzyme when E1 and E2 physically associate; allowing the C terminus of ubiquitin to be transferred to the catalytic cysteine residue of the E2 enzyme (Schulman and Harper, 2009) ('Conjugating', Fig. 2A). Studies have revealed that before ubiquitin can be transferred to the substrate by E3 from E2, E2 must first be dissociated from E1 (Eletr et al., 2005). E3 enzymes confer specificity to the system as they recognise their substrates by specific attributes

such as amino acid sequence or phosphorylation events. As such, there are over 1000 E3 ligases (Lin and Mak, 2007, Jackson and Xiong, 2009). Binding of the substrate and the E2 conjugating enzyme occurs simultaneously and at separate sites (Berndsen and Wolberger, 2014) ('Ligating', Fig. 2A). However, transfer of ubiquitin to the substrate occurs differently depending on the type of E3 ligase. For example, those with a RING finger domain bring the E2 and substrate close together, allowing ubiquitin to be transferred directly from the E2 to the substrate whereas those with a HECT domain transfer the ubiquitin first to a cysteine residue within the E3 before completing the transfer to the substrate. This leaves a substrate with one ubiquitin monomer attached. This cycle can then be repeated forming poly-ubiquitin chains using different lysine residues to form the links between monomers or can end, leaving a mono-ubiquitylated substrate (Fig. 2B). Polyubiquitylated substrates are recognised by the 26S proteasome (Figs. 3A and B) and degraded (Glickman and Ciechanover, 2002, Lecker et al., 2006).

The main complex used by this system responsible for the breakdown of proteins is the 26S proteasome (Bedford et al., 2010). The 26S proteasome is composed of two subunits: the core particle (CP, 20S) and the regulatory particle (RP, 19S) (Fig. 3C). Substrates are first recognised by and enter the RP where they are deubiquitylated and unfolded in an active process that requires ATP before they are transported to the CP where peptidases aid in protein breakdown and single amino acids or short amino acid chains are released and are either recycled or used for antigen presentation (Fig. 3C) (Hochstrasser, 2009). The exact mechanisms used to perform these tasks are unclear but conformational changes have been associated with the function. Assembly of this structure is very precise and is tightly regulated by a number of chaperones whose specific functions are to ensure the correct assembly of the final product. These

chaperones are thought not to be involved in the function of the 26S proteasome (Bedford et al., 2010).

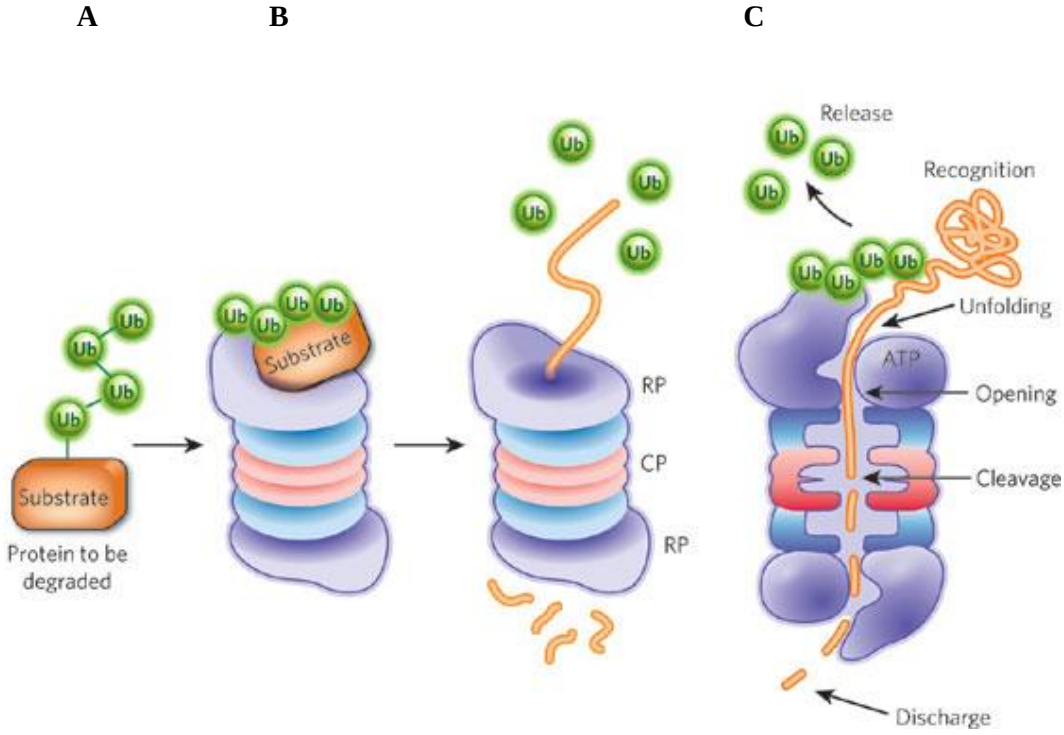

Figure 3: Pathway of a 26S proteasome substrate (Hochstrasser, 2009)
(A) Substrates are marked for degradation by poly-ubiquitylation. **(B)** Substrates are recognised by the 26S proteasome. **(C)** The 26S proteasome degrades the substrate and releases ubiquitin monomers.

1.3 E3 LIGASES CONTRIBUTE TO CONTROL OF CELL CYCLE PROGRESSION

The two principle E3 ligases responsible for the degradation of proteins involved in regulating the cell cycle are the Anaphase Promoting Complex / Cyclosome (APC/C) and the Skp, Cullin, F-box containing (SCF) complex and are active during distinct stages of the cell cycle (Vodermaier, 2004, Castro et al., 2005). Considering that progression of the cell cycle is tightly regulated; the functions of these two E3 ligases must also be tightly regulated.

SCF complexes recognise their substrates using the F-box protein which confers specificity. This requires specific modifications of the substrate at specific sites such as phosphorylation (Wang et al., 2014b). Phosphorylation of proteins by cyclin dependent kinases (CDK) is known to have several possible effects. For example, in the late G_1 phase, Cdh1; a protein that can form part of the APC/C complex, activating it and conferring specificity (Castro et al., 2005); is phosphorylated by CDKs causing it to dissociate from the APC/C complex and is then recognised by the $SCF^{\beta\text{-}TRCP}$ complex and ubiquitylated, marking it for degradation (Fig. 4B) (Kramer et al., 2000, Fukushima et al., 2013). In this way, the SCF complex regulates the APC/C complex and inactivation of APC/C^{Cdh1} is necessary for entry into the S phase (Hsu et al., 2002). However, APC/C^{Cdh1} regulates SCF^{Skp2} during the earlier stages of the G_1 phase by ubiquitylating Skp2, causing its degradation (Fig. 4A). As the cell cycle progresses towards the G_1/S phase transition, Skp2 is phosphorylated first by cyclin E-CDK2 and then cyclin A-CDK2. Skp2 itself regulates the activity of the CDK inhibitor proteins p21, p27 and p57 which, when active, inhibit cyclin E-CDK2, forming a positive feedback loop. These phosphorylation events increase protein stability, preventing ubiquitylation by APC/C^{Cdh1} and so Skp2 is no longer degraded (Fig. 4B) (Rizzardi and Cook, 2013, Vodermaier, 2004). This demonstrates that not only do SCF and APC/C regulate each other (Fig. 4), but that phosphorylation of proteins can either function as a mark for degradation or alternatively, protect against degradation (Wang et al., 2014b, Rizzardi and Cook, 2013). It is the combination of these events that ensure proteins are ubiquitylated and degraded during the correct stages of the cell cycle.

The APC/C complex recognises its substrates via specific sequences. It also requires the presence of an activating protein which simultaneously confers specificity. During

the initial stages of mitosis, Cdc20 binds to APC/C; causing ubiquitylation of substrates containing an RXXL motif, subsequently referred to as the destruction box (D-box). However, as most substrates of APC/C^{Cdc20} are required for mitotic spindle assembly until the checkpoint has been passed and Cdc20 is unable to bind activate APC/C during this stage since it forms part of the mitotic checkpoint complex (MCC); an alternative form of recognising substrates such as cyclin A that are degraded before this point by APC/C^{Cdc20} is required. Cyclin A has been found to contain a motif that binds Cdc20, allowing its degradation (Di Fiore et al., 2015). This motif has also been found in other proteins that form part of the MCC and studies have suggested that the motif, named ABBA, results in competitive binding between cyclin A and the MCC components with Cdc20 (Di Fiore et al., 2015). Cdh1 activates APC/C during late mitosis until late G_1 (Kramer et al., 2000, Li and Zhang, 2009) and recognises its substrates either by the D-box or the KEN box. Cdc20, a substrate of APC/C^{Cdh1}, is recognised by the KEN box (Pfleger and Kirschner, 2000).

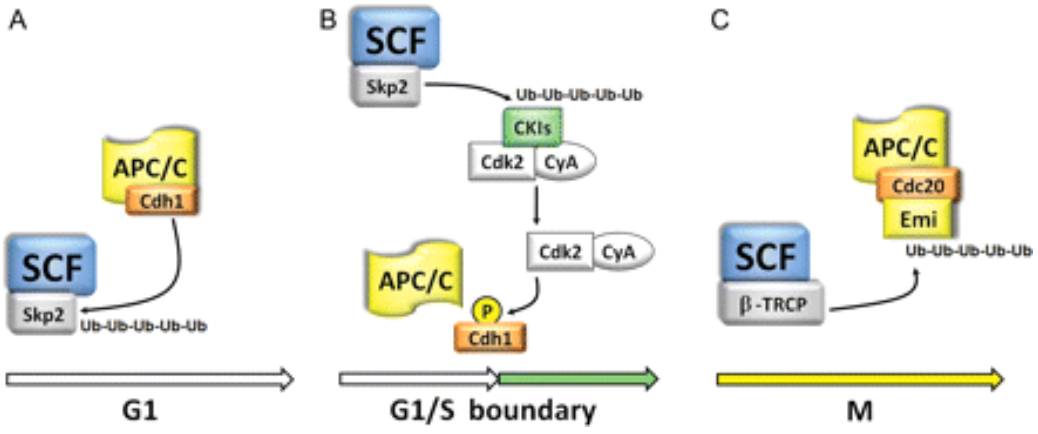

Figure 4: The APC/C and SCF complexes regulate each other during different stages of the cell cycle (Fasanaro et al., 2010)
(A) During the G_1 phase, APC/C^{Cdh1} regulates SCF^{Skp2} levels. **(B)** During late G_1, SCF^{Skp2} becomes the more dominant E3 ligase and Cdh1 is marked for degradation. **(C)** When the cell enters the M phase, APC/C becomes active once again, this time partnered with Cdc20.

It is known that APC/C^{Cdh1} ubiquitylates substrates in a specific order (Buschhorn and Peters, 2006). It has been hypothesised that there are two methods used to ubiquitylate proteins depending on when the functions of these substrates are required in the cell cycle. Substrates degraded during late mitosis and the early G_1 phase are 'early' substrates. These are bound by APC/C^{Cdh1} and are quickly poly-ubiquitylated. 'Late' substrates are continuously bound and unbound by the APC/C complex and are at first mono-ubiquitylated, due to preferential binding to 'early' substrates. Deubiquitylating enzymes can remove these ubiquitin monomers. As the cell progresses through G_1, competition in the form of 'early' substrates is removed and the 'late' substrates are bound more often by APC/C^{Cdh1}. This leads to poly-ubiquitylation and subsequent degradation of the substrate. Binding of APC/C^{Cdh1} to substrates is greatly influenced by the D-box (Rape et al., 2006).

1.4 EMERGING ROLE OF THE UPS IN CANCER BIOLOGY

The importance of the SCF and APC/C complexes being tightly regulated is highlighted when mutations of certain components of these complexes occurs. Mutations of associated genes can lead to a variety of cancers. For example, Skp2 has been observed to be overexpressed in several cancers such as lung cancers and breast cancers. This overexpression has many consequences since Skp2 targets several substrates including p27, a CDK inhibitor, as well as several cyclins (Nakayama and Nakayama, 2006, Wang et al., 2014b). Another example is the reduced expression of Cdh1 in the malignant progression of a B lymphoma cell line. This again has drastic consequences as APC/C^{Cdh1} is responsible for degrading several inhibitors of pre-RC assembly such as mitotic cyclins and Skp2. These inhibit pre-RC assembly by inhibiting high cyclin-CDK activity, which when elevated, could lead to premature activation and entry into S phase (Nakayama and Nakayama, 2006).

Other minor E3 ligases can also contribute to cancer development and progression such as the Human double minute 2 (Hdm2), an E3 ligase made up of a single protein. Overexpression of this protein has been observed in several cancer types including breast carcinomas and malignant melanomas (Sun, 2003, Yin et al., 2005). Hdm2 is responsible for binding to p53 and causing its ubiquitylation, leading to the eventual degradation. When Hdm2 is overexpressed p53 degradation is excessive (Sun, 2003) and since p53 is responsible for a number of functions including apoptosis and cell cycle progression; loss of p53 leads to deregulation of the cell cycle, eventually resulting in cancer (Kastan et al., 1995).

Mutated E3 ligases have been observed in many cancer types. These involve those that are directly responsible for ubiquitylating proteins that regulate progression of the cell cycle such as SCF^{Skp2}; a target of which includes p27, a CDK inhibitor responsible for inhibiting cell cycle progression (Nakayama and Nakayama, 2006, Wang et al., 2014b); but also include those that are indirectly responsible for cell cycle regulation such as Hdm2 (Sun, 2003) and HECTH9, responsible for ubiquitylation of the transcription factor Myc and has been observed to be over-expressed in a number of cancers causing Myc-induced cell proliferation (Adhikary et al., 2005). For this reason, E3 ligases have been investigated as potential cancer therapy targets. Initially, the 26S proteasome was considered the ideal target for inhibition; however it was considered by many that this treatment type would be highly toxic to normal cells as well. Surprisingly, it was quickly observed that cancer cells are highly susceptible to proteasomal inhibition, ultimately resulting in cell death (Rizzardi and Cook, 2013).

More recently, E3 ligases as targets of cancer therapy have been investigated. One such E3 ligase is the murine double minute 2 (Mdm2) (Vassilev, 2007). As stated previously, Mdm2 is responsible for ubiquitylation of p53 and has been observed to be

over-expressed in certain cancers (Sun, 2003, Yin et al., 2005). Inhibitors of Mdm2 ubiquitin ligase activity have been found to have low potency and selectivity. However, inhibitors of the Mdm2-p53 interaction such as the nutlins have been found to show more promise as they have a higher specificity and potency and when administered to cultured cells, have been shown to lead to activation of the p53 pathway due to increased protein stability. Other small molecule inhibitors have also been identified although nutlins remain the most promising (Vassilev, 2007). Skp2 has also been investigated as a target of small molecule inhibitors; with two compounds identified as Compound A, which induces apoptosis and cell cycle arrest in multiple myeloma cells; and SZL‐P1‐41, which suppresses E3 ligase activity of Skp2 but no other SCF components (Wang et al., 2014b).

1.5 CIZ1 PROMOTES CELL CYCLE PROGRESSION

The *CIZ1* gene is located at 9q34.1 (Gilley and Fried, 1999). Ciz1 has been functionally linked to regulation of the cell cycle and directly associates with several cell cycle regulators including $p21^{Cip1/Waf1}$ (Mitsui et al., 1999), cyclin A and cyclin E (Copeland et al., 2010b) and CDK2 (den Hollander and Kumar, 2006). The protein has been found to bind to the N-terminal region of $p21^{Cip1/Waf1}$, which is the same region that binds to CDK2, indicating that this binding occurs in a competitive manner. Binding affinities of $p21^{Cip1/Waf1}$, CDK2 and Ciz1 show that $p21^{Cip1/Waf1}$ binds CDK2 preferentially. This interaction involves the first of three zinc finger motifs, with initial studies indicating that Ciz1 is also responsible for regulating the location of $p21^{Cip1/Waf1}$ within the cell. In the absence of Ciz1, $p21^{Cip1/Waf1}$ is largely located in the nucleus whereas when bound to Ciz1, the complex formed is mainly found in the cytoplasm; indicating that Ciz1 not only competitively binds the CKI in place of CDK2 but also sequesters it away from the nucleus: the site of pre-RC and pre-IC

formation (Mitsui et al., 1999). It was also found that p21 binding is dispensable for Ciz1 function in promoting cell cycle progression using p21 null fibroblasts (Coverley et al., 2005) suggesting that Ciz1 does not promote cell cycle progression solely by sequestering the CDK inhibitor $p21^{Cip1/Waf1}$ in the cytoplasm.

More recently, Ciz1 has been shown to promote cellular proliferation through stimulation of initiation of DNA replication in cell-based and cell-free assays. This function is independent of the interaction of Ciz1 with p21 as both $p21^{Cip1}$ null cells as well as wild type cells showed this stimulation in the presence of Ciz1(Coverley et al., 2005). It also explains the observation that Ciz1 is largely located at sites of initiation of DNA replication within the nucleus rather than in the cytoplasm. A more focussed study on Ciz1 localisation revealed that the C-terminal domain encodes a tag for the nuclear matrix localisation, whereas the N-terminal domain contains the replication domain and is therefore responsible for localisation at DNA replication specific foci (Coverley et al., 2005, Ainscough et al., 2007). Results obtained suggest that Ciz1 plays a role in the later stages of the G1 phase after formation of the pre-RC is complete by recruiting cyclin A to these sites of DNA replication (Copeland et al., 2010b). This allows activation of DNA replication due to increased cyclin A-CDK2 activity; causing phosphorylation of several proteins (Petersen et al., 1999, Lei and Tye, 2001).

In the study by Coverley et al. (2005), a link between cyclin A-CDK2 and Ciz1 was discovered, suggesting that Ciz1 may also have a function during the S phase. However, the precise relationship between the two was not elucidated. Since then, further investigations have revealed that Ciz1 functions in conjunction with cyclin A-CDK2 to activate DNA replication (Copeland et al., 2010a).

Subjecting replication-competent nuclei to recombinant cyclin A-CDK2 within a specific concentration range results in a larger number of nuclei where DNA replication is initiated *in vitro* than in the absence of this complex. A similar effect is observed when adding recombinant embryonic Ciz1 (ECiz1), which differs slightly from Ciz1 due to alternative splicing in exons 2/3, 6 and 8 (Coverley et al., 2005, Copeland et al., 2010a). However, when ECiz1 is added together with recombinant cyclin A-CDK2, the concentration range at which recombinant cyclin A-CDK2 stimulates initiation of DNA replication becomes larger, expanding at both ends of the scale (Copeland et al., 2010a). These observations support those previously made, whilst also providing further evidence of a relationship between Ciz1 and cyclin A-CDK2.

Ciz1 has been shown to directly bind both cyclin E and cyclin A using a Cy motif, located close to the CDK-binding domain (Copeland et al., 2010b). This Cy motif is a cyclin-binding sequence and is found in inhibitors, activators and substrates of CDKs, including $p21^{Cip1/Waf1}$ (Wohlschlegel et al., 2001). Ciz1 has 3 Cy motifs located within the N-terminal domain: the region containing the replication domain. The second motif has been found to be essential for function as mutations within this sequence result in an inability to influence DNA replication; which could be due to the impaired binding with both cyclin A and cyclin E when mutations in this region are present. Binding of Ciz1 to cyclin A and cyclin E is not identical (Copeland et al., 2010a); as might be possible to occur when considering levels of these cyclins do not reach their peaks during the same stage of the replication cycle. Evidence has shown that as cyclin A levels increase as the cell enters the S phase; cyclin E, whose levels are highest during the second part of the G_1 phase; is displaced from Ciz1 which in turn,

binds to cyclin A. This could mean that cyclin A is partly responsible for the displacement of cyclin E from Ciz1 (Copeland et al., 2010b).

The influence of Ciz1 on cyclin A-CDK2 activity was shown when small interfering RNA (siRNA) against Ciz1 transcripts was added during the G_1 phase, effectively reducing Ciz1 protein levels. This led to a significant reduction in recruitment of cyclin A to the nucleus, resulting in the number of cells entering S phase to be greatly reduced. It was also shown that a reduction in Ciz1 levels did not affect recruitment of cyclin E. Together with the observation that cyclin A displaces cyclin E from Ciz1, this strongly suggests that Ciz1 first binds to cyclin E which is located at specific foci within the nucleus, then recruits cyclin A to these foci and exchanges binding partners (Copeland et al., 2010a).

It is clear that Ciz1 is somehow involved in the initiation process of DNA replication. Evidence suggests that Ciz1 has a regulatory role in this process as low levels of this protein have been shown to have a detrimental effect on the recruitment of cyclin A-CDK2 to the required locations, resulting in the inhibition of the initiation of DNA replication. Further evidence of a regulatory role is shown in certain cancers where Ciz1 is mutated (Nishibe et al., 2013). Other binding partners such as $p21^{Cip1/Waf1}$, a known inhibitor of cyclin E-CDK2 that is normally sequestered unless activated as part of the DNA damage response, also support this (Sherr and Roberts, 1999, Satyanarayana et al., 2008). It has also been shown that the knockdown of Ciz1 results in reduced CDK2 activity (den Hollander and Kumar, 2006); revealing that not only is Ciz1 required for recruitment of cyclin A but is also required for the function of its CDK counterpart.

More recent evidence has provided more evidence of the relationship between cyclin A-CDK2 and Ciz1. This evidence has shown that not only are cyclin A-CDK2 and Ciz1 binding partners, but that Ciz1 is actually also a substrate of this cyclin-CDK complex. Phosphorylation at threonine residues 144, 192 and 293 result in the direct interaction between Ciz1 and cyclin A-CDK2 to be blocked, resulting in cyclin A no longer being recruited to sites of DNA replication. However, Ciz1 nuclear matrix localisation is retained. Phospho-specific antibodies monitoring Ciz1 phosphorylation status demonstrated that Ciz1 is not phosphorylated until mid-S phase, suggesting that cyclin A-CDK2 plays a role in inhibiting re-replication of DNA as formation of the replisome no longer occurs when Ciz1 is phosphorylated at these sites (Copeland et al., 2015). This also provides evidence that Ciz1 is one of the many factors involved in ensuring that DNA replication and the preparation for this event beforehand occurs when kinase levels are relatively low.

1.6 ALTERNATIVE FUNCTIONS OF CIZ1

Ciz1 is expressed at varying levels in a wide range of tissues, indicating that this protein is not just required for a specific cell type, but is rather utilised more generally. This emphasises the role of Ciz1 during the generic cell cycle; although varying levels of expression indicate that regulation of this protein does differ depending on cell type. The tissues in which Ciz1 is known to be expressed include the brain, heart, placenta, lung, liver, skeletal muscle, kidney and pancreas (Warder and Keherly, 2003). Ciz1 has since been observed in other tissues as well, including male germ cells (Greaves et al., 2012).

Ciz1 has more recently been found to bind Enhancer of Rudimentary Homolog (ERH). Co-expression of these proteins results in Ciz1 recruiting ERH to DNA

replication foci (Łukasik et al., 2008). ERH was first identified some years ago as an orthologue of a gene found in *Drosophila*. However, the precise function of this protein has still not been fully explained. ERH is known to be located in the nucleus and various proteins have been shown to interact with it; the functions of which have led to suggestions that ERH is involved in regulating various processes including transcription, cell shape and the cell cycle. Compiling all the evidence regarding the human orthologue as well as those from other species including *Caenorhabditis elegans* and yeast has led to a complex map of protein-protein interactions. This map includes proteins involved in regulating the cell cycle including skpA and skpB (components of the SCF complex in *Drosophila*) which are important components of several ubiquitin E3 ligase complexes. It has also been shown that the ERH orthologue protein in *Drosophila* interacts with CDK4 and *Rux*, a CKI that interacts directly with cyclin B (Jin et al., 2007). Considering that Ciz1 has now been shown to bind ERH at a site that overlaps the $p21^{Cip1/Waf1}$ binding site, containing the first zinc finger; it appears that ERH is recruited to sites of DNA replication by Ciz1 when all proteins concerned are at the correct levels, blocking binding between Ciz1 and p21 (Łukasik et al., 2008). Also, in taking into account the other binding partners of ERH as well as their functions; it appears that Ciz1 helps regulate the cell cycle indirectly as well. This further supports the hypothesis that Ciz1 binds other proteins using the DNA-binding sequence identified previously (Warder and Keherly, 2003).

It has been shown that Ciz1 interacts together with dynein light chain 1 (DLC1) to regulate the oestrogen receptor (ER) and also appears to influence $p21^{Cip1/Waf1}$ indirectly (den Hollander et al., 2006). DLC1 is best known as a component of cytoskeleton signalling as it makes up part of the dynein complex involved in trafficking vesicles and organelles along microtubules in a retrograde fashion.

However, it has also been found to have functions independent of the motor protein complex. Oestrogen influences the cell cycle in multiple ways. More recently, it was discovered that overexpression of DLC1 has been found to result in an accelerated G_1-S phase transition in an oestrogen-dependent manner as well as stimulating CDK2 activity (den Hollander and Kumar, 2006).

An investigation into the mechanism by which DLC1 influences cell cycle progression in response to oestrogen led to protein interaction studies which identified DLC1 as a novel binding partner for Ciz1. Following experiments showed that DLC1, CDK2 and Ciz1 form a trimeric complex (den Hollander and Kumar, 2006); suggesting that Ciz1 is not solely responsible for the reduced kinase activity when its levels are low as mentioned previously. Knowing that Ciz1 sequesters $p21^{Cip1/Waf1}$ in the cytoplasm, thus allowing CDK activity, experiments were performed in order to determine whether DLC1 also plays a role in this process as it was previously shown that this protein is located both in the cytoplasm and the nucleus. Results indicated that DLC1 is indeed involved in this process leading to a modified model of that proposed by Mitsui et al. (1999) in which DLC1 forms a complex with Ciz1 before sequestering $p21^{Cip1/Waf1}$ together (den Hollander and Kumar, 2006).

Following on from the discovery of this interaction as well as the knowledge that DLC1 is a coactivator of the ER; targeting it to oestrogen response elements (ERE) causing the expression of genes downstream to these sequences as well as genes within which EREs are located; further studies revealed that Ciz1 is the other half of the activating complex of the ER. It was found that Ciz1 interacts with ER via the second glutamine-rich domain located in the N-terminal domain and binds to the DNA-binding domain of the ER and that this interaction is enhanced by the presence of oestrogen (den Hollander et al., 2006). The fact that Ciz1 binds ER at the DNA-

binding region provides further evidence that the consensus DNA-binding sequence within Ciz1 mentioned previously (Warder and Keherly, 2003), allows this protein to interact with other DNA-binding proteins and might even confer a greater specificity for certain DNA sequences.

The *CIZ1* gene itself is induced by oestrogen in oestrogen-responsive cell lines. It was discovered that within this gene, there are multiple partial and complete EREs located upstream of exon 1 and the intron between the first two exons. The two complete EREs are located within the first intron. A study of Ciz1 mRNA levels revealed that oestrogen only induces *CIZ1* expression in the presence of the ER. Chromatin Immunoprecipitation assays (ChIP) revealed that ERs are recruited to both complete EREs. This was followed by a double ChIP with RNA polymerase II and ER which confirmed that both EREs are bound by ER and RNA polymerase II in an oestrogen-dependent manner, thus inducing expression of the *CIZ1* gene (den Hollander et al., 2006). These studies revealed that Ciz1 acts as a coactivator of ER together with DLC1 and is itself induced by oestrogen, which suggests a cycle with each complete one resulting in increased levels of mRNA transcripts of genes induced by oestrogen including Ciz1 that is also responsible for the activation of the ER; effectively forming a positive feedback loop. This process would obviously require a system to monitor and limit it to maintain proteins at the correct levels.

An investigation into the regulation of transcription of glucocorticoid receptors (GR) was performed using a chromosome conformation capture based technique since most glucocorticoid response elements (GRE) are not located proximal to promoters. The GRE chosen for this experiment is responsible for the activation of the lipocalin2 gene (*LCN2)*. The screening revealed that this GRE also interacts with the *CIZ1* gene roughly 30kb upstream. Further studies of the chromosome structure around these two

genes revealed a loop, resulting in the two genes being physically close together. Following on from this observation, it was then determined that like *LCN2*, *CIZ1* is also a glucocorticoid responsive gene. This was shown when glucocorticoids were added and transcript levels of both these genes were observed to increase in response (Hakim et al., 2009).

Interestingly, glucocorticoids inhibit the activity of oestrogen by negatively regulating the signalling pathway of ERα. ChIP studies revealed that the glucocorticoid receptor (GR) binds to several binding regions normally occupied by ERα when both glucocorticoids and oestrogen are present but not when only one of these ligands is present. The binding of GR to these regions causes the displacement of ERα from these sites and destabilises the complex of ERα and the steroid receptor coactivator SRC-3 but binding itself is mediated by ERα. However, as a consequence of the displacement of ERα, transcription of genes normally activated by ERα is repressed (Karmakar et al., 2013). This phenomenon has revealed a possible target for oestrogen-responsive cancers. Considering that *CIZ1* has been identified as being both an oestrogen responsive gene and a glucocorticoid responsive gene, this suggests that despite fluctuations in oestrogen and glucocorticoid levels, production of Ciz1 should remain relatively constant.

1.7 ROLE OF CIZ1 IN CANCER BIOLOGY

It has been noted that alternative splicing of Ciz1, resulting in a lack of exon 4, occurs in Ewing tumour cell lines (Rahman et al., 2007). This alternatively spliced protein no longer localises at sites of initiation of DNA replication, although it is still located in the nucleus. However it is still able to stimulate replication activity. Since this observation was made, alternatively spliced Ciz1 has been observed in several other

cancer types. Notably, the variant delta 8-12 lacks key functional sites but was found to be over-expressed in many cancer cell lines, including over half of a panel of primary lung tumours tested (Rahman et al., 2010). This novel variant could be a useful biomarker of certain cancer types.

A study of Ciz1 in lung cancer found that an alternatively spliced form of Ciz1 (in exon 14) was present in 34 out of 35 lung tumours but not in the adjacent tissue. Further testing revealed that this variant of Ciz1 could be used as a circulating biomarker for early-stage lung cancer (Higgins et al., 2012). This variant of Ciz1 was still found to be located at the same foci within nuclei as the normal Ciz1 but as larger aggregates and also some localisation at the edge of the nucleus. Depletion of both the variant and normal forms of Ciz1 resulted in inhibition of DNA replication in cell culture (Higgins et al., 2012).

Ciz1 has since been shown to function as a tumour suppressor *in vivo* using $Ciz1^{-/-}$ mice (Nishibe et al., 2013). Ciz1 has also been shown to play an indirect role in breast cancers (Okumura et al., 2011) as well as human colon cancer (Wang et al., 2014a). Ciz1 was found to be significantly upregulated in the majority of samples tested. It was also found to be a prognostic factor of disease free survival after colectomy in patients with colon cancer (Wang et al., 2014a).

In all cancers where Ciz1 was observed to be altered, over-expression of this protein was associated with tumour growth (Rahman et al., 2010, Higgins et al., 2012, Wang et al., 2014a). Ciz1 should therefore be considered as a potential target in cancer therapy where Ciz1 has been observed to be over-expressed; considering that cell culture work has demonstrated that targeted depletion of Ciz1 inhibits cell proliferation (Higgins et al., 2012).

1.8 POST-TRANSLATIONAL REGULATION OF CIZ1

Although *CIZ1* gene expression has been shown to be regulated in part by the ERE and GRE (den Hollander et al., 2006, Hakim et al., 2009), post-translational regulation of this protein is not fully understood.

Ciz1 has been shown to be phosphorylated by ATM kinases as part of the DNA damage response; thought to form part of a pathway responsible for regulating cyclin E such that cell cycle progression is inhibited. The CKI p27, an inhibitor of cyclin E-CDK2, and FBW7, a component of the SCF complex that targets cyclin E for degradation (Welcker and Clurman, 2008), also form part of this pathway network (Matsuoka et al., 2007).

However, Ciz1 is also phosphorylated as part of normal cell cycle progression by CDKs. Studies have shown that Ciz1 interacts with both cyclin E-CDK2 and cyclin A-CDK2 in a sequential manner (Coverley et al., 2005, Copeland et al., 2010b) although binding with cyclin E-CDK2 has as yet an unknown function. More recently, Ciz1 has also been shown to be a substrate of cyclin A-CDK2 (Copeland et al., 2015).

In contrast to the observations that phosphorylation of Ciz1 prevents binding to cyclin A-CDK2; it has also been shown that depletion of cyclin A leads to a reduction in Ciz1 protein levels; which are recovered with the addition of a proteasomal inhibitor MG132 (Fig.5A) (Copeland, unpublished data). This suggests that the cyclin A-CDK2 complex also stabilises the Ciz1 protein, which actively prevents degradation by the ubiquitin proteasome system. In order to determine if Ciz1 could also be destabilised by chemical means, addition of roscovitine, a known CDK inhibitor was also used (Figs. 5B and C) (Copeland, unpublished data). These results suggest that CDK-mediated phosphorylation of Ciz1 stabilises this protein. Taken together with the

results showing that Ciz1 phosphorylation prevents binding to cyclin A-CDK2; one possible reason for the apparent opposite situations presented is that low level phosphorylation of Ciz1 at perhaps a different CDK phosphorylation site to those involved in cyclin A-CDK2 binding is responsible for protein stability.

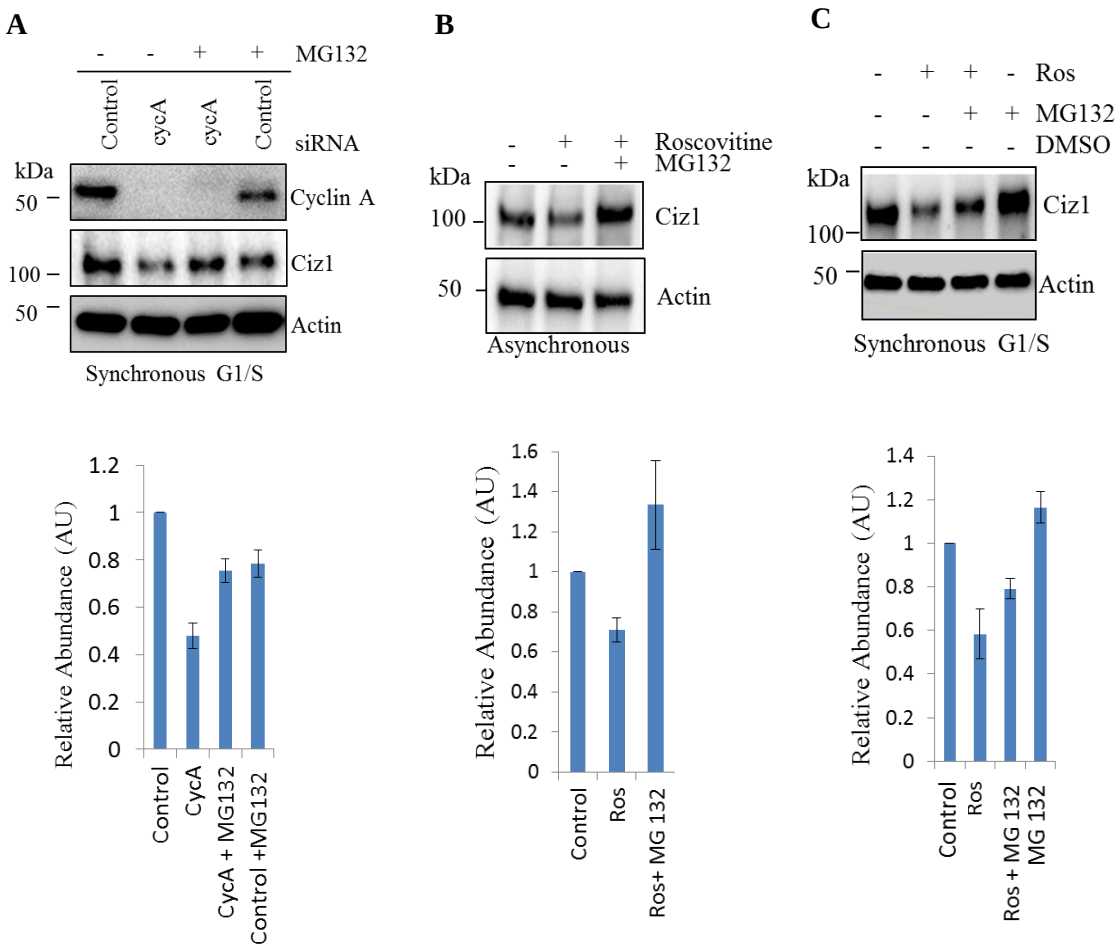

Figure 5: Ciz1 is destabilised by reduction of cyclin A-CDK2 and is recovered by inhibition of the ubiquitin proteasome system
Ciz1 levels relative to actin are shown in the accompanying histograms below. Cells were harvested four hours post-drug treatment and samples were used for western blots. The anti-N471 antibody was used to observe Ciz1. **(A)** Cells were depleted of cyclin A by transfection of a synchronised population of cells with *a-ccna2* siRNA. Cells were also treated with the chemical proteasomal inhibitor MG132 as shown. **(B)** Cells were treated with a chemical CDK inhibitor roscovitine, in an asynchronous population of cells and MG132 as indicated. **(C)** A synchronised population of cells was treated with roscovitine and MG132 as indicated.

1.9 PROJECT AIMS

This project aims to better understand how the protein Ciz1 is regulated within the cell cycle.

1. Does CDK-mediated phosphorylation of Ciz1 contribute to protein stability? This will be investigated by attempting to chemically destabilise the Ciz1 protein by targeting CDK activity and attempting to identify which site(s), if any, contribute to protein stability when phosphorylated by CDK activity.
2. Preliminary investigation into the potential E3 ligase that regulates Ciz1 levels via UPS. Ciz1 ubiquitylation status will first be investigated followed by *in vitro* protein studies to investigate whether the candidate E3 ligase can bind Ciz1.
3. Characterisation of Ciz1 phospho-specific antibodies and enzymological analysis of cyclin A-CDK2 mediated Ciz1 phosphorylation. This will involve *in vitro* protein work to determine whether the site of interest, S331, is a potential candidate as a site responsible for contributing to increased protein stability.

2. MATERIALS & METHODS

2.1 Materials

All chemicals used were obtained from Sigma-Aldrich except where stated otherwise.

2.2 Cell Culture

Mouse fibroblasts (D3T3) were cultured in Dulbecco's Modified Eagle's Medium (DMEM) supplemented with 10% foetal bovine serum and 1x penicillin-streptomycin-glutamine. These were incubated at 37^{o}C in 5% CO_2. When confluency reached 50-60%, cells were passaged with trypsin-EDTA (Gibco®) using a final 1x concentration diluted in phosphate buffered saline (PBS) and incubated at 37^{o}C until the cells no longer adhered to the plate before being split onto fresh plates with DMEM; inactivating the trypsin-EDTA. Cells were typically split in a 1:2 or 1:4 ratio.

Populations of cells were synchronised by growing cells by contact inhibition and serum starvation. Cells were cultured until they had reached 100% confluency. At this point, fresh media was added and cells were left for a further 48 hours, allowing them to enter quiescence. Cells were then released back into the cell cycle by trypsinisation as described except 2x trypsin was used to break cell-cell interactions. Cells were diluted 1:4 and placed in fresh supplemented DMEM on new plates. If cells were transfected, this process occurred when cells were trypsinised.

Two drugs were used in these experiments: roscovitine (Sigma-Aldrich) and MG132. Roscovitine was dissolved in DMSO, with the final concentration ranging between 0.9µM-100µM. MG132 was also dissolved in DMSO and was used at concentrations of 1µM or 10µM. Cells were harvested 4 hours after treatment.

2.3 Whole plasmid mutagenesis

Phosphorylation sites were identified by locating serine and threonine residues as well as the putative destruction box in the N-terminal region (denoted by the classic

sequence RXXL). Primers were then designed containing the intended mutations to each of these sites. Substitution mutations were introduced such that the new residue became an aspartate for the phosphomimetic mutants and alanine for all other mutants. Primers were typically 30 nucleotides long with melting temperatures (T_m) between 65^{o}C and 80^{o}C. Primers were synthesised by Eurofins MWG Genomics.

Primers were received and dissolved in nuclease-free water to obtain a concentration of 100µM. To perform PCR of plasmids >10kb, 0.4µM of forward and reverse primers is required according to the protocol provided by Agilent Technologies for the PfuUltra II Hotstart 2x PCR Master Mix. Briefly, reactions occurred in a mixture containing 0.4µM each of the complementary forward and reverse primers, 20ng of template DNA (WT Ciz1) and a final 1x concentration of Master Mix. The rest of the volume was made up with nuclease-free water. This was prepared in PCR tubes. Samples were then placed in the PCR machine (Techne TC-312; Jencons-PLS) and run at the appropriate program (Table 1). Following PCR, plasmids were subjected to digestion with DpnI.

1	1 cycle	92^{o}C	2 minutes
2	30 cycles	92^{o}C	20 seconds
		Primer T_m- 5^{o}C	20 seconds
		68^{o}C	30 seconds/kb
3	1 cycle	68^{o}C	5 minutes

Table 1: Conditions required for PCR of the plasmid containing Ciz1 with mutated primers

2.4 Preparation of an agarose gel

The 0.7% agarose gel was prepared by using powdered agarose with low electroendosmosis (EEO) and 1x Tris/Borate/EDTA (TBE) buffer. This mixture was heated until all the agarose had been dissolved before addition of ethidium bromide

when the solution had cooled to ~50^{o}C. This mixture was then added to the gel tank and left to set.

2.5 Confirming success of PCR

To confirm the PCR had been successful, samples were subjected to agarose gel electrophoresis. A 0.7% gel was prepared (section 2.4) and loaded with an equal mixture of plasmid and 6x Gel Loading Dye (BioLabs) with a 1kb ladder (BioLabs) for reference. The DNA was separated by electrophoresis at 100V for one hour. The gel was imaged using the Bio-RAD ChemiDoc^{TM} MP System and the accompanying Image Lab^{TM} 4.1 Software.

2.6 Preparing competent Top 10 *E. coli*

Competent *E. coli* cells were prepared by inoculating 5ml of LB medium with 1µl of Top 10 *E.coli* cells which were left to grow overnight at 37^{o}C at 150rpm. 750µl of the *E. coli* was used to inoculate 75ml of fresh LB medium, incubated for approximately two hours until the OD600 was between 0.3 and 0.6. At this point, the broth was centrifuged at 3000g for 10 minutes at 4^{o}C after which the medium was removed. The pellet was resuspended in 30ml ice cold CCMB80 buffer prepared on the day and left to incubate for 20 minutes on ice following another round of centrifugation. The pellet was resuspended in 4ml of ice cold CCMB80 buffer before being placed in cooled eppendorfs in 200µl aliquots. These were frozen at -80^{o}C.

- CCMB80 buffer composition: 10mM Potassium acetate pH 7.0
  80mM $CaCl_2.2H_2O$
  20mM $MnCl_2.4H_2O$
  10mM $MgCl_2.6H_2O$
  10% glycerol

2.7 Preparation of *E. coli* for plasmid isolation and DNA sequencing

To confirm introduction of each mutation had been successful for the phosphomimetic mutants and D-box mutant, competent Top 10 *Escherichia coli* were transformed with the mutated plasmids. Transformation was performed by adding 1µl of plasmid to competent cells and incubated for 30 minutes on ice, 1 minute at 42^{o}C then another 5 minutes on ice before being left on a shaker at 37^{o}C for 1 hour following addition of 500µl of SOC medium (Super Optimal broth with Catabolite repression, Thermo Fisher Scirntific) to maximise transformation efficiency. This was plated onto LB agar (Thermo Fisher Scientific) supplemented with kanamycin (50µg/ml) and incubated overnight at 37^{o}C.

A single colony was used to inoculate 5ml of LB medium supplemented with kanamycin (50µg/ml) which was incubated at 37^{o}C and 150rpm for a maximum of 16 hours. This was followed by DNA extraction according to the protocol provided either with the QIAprep® Spin Miniprep Kit or GeneJET Plasmid Miniprep Kit (Thermo Scientific). DNA samples were then sent to Eurofins MWG Genomics at 50-100µg/ml for sequencing and presence of the correct mutations was verified.

For pGEX-6P3 plasmids, BL-21 (DE3) *E. coli* cells were used for transformation. The LB agar and LB medium were supplemented with ampicillin (100µg/ml).

***Escherichia coli* strain**	**Genotype**
Competent Top 10	F–mcrA Δ(mrr-hsdRMS-mcrBC)Φ80lacZΔM15ΔlacX74recA1araD139Δ(ara leu)7697galU galK rpsL (StrR) endA1 nupG (Inviitrogen)
BL-21 (DE3)	fhuA2 [lon] ompT gal (λ DE3) [dcm] ΔhsdS λ DE3 = λ sBamHIo ΔEcoRI-B int::(lacI::PlacUV5::T7 gene1) i21 Δnin5 (BioLabs)

Table 2: *E. coli* strains and their genotypes used in these experiments

2.8 Transfection of mouse fibroblasts

For asynchronous cell experiments; when confluency of cells reached over 70%, cells were trypsinised as described previously, cells placed in 5-10ml DMEM. Cells were harvested by centrifugation at 500g for 5 minutes to form a pellet. This pellet was resuspended in 100µl Nucleofector® Solution with Nucleofector® Supplement added before 5µl of plasmid or siRNA was added. This mixture was placed in a cuvette which in turn was placed in the Lonza Nucleofector™ 2b Device with the appropriate program selected for cell type (Program 30 – NIH-3T3). Following this process, living cells were then plated out in supplemented DMEM (10% FBS and 1x penicillin-streptomycine-glutamine) and incubated for 12-24 hours at 37^{o}C in 5% CO_2.

For synchronous cell experiments; cells were transfected as described (section 2.2). One 15cm diameter plate was used for two transfections.

2.9 Scrape harvesting cells for protein isolation

After appropriate incubation periods (16-24hrs post-transfection, 4hrs post-drug treatments), cells were harvested using Cytoskeleton Buffer (CSK) supplemented with a protease inhibitor tablet and 1mM Dithiothreitol (DTT) in order to remove a large proportion of proteins not bound to the scaffold or the chromatin. Once harvested, phenylmethanesulfonylfluoride (PMSF), a serine protease inhibitor was added to the cell mixture at a final concentration of 2mM. This constituted the total protein fraction. Half of this fraction was removed and 1% Triton X-100 was added before the sample was spun at 14 000g for 5 minutes. The supernatant represents the detergent soluble fraction and the pellet contains the chromatin fraction. Each of the three fractions was placed in equal volumes of a 4x SDS-PAGE loading buffer supplemented with DTT at a final concentration of 200mM before being boiled for 10 minutes. Samples were stored at -20^{o}C until use.

- CSK buffer composition: 10mM PIPES pH6.8
  300mM Sucrose
  100mM Sodium chloride
  3mM Magnesium chloride

- 4x SDS-PAGE loading buffer composition: 240mM Tris-HCl pH 6.8
  8% SDS
  40% Glycerol
  Pinch of Bromophenol Blue

2.10 Determination of the proportion of cells in the S phase by 5-ethynyl-2'-deoxyuridine (EdU) incorporation

Synchronisation of cells (section 2.2) was confirmed using EdU labelling (EdU Click-iT method - Invitrogen) of cells grown on coverslips. Time points occurred 16-24 hours post-transfection at 2 hour intervals after release from quiescence. At 15.5 hours post-release from quiescence, coverslips with cells were placed individually into a 24-well plate containing 1ml media. Addition of 2μM EdU occurred 30 minutes prior to the first time point. After labelling with EdU, coverslips were removed from media and washed twice with PBS before fixing with 4% PFA for 15 minutes. Coverslips were then washed with 3% BSA in PBS twice followed by incubation with 0.5% Triton X-100 for 20 minutes at room temperature. After washing with 3% BSA in PBS twice again, EdU Click-iT cocktail was added to each coverslip so that the surface was completely covered (as described in manufacturer's instructions). This was incubated for 30 minutes in the dark. Prior to mounting on slides using mounting medium + DAPI, coverslips were washed again three times with 3% BSA in PBS, then twice again in PBS. For each coverslip, 100 nuclei were scored and the

percentage of cells in S phase was calculated by determining the number of EdU positive nuclei.

2.11 Isolating RNA from synchronised cell populations for qPCR analysis

Cells were trypsinised as described (section 2.2). Following trypsinisation, cells were centrifuged at 500g for minutes to form a pellet, which was then frozen at -80^{o}C.

RNA extraction was performed using the PureLink^{TM} RNA Mini Kit (ambion by life technologies) according to manufacturer's instructions. Briefly, fresh lysis buffer was prepared by adding 1% v/v 2-mercaptoethanol. The pellet was thawed and 0.6ml lysis buffer was added. This mixture was vortexed in order to lyse the cells. Homogenisation was performed at room temperature by passing the lysate through an 18-21 gauge syringe needle 5-10 times. All other steps occurred on ice. To each volume of cell homogenate, 0.6ml of 70% ethanol was added followed by vortexing to mix. The sample was then placed in a spin column and centrifuged at 12 000g for 15 seconds at room temperature. The flow-through was discarded. 700µl Wash Buffer I was added twice to the spin cartridge and centrifuged as before; followed by two washes with Wash Buffer II. An extra centrifugation step was performed in order to dry the membrane before adding 30-100µl RNase free water to the centre of the spin cartridge. This was incubated at room temperature for 1 minute followed by centrifugation at 2000g for 2 minutes to elute the RNA from the membrane. Purified RNA was stored at -80^{o}C.

2.12 Determining mRNA levels by real time quantitative PCR

RNA extractions for transcript level analyses by qPCR were prepared using an EXPRESS One-Step SuperScript® qRT-PCR Kit with Premixed ROX (Invitrogen). Each reaction required 20µl master mix containing both the sample and the primers. For every 20µl, half the volume consisted of EXPRESS qPCR SuperMix with

Premixed ROX. 2µl EXPRESS SuperScript® Mix for One-Step qPCR and equal concentrations of template RNA were added. The rest of the volume was made up by DEPC-treated water. To each well of the PCR plate, 19.6µl of master mix was added before 0.4µl of the fluorescent primer mix was added. The 96-well PCR plate was then placed in the qRT-PCR machine with the correct program selected. GAPDH was used as the reference. The cycle threshold (Ct) was determined as the number of PCR cycles required to reach the detectable threshold of fluorescence emitted by PCR products, which occurs during the exponential phase of the reaction. The Ct value is inversely proportionate to the original amount of transcript.

1	50°C		15 minutes
2	95°C		2 minutes
3	40 cycles	95°C	15 seconds
		60°C	1 minute

Table 3: Conditions required for qPCR to determine RNA levels

2.13 Subcellular fractionation isolating chromatin, high salt resistant and nuclear matrix fractions

The method described here is a modified version of that used by Ainscough et al. (2007). Cells were harvested as described (section 2.9) before 1% Triton X-100 was added. An aliquot of this mixture was removed, forming the total protein fraction. The remaining mixture was centrifuged at 10 000g for 5 minutes; the supernatant containing the detergent soluble fraction. The high salt soluble fraction was prepared by resuspending the pellet in high salt CSK buffer (CSK + 0.5M NaCl). Following centrifugation at 10000g for 5 minutes, the supernatant was removed. The pellet was then washed 3 times with 1x DNase I buffer to reduce salt concentration prior to DNase I digestion (diluted 1:10 in 1x DNase I buffer – Thermo Fisher Scientific) was added; followed by an hour incubation period at room temperature. After

centrifugation at 17 000g for 5 minutes, the supernatant was placed in a fresh Eppendorf (Dnase supernatant). This was followed by repeating incubation with high salt CSK to remove the digested DNA, making up the DNA-free fraction following centrifugation. The pellet was resuspended in 4x SDS-PAGE loading buffer. An incubation period of 5 minutes occurred prior to each centrifugation step unless stated otherwise. All steps were performed on ice unless indicated.

- DNase I buffer composition: 100mM Tris-HCl pH 7.5
  25mM Magnesium chloride
  1mM Calcium chloride

2.14 SDS-PAGE gel electrophoresis

Samples were boiled at 95^{o}C for 10 minutes prior to loading in Mini-PROTEAN® Precast Gels (BIO-RAD). Gels were placed in a Mini-PROTEAN® Vertical Electrophoresis Cell (BIO-RAD) containing 1x Tris-Glycine-SDS PAGE Buffer (National Diagnostics) and samples were loaded. Proteins were separated by electrophoresis for approximately 30 minutes at 200V.

2.15 Western blots

Semi-dry western blots were prepared by incubation of Mini-PROTEAN® Precast Gels (BIO-RAD) in transfer buffer for 5 minutes and sandwiching between 4 pieces of filter paper saturated in transfer buffer, nitrocellulose 0.4µm membrane (GE Healthcare Life Sciences), gel and 4 more pieces of filter paper. Proteins were transferred by semi-dry blotting at 0.8mAmp/cm^2 (typically 63mA per blot) for 1.5-2 hours. Blots were then blocked for a minimum of 30 minutes with TBST+1% w/v BSA (Tris-Buffered Saline + Tween-20 and Bovine Serum Albumin) or 5% milk powder in TBST before the primary antibody was added at the appropriate dilution.

This was incubated for 1-2 hours at room temperature or overnight at 4^{o}C. Washing with TBST+BSA was performed four times for 5 minutes each before adding the appropriate secondary antibody at a dilution of 1:5000. Following an incubation period of one hour, washing was performed as before, this time using TBST. Peroxide solution and luminol enhancer solution (Cynagen Westar ηC) were mixed together (1:1 ratio), then placed on the blot after positioning in the BIO-RAD ChemiDoc^{TM} MP System. The blots were then developed. The blots were first probed with α-actin and actin was quantified using the Image Lab^{TM} 4.1 Software to ensure loading of samples was equal for most cell samples. Ciz1 levels were quantified relative to actin quantification levels.

Antibody	**Dilution**	**Antigen**	**Secondary antibody (+HRP) (1:5000)**
α-β actin	1:2000	β-actin	α-mouse
α-N471	1:500	Ciz1	α-rabbit
α-pT293	1:200	pT293 in Ciz1	α-rabbit
α-pS331	1:200	pS331 in Ciz1	α-rabbit
α-cyclin A	1:500	Cyclin A	α-mouse
α-cyclin E	1:1000	Cyclin E	α-rabbit
α-HA HRP	1:1000	Haemaglutinin	N/A

Table 4: Primary and secondary antibodies used to probe western blots

pIMAGO-biotin Phosphoprotein Detection (Expedeon)

Labelling reactions were performed according to manufacturer's instructions (Expedeon). Briefly, samples were boiled and allowed to cool down before adding 1x IAA solution. Samples were incubated for 15 minutes before being loaded onto a gel. When transferring to the nitrocellulose membrane, a second piece of membrane was placed before the gel as well in order to bind any contaminants, thus reducing

nonspecific background signal later on. The rest of the transfer process occurred as normal. The membrane was the blocked for 1 hour with 1x Blocking buffer. A 1:1000 mixture of pIMAGO reagent in 1x pIMAGO buffer was prepared before adding to the membrane followed by another 1 hour incubation. The membrane was washed three times with 1x Wash buffer and once with TBST. A 1:1000 mixture of avidin-HRP in 1x blocking buffer was prepared before adding to the membrane and incubating for 1 hour. The membrane was washed three times with TBST and a signal was obtained as before except Cynagen Westar Supernova enhanced chemiluminescence solution was used instead.

- Transfer Buffer (200ml): 7.2g Trizma base
  0.44g CAPS
  20ml 100% ethanol
  0.4ml 10% w/v SDS

2.16 Immunofluorescence

Success of transfection and confirmation of the location of ECiz1 were determined using immunofluorescence as the plasmid containing Ciz1 also contains a GFP (Green Fluorescent Protein) tag. Slides were prepared by growing transfected cells on coverslips. These coverslips were then washed twice with CSK before being placed in a 24 well plate. For the total protein fraction, cells were fixed using 4% PFA (Paraformaldehyde). The following treatments were all performed on ice. For the detergent resistant fraction, cells were treated with 1% Triton X-100 in CSK for 5 minutes, followed by fixing with 4% PFA. The high salt resistant fraction was formed by adding high salt CSK as used previously for 5 minutes before being fixed. The remaining nuclear matrix was prepared by washing first with DNaseI buffer before incubating with DNaseI (diluted 1:10 in 1x DNaseI buffer) at room temperature for

one hour. This was followed by washing with high salt CSK and fixing. Once fixing with 4% PFA was complete, coverslips were washed with PBS (Phosphate Buffered Saline). For each coverslip, a drop of VECTASHIELD® Mounting Medium with DAPI (Vector Laboratories) was placed on a microscope slide before placing the dried coverslip on top. A LSM510 laser scanning confocal microscope was used for viewing these treated cells and images taken along with the accompanying software.

2.17 Immunoprecipitation

Mouse fibroblasts (D3T3) were transfected with GFP-Ciz1 constructs and HA-Ubiquitin (HA-Ub) 24 hours before commencing this procedure. At the time of harvesting, cells had reached ~80% confluency. Cells were harvested using lysis buffer and had 1% v/v Triton X-100 added before being left to incubate on ice for 5 minutes. This was followed by centrifugation at 13000g to extract the Ciz1 protein. The supernatant containing the protein had 3x v/v binding buffer added prior to addition of 4x SDS-PAGE buffer followed by boiling for 10 minutes. These samples were used to confirm the presence of Ciz1 within the supernatant. Following this step, 5µl of 2-10µg of affinity-purified α-N471 was added to each sample. Control samples had no antibody added. Samples were then incubated for a minimum of 2 hours in order to form the immune complex.

The Pierce® Classic IP kit (Thermo Scientific) was used for these experiments. Pierce Protein A/G Agarose was placed into a Pierce Spin Column and spun down to leave only the resin. This was then washed twice with ice-cold binding buffer before addition of the antibody/lysate sample and incubation with gentle end-over-end mixing for 1 hour. Following centrifugation, the flow-through was saved until the IP was confirmed as successful. The resin was then washed three times with binding buffer before 50µl of 4x SDS-PAGE loading buffer was added and the samples boiled

for 10 minutes. Finally, samples were then centrifuged for 1 minute at 1000g and the flow-through was used to perform western blots. Each western blot was duplicated with separate gels probed with α-N471 and α-HA HRP respectively.

- Lysis buffer (50ml): 1x Phosphate Buffered Saline
  1x Complete Protease Inhibitors (Roche)
  1mM DTT
- Binding/Wash buffer (50ml): 50mM HEPES pH 7.8
  10mM Magnesium chloride
  20mM Calcium chloride
  130mM Potassium chloride
  0.02% Triton X-100
  1mM DTT
  1x Complete Protease Inhibitors (Roche)

2.18 Ni^{2+}-NTA immobilisation of His-Ub

Cells were transfected with His-Ub 24 hours prior to harvesting. Cells were then washed with ice cold lysis buffer (PBS, 100mM NaCl, 1mM DTT, 10mM Imidazole, 1x protease inhibitor tablet) followed by incubation for 5 minutes on ice in lysis buffer. Cells were then scrape harvested and made up to a volume of 200µl with lysis buffer to which 100µM PMSF and 0.5% Triton X-100 were added. Following incubation on ice for 5 minutes, samples were centrifuged at 10 000g for 5 minutes. The supernatant contained the low salt extract. The pellet was then resuspended in in 200µl high salt buffer (lysis buffer + final concentration of 500mM NaCl). This was centrifuged again at 17 000g for 5 minutes, with the supernatant containing the high salt extract. IP spin columns were prepared with 30µl Ni^{2+}-NTA resin for each reaction. These were washed three times with lysis buffer prior to addition of cell

lysates. The final volume of each sample as made up to 400µl with lysis buffer and an aliquot was removed from each sample to confirm presence of the protein of interest prior to immobilisation. The cell lysates were then added to the resin and allowed to bind for 1 hour on a mixer at 4^{o}C. This was followed by washing four times with lysis buffer before addition of 4x SDS-PAGE loading buffer and boiling for 10 minutes. The denatured protein was then collected by centrifugation.

2.19 Preparation of autoinduction media

For each recombinant protein, 750ml ZY was prepared. This contained 7.5g Tryptone (BD Biosciences) and 3.75g Yeast extract (Fisher Scientific). A 20x stock concentration of NPS was prepared with 0.5M ammonium sulphate, 1M potassium phosphate monobasic and 1M sodium phosphate dibasic. A 50x stock concentration of 5052 was prepared containing 25% glycerol, 0.139M glucose (Fisher Scientific) and 0.278M α-lactose monohydrate. These mixtures were then autoclaved for 15 minutes at 121^{o}C. Magnesium sulphate and 1000x trace metals mixtures were filter sterilised.

- **1000x trace metals (100ml):**

Metal (volume)	**1x concentration**
0.1M $FeCl_3.6H_2O$ (50ml)	50µM Fe
1M $CaCl_2$ (2ml)	20µM Ca
1M $MnCl_2.4H_2O$ (1ml)	10µM Mn
1M $ZnSO_4.7H_2O$ (1ml)	10µM Zn
0.2M $CoCl_2.6H_2O$ (1ml)	2µM Co
0.1M $CuCl_2.2H_2O$ (2ml)	2µM Cu
0.2M $NiCl_2.6H_2O$ (1ml)	2µM Ni
0.1M $Na_2MoO_4.2H_2O$ (2ml)	2µM Mo

0.1M $Na_2SeO_3.5H_2O$ (2ml)	2µM Se
0.1M H_3BO_3 (2ml)	2µM H_3BO_3

2.20 Over-expression of recombinant protein using autoinduction in *E. coli*

Autoinduction was used to produce the proteins of interest. BL-21 *E. coli* were transformed with pGEX-6P3 plasmids containing various protein constructs using the same protocol as that used for the transformation of Top 10 *E. coli* with ampicillin (1:1000) used instead of kanamycin. Following growth on LB agar, a single colony was used to inoculate 5 ml of LB supplemented with ampicillin (100µg/ml) and incubated overnight at 37^{o}C, shaking at 200rpm; followed by inoculation of 75ml of LB and ampicillin for another night. This culture was then added to 750ml of a mixture of ZY, 1mM $MgSO_4$, 1x 5052, 1x NPS, 100µg/ml ampicillin and 1:1000 dilution of trace metals. This mixture was incubated at 20^{o}C for 24 hours, shaking at 150rpm. The culture was then centrifuged for 15 minutes at 4500g and the majority of the supernatant removed followed by centrifugation at 3000g for 15 minutes. The remaining pellet was stored at -80^{o}C.

The pellet was resuspended in 25ml HEPES buffered saline (HBS – 10mM HEPES pH7.8, 135mM NaCl, 1mM EDTA) supplemented with DTT and one protease inhibitor tablet. Once the pellet had been resuspended, the cells were sonicated at maximum power for 15 seconds 5 times with a one minute rest between sonication. The cell mixture was then placed in a sorval tube and spun at 20 000g for 30 minutes at 4^{o}C in a JA 25.5 rotor. During centrifugation, 0.75ml of Glutathione Sepharose^{TM} 4B beads (GE Healthcare) were placed in 50ml bead wash buffer (HBS+DTT) and left on a roller for a minimum of one hour to rehydrate them. Subsequently, the wash buffer was removed from the beads and the cell lysate was placed on them. To allow GST tag immobilisation, the tube was placed on a wheel for 1 hour at 4^{o}C. The

mixture was then centrifuged at 1000g for 1 minute and the supernatant removed, with a 20µl aliquot removed to show purification levels at each wash stage. The beads were washed five times with 10ml of wash buffer (HBS + 1x protease inhibitor tablet + DTT), followed by centrifugation at 1000g for 1 minute after being placed on ice for a few minutes. After each centrifugation, an aliquot was removed.

2.21 Protein interaction studies

To cleave the beads from the protein, the mixture was washed 3 times with 3C cleavage buffer (50mM TrisHCl pH 7.35, 15mM NaCl) in the same manner as above. 10µl of 3C PreScission™ Protease (GE Healthcare) was then added to the mixture in a 1.5ml eppendorf with about 200µl head-space to avoid shearing of the protein due to mechanical stress. This was then left on a wheel at 4°C overnight.

To elute the protein, the mixture was placed in a spin column and spun at 1000g for 1 minute. The flow-through containing the protein was aliquoted and stored at -80°C. A smaller aliquot was used for purification identification and the beads were resuspended in 3C cleavage buffer so an aliquot could be removed for this purpose as well. These samples were mixed with 4x SDS-PAGE loading buffer + DTT and run on a gel. This was stained with Instant*Blue*™ (Coomassie Based Staining Solution) for an hour, then imaged. To prove the presence of the protein of interest, a western blot was also performed.

For protein-protein binding studies, one protein cleaved from the glutathione sepharose beads was added to another protein still bound to these beads. The mixture was placed in a 1.5ml eppendorf and an aliquot removed for a sample before binding. 3C buffer was added with about 200µl head space. The eppendorfs were placed on a wheel and left to bind for an hour at 4°C. The beads were then washed three times

with 3C buffer as described previously before adding 4x SDS-PAGE loading buffer and boiling for ten minutes.

2.22 Determining protein concentration

Protein concentrations following purification were determined using a Pierce® BCA Protein Assay Kit as per manufacturer's instructions (Thermo Scientific). The standard curve was produced using an albumin standard (bovine serum albumin) at 2mg.ml diluted in 3C cleavage buffer, containing 1mM DTT. Compatibility Reagent Stock Solution was added at an equal volume to each standard and sample and allowed to incubate at 37^{o}C for 15 minutes to degrade DTT. The BCA Working Reagent containing Cu^{2+} was then added followed by further incubation at 37^{o}C for 30 minutes. Absorbance of each standard and sample was read at 562nm.

2.23 *In vitro* kinase assays to determine phosphorylation kinetics of Ciz1 by cyclin A-CDK2

These reactions were performed under pseudo-first order reaction conditions in a buffer containing 50mM HEPES pH 7.8, 20mM $MgCl_2$, 10mM ATP and 1mM DTT. In the initial experiments, 50nM cyclin A-CDK2 and 1µM Ciz1 were used. Later experiments were performed with 5nM cyclin A-CDK2 and Ciz1 concentrations between 50nM-2µM. Each reaction had a total buffer volume of 200µl contained in a 1.5ml eppendorf before the correct volume of Ciz1 was added. The eppendorf was then placed in heat block at 37^{o}C. At t=0, the appropriate volume of cyclin A-CDK2 was added and an aliquot of 25µl immediately removed. Further aliquots were removed at appropriate time points. Removed aliquots were mixed with an equal volume of 2x SDS-PAGE loading buffer and boiled straight away for 10 minutes.

3. RESULTS

3.1 REGULATION OF CIZ1 STABILITY BY CYCLIN DEPENDENT KINASE-MEDIATED PHOSPHORYLATION

3.1.1 Identification of phosphorylation sites responsible for protein stability

Since the data presented previously in Figure 5 suggests that Ciz1 is stabilised when phosphorylated by CDK, it was decided to investigate which sites within the protein are phosphorylated that are responsible for this stabilisation. ECiz1 (embryonic Ciz1) has fourteen phosphorylation sites as illustrated in Figure 6, half of which are contained within the active-replication fragment Ciz1-N471 as identified by Copeland et al. (2010b). One method of testing each individual putative CDK-phosphorylation site is using phosphomimetic mutants of Ciz1.

Phosphomimetic mutants have an acidic residue that is introduced at putative CDK-phosphorylation sites that mimic the negative charge introduced by phosphorylation at these sites. Analyses of such mutants have been used in many studies to investigate the role of phosphorylation in protein function. Aspartate as a phosphomimetic amino acid and alanine as a non-phosphorylatable amino acid are commonly used (Lamia et al., 2009, Gu et al., 2009, Copeland et al., 2015). Using these phosphomimetic mutants, the aim was to determine whether Ciz1 could be stabilised; that is protected from poly-ubiquitylation and proteasomal degradation after inhibition of CDK activity. Mutant Ciz1 proteins could be assayed after addition of a CDK inhibitor in the presence and absence of a proteasomal inhibitor in order to identify which, if any, sites contributed to protein stability. If phosphorylation of a certain site does contribute to protein stability, inhibition of CDK activity should not have any, or have little, effect on protein levels as opposed to decreased protein levels when that site is not phosphorylated. These phosphomimetic mutants would be created by designing

primers followed by whole plasmid mutagenesis by PCR to introduce the desired mutations followed by DNA sequencing (Eurofins Genomics) to verify the presence of these mutations.

No 3D structure of Ciz1 has been determined yet so establishing which of these putative CDK-phosphorylation sites are the most likely candidates for being phosphorylated by CDKs and increasing protein stability by observing whether sites are easily accessible to CDKs in the first place is not possible. However, previous studies have revealed four sites that are phosphorylated by CDKs: T144, T192, T293 and S331 (Copeland et al., 2015). Functions of these phosphorylation events have been established for the first three sites but not the fourth. It is therefore possible that phosphorylation of S331 could lead to increased protein stability. A putative destruction box, denoted by the sequence 'RXXL' was also identified. Therefore, putative CDK-phosphorylation sites situated closest to the D-box in the primary sequence are also of particular interest as it is possible that if these sites are phosphorylated, a physical block could be put into place as a consequence such that an E3 ligase could not actually bind to the D-box, thus preventing ubiquitylation from occurring.

Several proteomic analyses of post-translational modifications have revealed other phosphorylated sites within Ciz1 in several species including humans and mice (Sharma et al., 2014, Mertins et al., 2013). Identification of these sites within ECiz1 that are equivalent to those in Ciz1 in other species as well as humans would also be sites of interest.

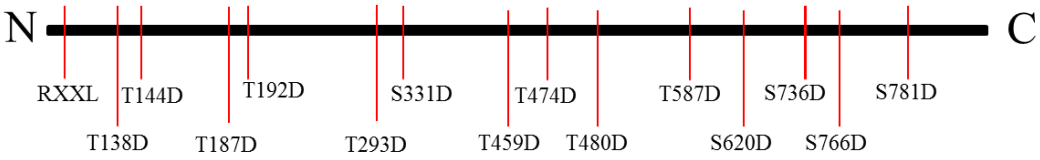

Figure 6: Identification of putative CDK phosphorylation sites and creation of phosphomimetic mutants
Diagram of the full-length Ciz1 protein and location of each putative CDK phosphorylation site identified for the creation of the phosphomimetic mutants.

3.1.2 Optimising conditions and drug concentrations for Ciz1-phosphomimetic mutant stability assays

In order to use these phosphomimetic mutants, an assay first needed to be set up that would allow conditions to be changed in an attempt to destabilise the Ciz1 protein. All experiments using Ciz1 constructs were ECiz1 forms and were set up such that both endogenous Ciz1 protein and transfected GFP-Ciz1 constructs were tested. Cells were harvested four hours post-drug treatments and, if transfected, 16-24 hours post-transfection. A range of drug concentrations were used. The CDK inhibitor roscovitine was used at final concentrations between 0.9µM and 100µM whereas the proteasomal inhibitor MG132 was used at a final concentration of either 1µM or 10µM. All experiments were conducted using asynchronous populations of cells.

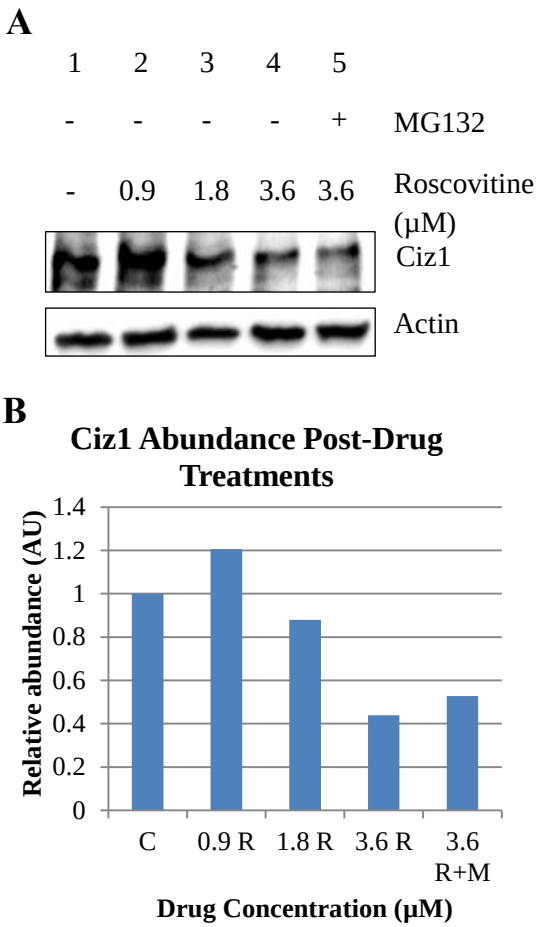

Figure 7: Treating cells with 0.9μM-3.6μM Roscovitine and 1μM MG132.
Cells were treated with 0.9-3.6uM roscovitine and 1uM MG132 as indicated. Cells were harvested four hours post-drug treatments and samples were used to perform western blots. Total protein fractions were used. **(A)** Western blot showing endogenous Ciz1 levels following drug treatments. Actin was used as a loading control. **(B)** Densitometry of the bands shown in (A) was performed in order to quantify Ciz1 levels. The histogram shows Ciz1 levels when quantified relative to actin.

Roscovitine is generally used at concentrations between 10μM and 50μM (Alessi et al., 1998, Planchais et al., 1997, Kang et al., 2011, Hahntow et al., 2004). Roscovitine is mainly used to observe effects of inhibiting CDK1/2 phosphorylation; although a study into roscovitine itself revealed that this drug is only effective against certain kinases and to varying degrees (Bach et al., 2005). A study performed by Meijer et al. (1997) revealed that roscovitine inhibits cyclin E-CDK2 and cyclin A-CDK2; with IC_{50} values of 0.7μM for both. Roscovitine also inhibits CDKs 1, 5 and 7. It does not

however, inhibit cyclin D-CDK4/6. However, since lower and higher drug concentrations have also been used, a range of concentrations were tested.

The lowest concentrations tested started with a concentration of 0.9µM (Fig. 7), with 1.8µM and 3.6µM also tested to observe whether any effects that occurred were concentration-dependent. The western blot showing drug effects on endogenous Ciz1 (Fig. 7A) indicates no significant change in protein levels as would be expected when compared to previous results presented in Figure 5. The accompanying histogram shows that although Ciz1 levels are not constant, changes do occur. However, as can be seen in Figure 7B, at 0.9µM (lane 2), endogenous Ciz1 levels appear to increase relative to the controls whereas the higher concentrations (lanes 3 and 4) do cause Ciz1 levels to decrease, with a slight recovery with addition of MG132 (lane 5), although this is not immediately evident in the western blot (Fig. 7A).

It was reasoned that if the correct conditions could be determined in order to test the stability of each of the fourteen phosphomimetic mutants, drug concentrations required would need to be ideal for affecting transfected Ciz1 protein levels. As small changes in endogenous protein expression were observed when cells were treated with 1.8uM and 3.6uM roscovitine, similar changes in exogenous Ciz1 protein expression were expected to be observed at slightly higher drug concentrations. This was determined by taking into account not only higher levels of the protein of interest after transfection of cells with the Ciz1 construct, but also the desire to observe a greater change in protein expression, if indeed one was present. The following concentrations of roscovitine tested therefore were 9.9µM, 19.7µM and 39.5µM on cells transfected with WT-GFP-Ciz1. However, no visible difference is seen in GFP-WT-Ciz1 protein levels in the western blot (Fig. 8A) and quantifications again show that GFP-WT-Ciz1

levels are not altered as expected, instead appearing to increase slightly at higher drug concentrations (lanes 3 and 4, Fig. 8B).

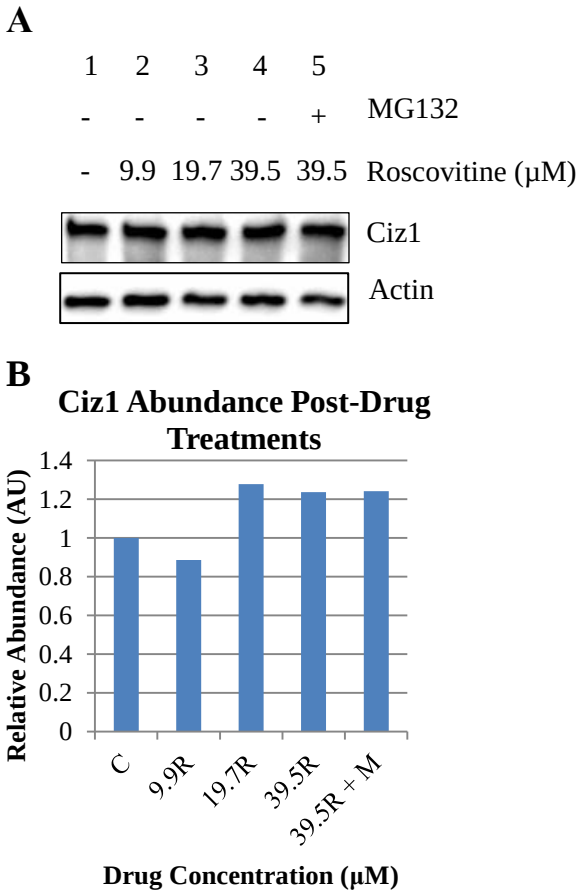

Figure 8: Treating cells with 9.9µM-39.5µM Roscovitine and 10µM MG132. Cells were transfected with WT-GFP-Ciz1 twenty hours prior to drug treatments and were treated with 9.9-39.5uM roscovitine and 10uM MG132 as indicated. Cells were harvested four hours post-drug treatments and total protein fractions were used to perform western blots. **(A)** Western blot showing transfected GFP-WT-Ciz1 levels following drug treatments. Actin was used as a loading control. **(B)** Densitometry of the bands shown in (A) was performed in order to quantify Ciz1 levels. The histogram shows Ciz1 levels when quantified relative to actin.

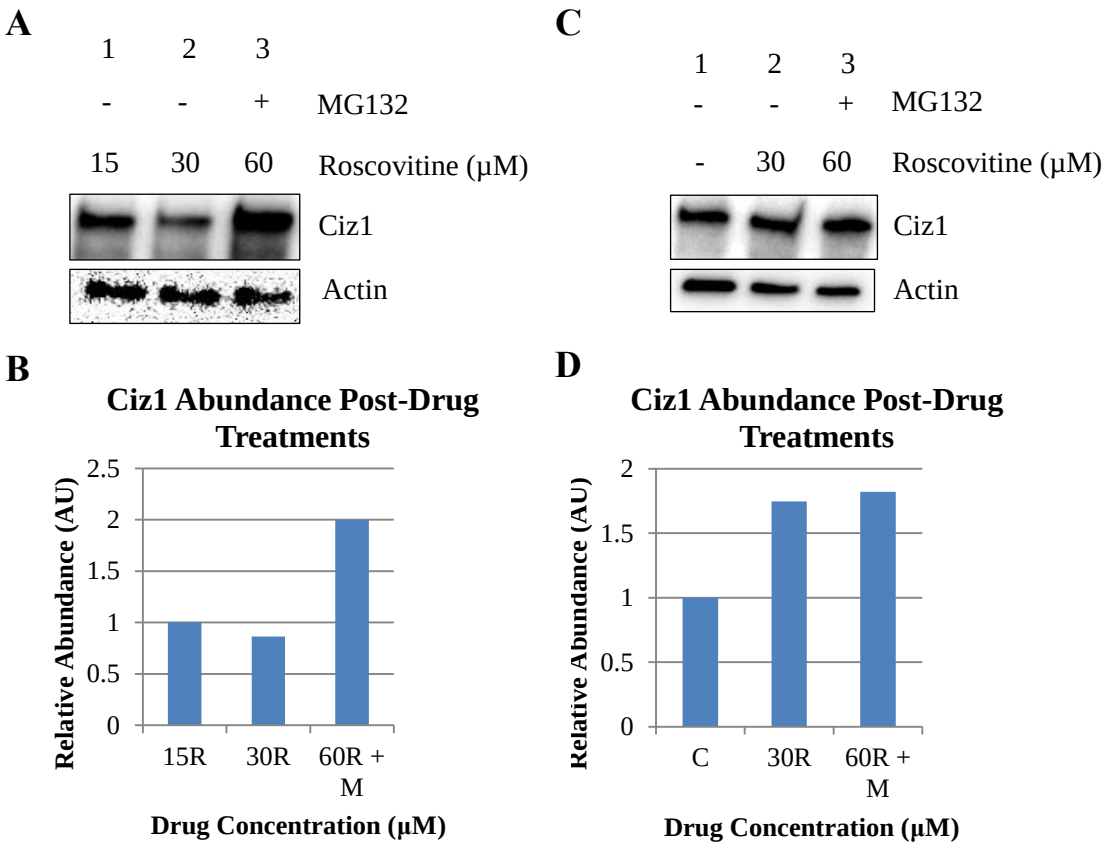

Figure 9: Treating cells with 15µM-60µM Roscovitine and 1µM MG132.
Cells were transfected with WT-GFP-Ciz1 and treated twenty hours later with 15-60uM roscovitine and 1uM MG132 as indicated. Cells were harvested four hours post-drug treatments and total protein fractions were used to perform western blots. Actin was used as a loading control. **(A)** Western blot showing transfected GFP-WT-Ciz1 levels following drug treatments. **(B)** The histogram of Ciz1 protein levels according to the western blot shown in (A). **(C)** Western blot showing transfected GFP-WT-Ciz1 levels following drug treatments. **(D)** The histogram of Ciz1 protein levels according to the western blot shown in (C).

The next highest concentrations of roscovitine tested were 15µM, 30µM and 60µM. The first time this experiment was performed, protein levels in the control sample were too low to detect. However, the western blot (Fig. 9A) did show visibly altered GFP-WT-Ciz1 protein levels as expected, which was confirmed following quantification (Fig. 9B). Unfortunately, when this experiment was repeated (Figs. 9C and D), GFP-WT-Ciz1 levels increased with addition of 30µM (lane 2) of roscovitine and continued to increase slightly with addition of MG132 (lane 3). This highlights the irreproducibility of results obtained. Using the approach of phosphomimetic

mutants requires a robust assay to determine the role for each phosphorylation site, which has not been achieved here with drug concentrations tested so far.

The highest concentration of roscovitine tested was 100μM. Effects of treatment with roscovitine at this concentration on GFP-WT-Ciz1 levels are different when comparing the total (Figs. 10A and B) and chromatin (Figs. 10C and D) fractions. The western blots do not show any significant changes in Ciz1 levels and quantifications indicate that in the total protein fraction, Ciz1 levels increase with increasing concentrations of roscovitine (lanes 2 and 3) and increase further with addition of MG132 (lane 4) whereas with the chromatin fraction, Ciz1 levels do drop with the addition of 100μM roscovitine (lane 3) compared to control levels but addition of MG132 (lane 4) does not lead to much recovery of Ciz1.

However, when observing GFP-Ciz1 levels in the presence of the proteasomal inhibitor MG132 in all experiments performed here, there appears to be a repeated increase of Ciz1 levels. This suggests that Ciz1 degradation is mediated by the ubiquitin proteasome system.

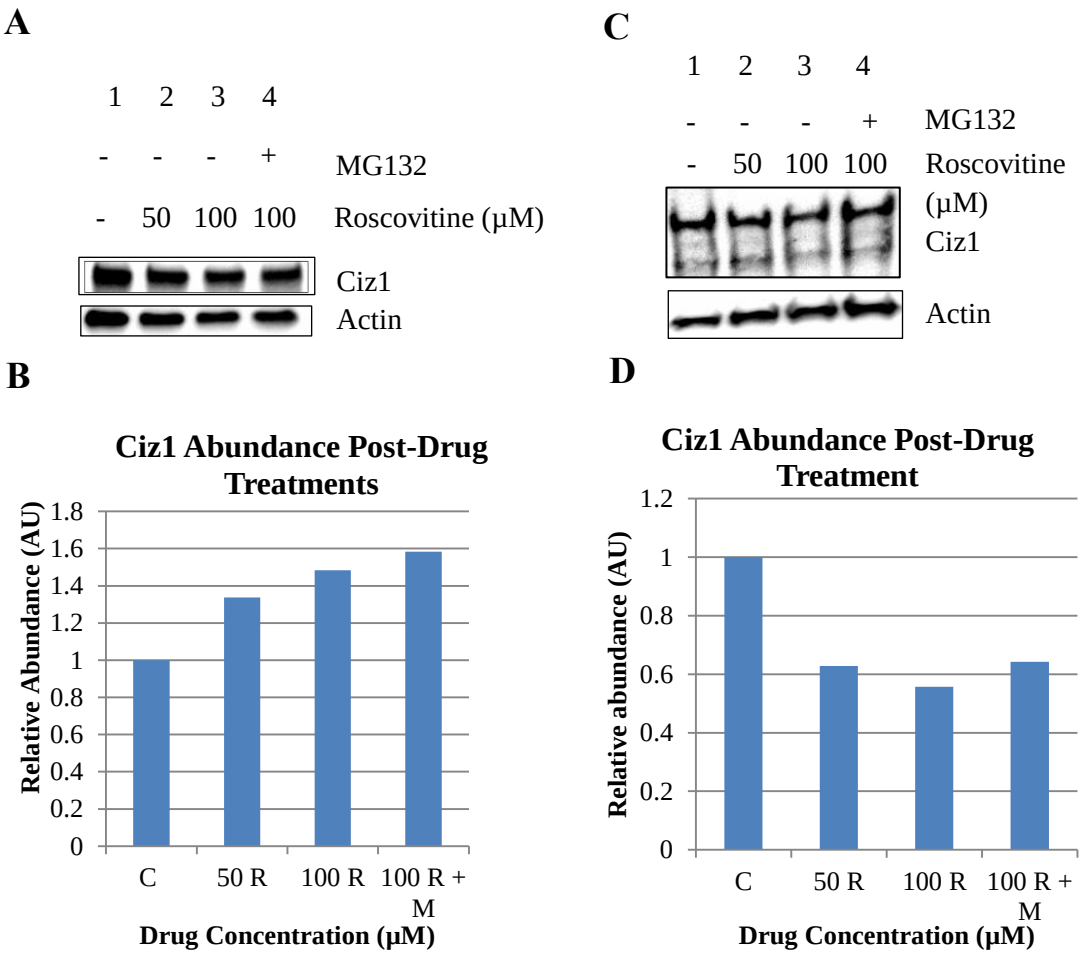

Figure 10: Treating cells with 50µM-100µM Roscovitine and 10µM MG132: observing GFP-WT-Ciz1
The accompanying histograms show quantified levels of Ciz1 protein relative to actin. **(A)** Western blot showing Ciz1 levels following drug treatments as indicated. This blot shows the total protein fraction. **(B)** The histogram of Ciz1 protein levels according to the western blot shown in (A). **(C)** Western blot showing Ciz1 levels following the same drug treatments as in (A). This blot shows the chromatin fraction. **(D)** The histogram of Ciz1 protein levels according to the western blot shown in (C).

3.1.3 Observing effects of Cyclin A knockdown on Ciz1 protein stability

Since it has also previously been shown that depletion of cyclin A affects Ciz1 protein levels in a manner similar to that of addition of a CDK inhibitor (Fig. 6) (Copeland, unpublished data); this approach was also tested in both synchronous (Fig. 11) and asynchronous populations of cells (Fig. 12). These experiments were performed as an attempt at an alternative method to chemiclly inhibiting CDK activity in order to destabilise the Ciz1 protein. It has recently been shown that cyclin A-CDK2 can

phosphorylate Ciz1 (Copeland et al., 2015); therefore by causing a depletion of cyclin A, phosphorylation of Ciz1 by this cyclin-CDK complex should no longer occur. Cells were synchronised (Fig. 11A) by contact inhibition and serum starvation for 48 hours, followed by release into the cell cycle once again, at which point transfection also occurred. Protein and RNA samples were harvested 24 hours post-release.

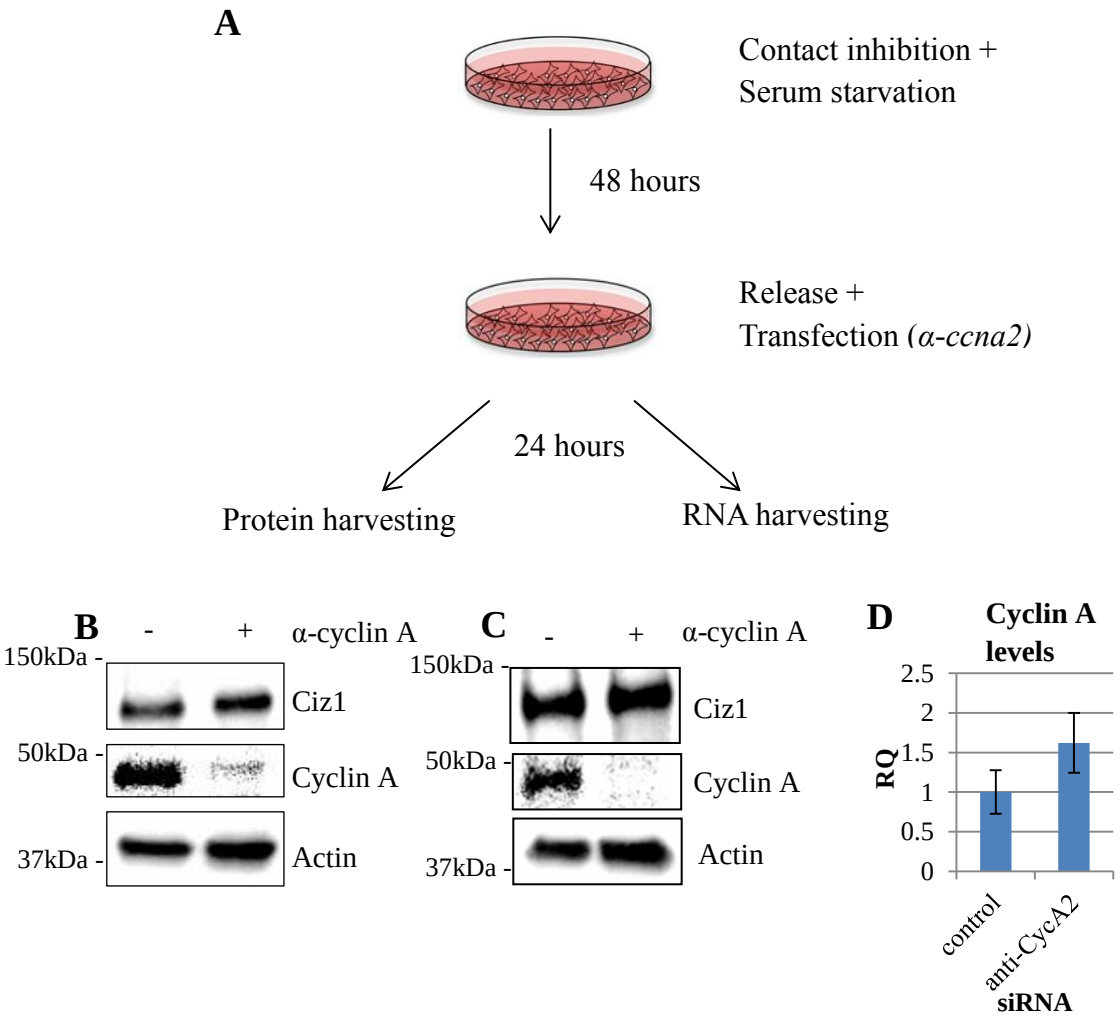

Figure 11: Effects of Cyclin A knockdown on Ciz1 protein levels in a synchronised population of cells
Western blots show levels of Ciz1 following cyclin A knockdown as indicated. MG132 was added at a final concentration of 10μM as indicated. Both proteins and RNA were harvested 24 hours post-transfection and four hours after drug-treatments. **(A)** Experimental design showing how cells are synchronised to G_0 then re-entered into the cell cycle and transfected with *α-ccna2* siRNA, followed by protein and RNA harvesting. **(B)** Cyclin A knockdown performed in a synchronised cell population; showing endogenous Ciz1 in the total protein fraction. **(C)** The chromatin fraction of the experiment shown in (A). **(D)** qPCR results showing levels of Cyclin A2.

As can be seen in Figure 11, cyclin A protein levels are significantly reduced in the synchronous cell populations. However, qPCR results show that levels of cyclin A2 RNA are actually increased following transfection with *α-ccna2* siRNA (Fig. 11D), and it appears that Ciz1 levels are not significantly affected (Figs. 11B and C).

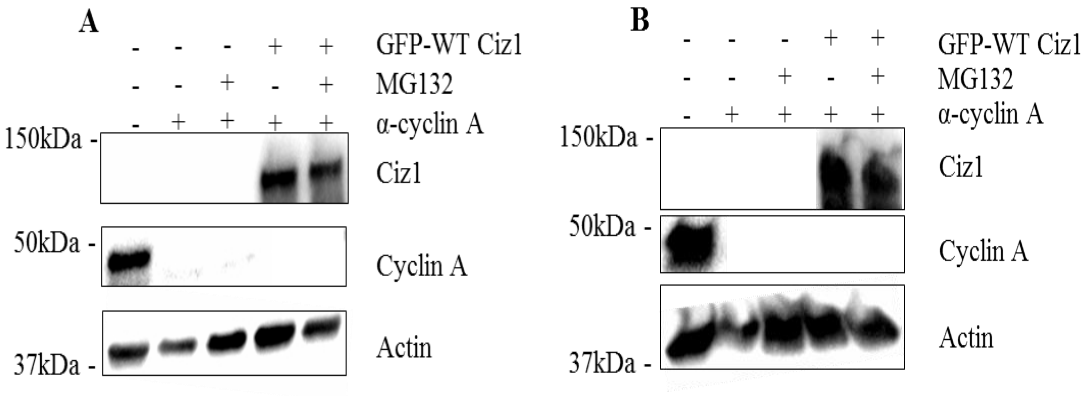

Figure 12: Effects of Cyclin A knockdown on Ciz1 protein levels in an asynchronous population of cells
Western blots show levels of Ciz1 following cyclin A knockdown as indicated. MG132 was added at a final concentration of 10μM as indicated. Proteins were harvested 24 hours post-transfection and four hours after drug-treatments. **(A)** Cyclin A knockdown performed in an asynchronous cell population; showing both endogenous and transfected GFP-WT-Ciz1 levels in the total protein fraction as indicated. **(B)** This blot shows the chromatin fraction of the experiment outlined in (A).

This can also be observed in the asynchronous cell populations (Figs. 12A and B) where GFP-WT-Ciz1 was co-transfected with the *α-ccna2* siRNA. This experiment also revealed that inhibiton of the ubiquitin proteasome system did not affect Ciz1 protein levels either. Endogenous Ciz1 protein was not detected in this experiment. The results presented in Figures 11 and 12 suggest that, contrary to previous data shown in Figure 5, absence of cyclin A does not affect Ciz1 protein stability. However, with an increase in cyclin A2 RNA levels in the synchronised cell population despite the decreased protein levels, it is possible that there was still enough cyclin A such that Ciz1 levels were not significantly affected. It is also important to note that the experimental results presented in Figure 11 requires

repeating due to a small sample size and a method of determining cell cycle status such as by EdU incorporation to determine S phase entry.

3.1.4 Discussion

Phosphorylation of certain proteins involved in regulating the cell cycle contributes to increased protein. This occurs due to the phosphorylation event preventing the specific E3 ligase from ubiquitylating its substrate, thus preventing it from being targeted by the 26S proteasome for degradation. This results in the levels of this protein being allowed to increase. Ciz1 has previously been shown to be phosphorylated at four distinct sites by cyclin A-CDK2. Phosphorylation of three of these sites leads to an inability of Ciz1 to bind cyclin A-CDK2; however a function of the phosphorylation event at the fourth site, S331, has not been attributed (Copeland et al., 2015). Since preliminary results shown in Figure 5 suggest that Ciz1 is degraded by the ubiquitin proteasome system (UPS), as evidenced by the fact that in the presence of the 26S proteasome chemical inhibitor MG132, Ciz1 protein levels are increased; and taking into account that many proteins degraded by this system are phosphorylated, causing them to be either marked for or protected from degradation (Mailand and Diffley, 2005, Fukushima et al., 2013); further investigation was required in order to determine whether Ciz1 is indeed stabilised by phosphorylation and if so, which sites are responsible for this stabilisation.

The identification of a putative destruction box within the primary sequence of Ciz1, found within many targets of the UPS, supported the preliminary findings shown in Figure 5 that suggested that Ciz1 is degraded by this system. Results presented here in Figures 7-10 further support this; as in the presence of a chemical inhibitor of the 26S proteasome MG132, Ciz1 levels consistently increase. Considering the fact that all

evidence presented to date shows that Ciz1 plays a role in regulating cell cycle progression (Coverley et al., 2005, Copeland et al., 2010a, Copeland et al., 2015), it seems logical that Ciz1 is itself partly regulated by the UPS as this system is largely responsible for the removal of other proteins involved in regulating the cell cycle at specific stages and is itself also tightly regulated (section 1.3).

Results presented here also support the preliminary findings shown in Figure 5 with regards to a link between Ciz1 and CDK activity. Figure 7 reveals that in the presence of 1.8uM and 3.6uM roscovitine, a chemical inhibitor of CDK activity, Ciz1 levels drop when compared to the control (lanes 3 and 4 respectively). As Ciz1 has previously been shown to be phosphorylated by cyclin A-CDK2 (Copeland et al., 2015) and inhibition of the proteasome results in a partial recovery of Ciz1 levels (lane 5, Figure 7), these results suggest that Ciz1 is phosphorylated by CDK activity and that this phosphorylation leads to increased protein stability. This observation, together with the identification of the putative destruction box, suggest that Ciz1 is a target of the APC/C E3 ligase since many other such targets also have a destruction box and phosphorylation at certain sites leads to increased protein stability (sections 1.2 and 1.3).

Having decided to create plasmids containing phosphomimetic mutants of Ciz1 in order to attempt to identify which site(s) within Ciz1 contribute(s) to increased protein stability when phosphorylated, it was unfortunate that in attempting to identify the correct conditions and drug concentrations required to destabilise the wild type form of the Ciz1 protein as previously observed (Fig. 5), a major problem was encountered. We were unable to reproduce the destabilisation of ectopically expressed GFP-Ciz1 under a wide range of roscovitine concentrations (0.9µM-100µM). Most drug concentrations of roscovitine were tested at least twice in separate experiments.

Multiple sets of results for the same drug concentrations show that even under the same conditions, results obtained the second time sometimes showed what seemed to be the opposite of results obtained the first time the experiment was performed. The levels of recombinant Ciz1 protein found after transfection were considerably higher than the endogenous protein, which may have masked the effect of loss of Ciz1 levels.

An inability to acquire reproducible results, whether or not they agreed with those previously observed (Fig. 5), led to a need to identify a different method that could be used to destabilise Ciz1 protein levels in order to study the effects of the phosphomimetic mutants on protein stability. Having previously observed that similar results were obtained following cyclin A knockdown, it was decided to attempt destabilisation using siRNAs instead of by chemical means since a possible explanation for not getting reproducible results is that the drugs used were causing side-effects previously not observed that led to the seemingly random changes in Ciz1 protein levels at times. Sychronised cell experiments were used because there may be a cell cycle dependence for Ciz1 stability (Figs. 5A and C).

Unfortunately, cyclin A knockdowns using *α-ccna2* siRNA in both synchronous and asynchronous populations of cells also proved not to show the desired effects on Ciz1 protein levels. However, this observation in the synchronised population of cells is slightly less clear as to the success of the cyclin A knockdown. This is because in the western blot (Figs. 11B and C), cyclin A protein levels have clearly decreased significantly. On the other hand, cyclin A transcript levels following qPCR suggest that cyclin A knockdown was not successful, which could explain why Ciz1 protein levels do not appear to have decreased as expected. The discrepancy between cyclin A transcript levels and cyclin A protein levels could be due to a number of factors. Since this experiment involved using a synchronised population of cells, a possible

explanation could be that cells were not properly synchronised, thus affecting protein levels and transcript levels differently. Considering that cyclin A knockdown was also performed in an asynchronous population of cells and cyclin A protein levels were successfully reduced but Ciz1 protein levels were unaffected, the failure to synchronise the cells is a possible explanation. Another possible explanation of course could be an experimental error, during the qPCR or preparation of the RNA samples, rather than analysis of the protein samples by western blot. To further analyse the reason behind the observed unaffected Ciz1 levels when cyclin A is knocked down in a synchronised population of cells, this experiment would have to be repeated and a method to observe cell cycle state, such as EdU labelling, would also have to be used. The lack of EdU labelling in this experiment makes the degree of synchronisation impossible to determine. Another attempt at performing a cyclin A knock-down and observing the effect on endogenous Ciz1 protein levels would also be performed.

The inability to produce a method allowing the investigation of the role of phosphorylation of specific sites within Ciz1 to occur using phosphomimetic mutants as described meant that it was not possible to identify which site(s) within Ciz1 is/are phosphorylated by CDK activity leading to increased protein stability, as was planned. However, results obtained did consistently suggest that Ciz1 is a substrate of the UPS.

3.2 IDENTIFYING CIZ1 AS A TARGET OF THE UBIQUITIN PROTEASOME SYSTEM

In section 3.1, treating cells with the chemical proteasome inhibitor MG132 consistenly resulted in increased levels of Ciz1 protein as shown in western blots (Figs. 7-10 in the last lanes). These results supported the preliminary findings shown in Figure 5 (Copeland, unpublished data) and suggest that Ciz1 is degraded by the ubiquitin proteasome system (UPS). This suggestion is supported by the observation made also in section 3.1 that Ciz1 has a putative destruction box as part of its primary sequence. This sequence is frequently found in targets of one othe E3 ligases that forms part of this system. E3 ligases attach ubiquitin monomers to their targets as described in section 1.2, leading to the formation of poly-ubiquitin chains; thus targetting the substrate to the 26S proteasome for degradation.

In order to determine whether or not Ciz1 is indeed a target of the UPS, it would first be useful to investigate if Ciz1 is poly-ubiquitylated. Multiple methods have been described to perform this determination including immunoprecipitation of the protein of interest after transfection with a plasmid containing ubiquitin and a tag such as haemaglutinin (HA) as well as transfection with a plasmid containing His-tagged ubiquitin followed by immobilisation with Ni^{2+}-NTA. In the latter method, no immune complex is formed eliminating the need for antibodies at multiple stages and instead, simply when running samples for observation by western blot. In this case, the His tag binds directly to the Ni^{2+}-NTA residue (Kirkpatrick et al., 2005) whereas in immunoprecipitation experiments, proteins bind to the protein A/G agarose resin via the antibodies.

3.2.1 Ubiquitylation of Ciz1

Analysis of the amino acid sequence of Ciz1 in *Mus musculus* revealed the presence of 37 lysine residues (Fig. 13) as well as a putative D-box.

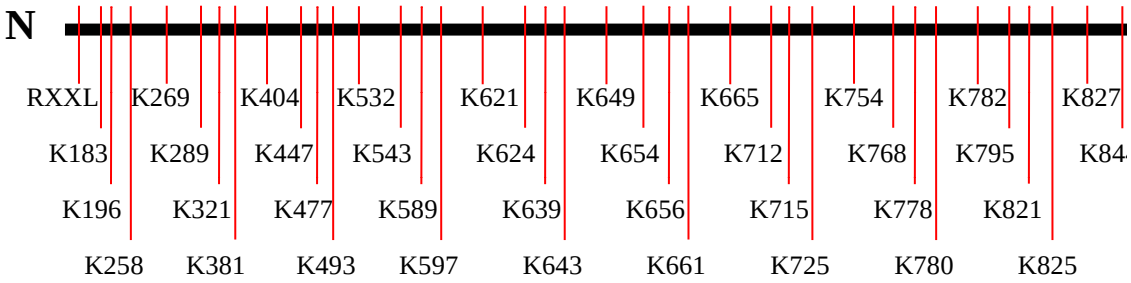

Figure 13: Identification of putative ubiquitylation sites in Ciz1
Representation of all lysine residues located within the murine form of Ciz1, denoting putative ubiquitylation sites. A putative destruction box was also identified.

Due to the large number of putative ubiquitylation sites within the Ciz1 protein, it was not feasible to mutate each individual site to create GFP-Ciz1 mutants. Ubiquitylation was therefore monitored in endogenous Ciz1 to first assess whether Ciz1 is indeed ubiquitylated.

3.2.2 Identifying soluble pools containing Ciz1 protein

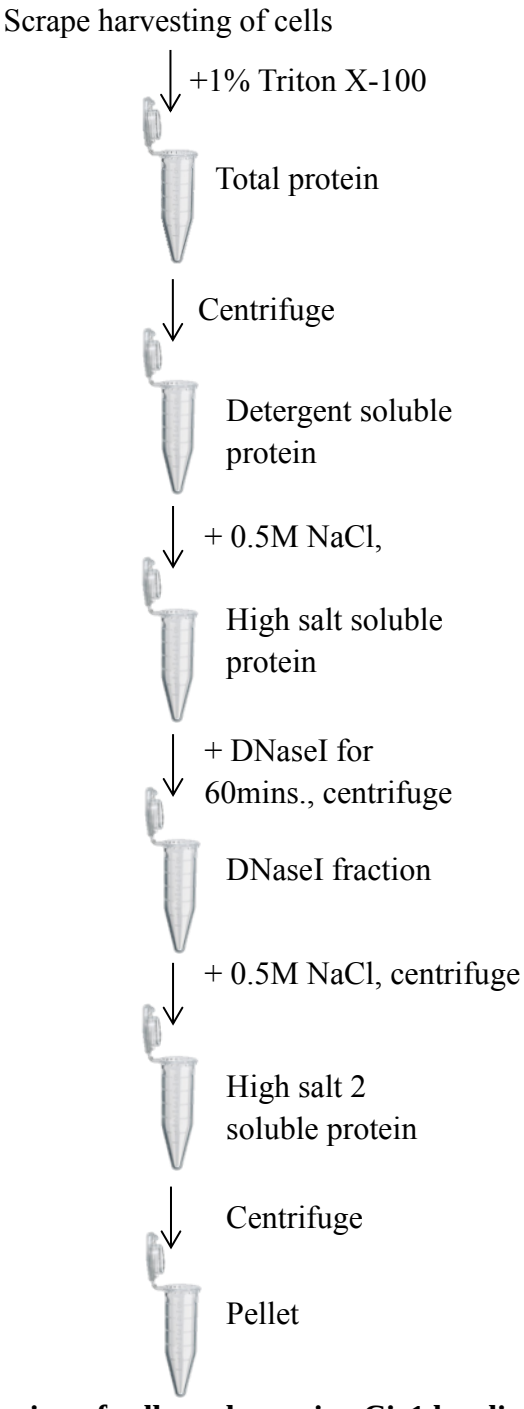

Figure 14: Fractionation of cells to determine Ciz1 localisation
Differential cellular fractionations was performed by treating cells with final concentrations of 1% Triton X-100, 0.5M NaCl and 1x DNaseI (diluted in 1x DNaseI buffer). Between each step, samples were centrifuged. After treatment with DNaseI, centrifugation occurred at 17 000xg. Prior centrifugations occurred at 10 000xg. An aliquot of the supernatant was removed for analysis and the remaining supernatant was removed. A similar method was used to prepare fractionated cells for analysis by immunofluorescence.

To perform investigations into ubiquitylation status of Ciz1, it was first necessary to identify if there were soluble pools of Ciz1 within cell extracts. Ciz1 is a protein that is integral to the nuclear matrix, a cellular fraction that resists high salt and nuclease treatment (Ainscough et al., 2007). Using cellular fractionation (Fig. 14), western blotting was used to identify whether soluble Ciz1 could be obtained for both endogenous Ciz1 and over-expressed recombinant Ciz1. Results show that localisation of the transfected GFP-WT-Ciz1 (Fig. 15B) is identical to the distribution of the endogenous protein (Fig. 15A). Both endogenous and exogenous Ciz1 localise predominantly to the nuclear matrix and could therefore be used in further studies such as observing the effects of mutants on localisation. The Ciz1 protein was found to be soluble in detergent and high salt fractions. These results concur with those previously obtained by Ainscough et al. (2007) who fractionated cells in a similar manner and found that Ciz1 associated with the nuclear matrix co-localised with newly synthesised DNA during the S phase.

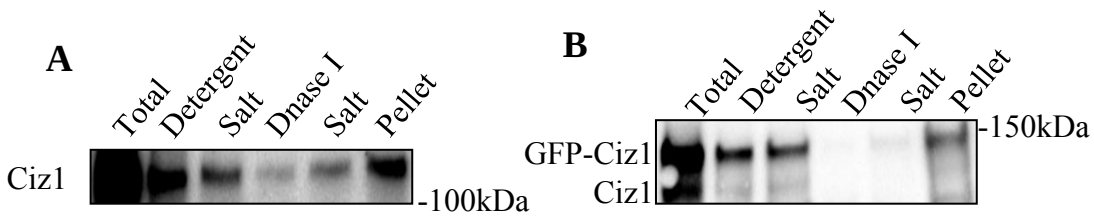

Figure 15: Identification of Ciz1 localisation
(A) Soluble protein pools following cell fractionation (see Figure 14) showing endogenous Ciz1. The detergent used was 1% Triton X-100 and the salt was 0.5M NaCl. **(B)** Soluble protein pools following fractionation showing both transfected GFP-WT-Ciz1 and endogenous Ciz1 can be found in the same soluble pools previously identified in (A).

3.2.3 Determining whether Ciz1 is ubiquitylated

Having identified the soluble pools in which the Ciz1 protein can be found, it was possible to perform experiments with Ciz1 and ubiquitin. Considering the multiple possible methods of determining whether Ciz1 is ubiquitylated (section 3.2). the following experiments were performed using His-tagged ubiquitin followed by immobilisation with Ni^{2+}-NTA, thus eliminating the need to use antibodies at multiple stages to form immune complexes and indirectly capturing proteins via these antibodies.

These experiments involved both transfection with His-Ub to detect endogenous Ciz1 and co-transfection with GFP-WT-Ciz1 and His-Ub. For these experiments, two soluble pools of protein were used for the initial experiments: the detergent soluble (referred to as the low salt extract) and the high salt soluble pools. This was performed in order to observe whether there might be a difference in ubiquitylation events of Ciz1 between separate cellular compartments. Effects of addition of the proteasomal inhibitor MG132 were also tested. The results obtained from the low salt extracts, largely containing cytoplasmic proteins, of cells with only endogenous Ciz1 protein are shown in Figure 16.

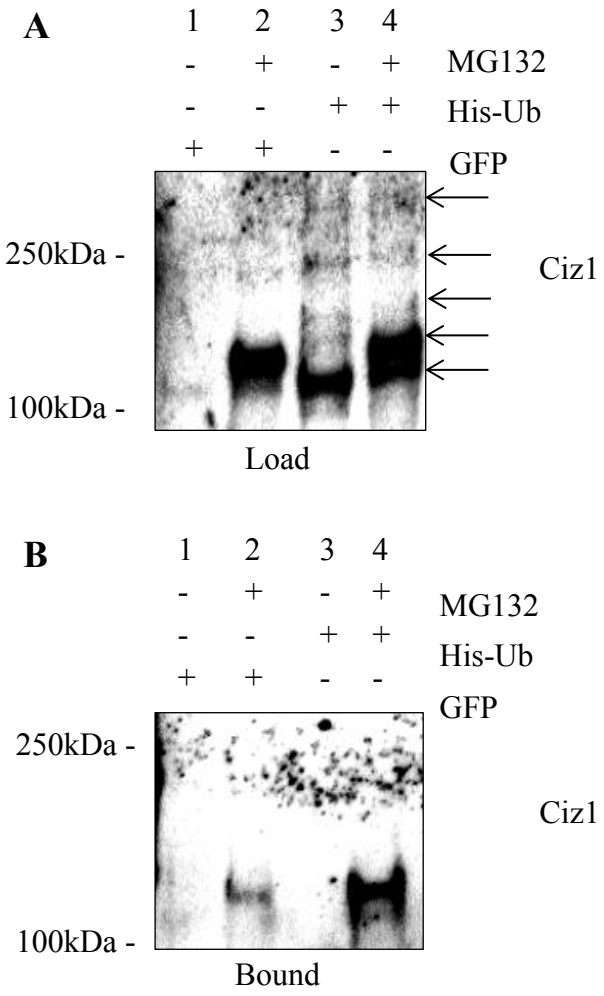

Figure 16: Determining ubiquitylation status of endogenous Ciz1 in the low salt fraction

Cells were transfected with His-Ub or GFP as indicated, 24 hours prior to harvesting. MG132 was added at a concentration of 10μM as indicated four hours prior to harvesting. The low salt cellular extract was applied to Ni^{2+}-NTA resin and allowed to bind. **(A)** Protein load for identifying endogenous Ciz1. **(B)** Ciz1 following Ni^{2+}-NTA immobilisation of the extract shown in (A).

In Figure 16A, low salt extracts of samples are shown before binding to the Ni^{2+}-NTA resin. It is immediately apparent that a difference exists between samples treated with MG132 (lanes 2 and 4) and those that were not (lanes 1 and 3). In the samples with no His-Ub but treated with MG132 (lane 2), a dark band appears at a slightly higher molecular weight to that of the darkest band in lane 3, containing the sample transfected with His-Ub but not treated with MG132. Interestingly, in the sample transfected with His-Ub and treated with MG132 (lane 4), there are two distinct bands corresponding to each band in the previous two samples. It should also be noted that

in lanes 3 and 4, there are multiple faint bands at higher molecular weights (see arrows) that are visible in both lanes. The detection of higher laddered molecular weight Ciz1 protein when transfected with His-Ub (lanes 3 and 4) is attributed to poly-ubiquitylation (Bloom and Pagano, 2005). After binding to the Ni^{2+}-NTA, shown in Figure 16B, Ciz1 is only detected in samples treated with MG132 (lanes 2 and 4), with a significantly more prominent band in lane 4 containing the sample that had also been transfected with His-Ub. The observation that a small amount of Ciz1 is present after binding to Ni^{2+}-NTA when no His-Ub is present in lane 2, is attributable to the fact that Ciz1 has three zinc fingers (Mitsui et al., 1999) that are capable of binding to the resin (Hanas et al., 2005). Addition of MG132 appears to have an effect on the ubiquitylation of endogenous Ciz1 as might be expected if Ciz1 is indeed a substrate of the 26S proteasome. This also suggests that there is a dependency on this chemical for the detection of ubiquitylation of this protein.

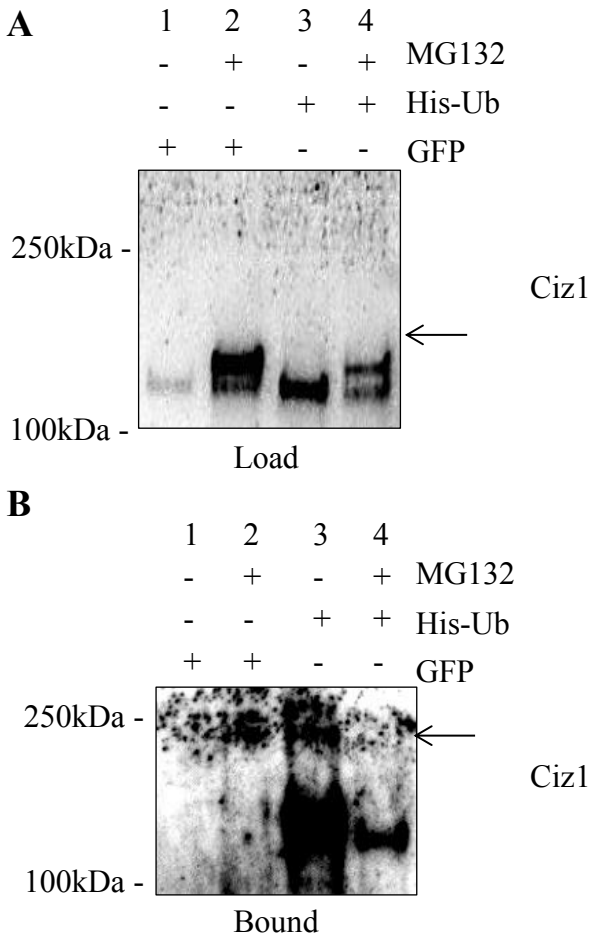

Figure 17: Determining ubiquitylation status of endogenous Ciz1 in the high salt fraction

Cells were transfected with GFP or His-Ub as indicated, 24 hours prior to harvesting. MG132 was added at a final concentration of 10μM as indicated, four hours prior to harvesting. The high salt cellular extract was applied to Ni^{2+}-NTA resin and allowed to bind. **(A)** Protein load for identifying endogenous Ciz1. **(B)** Ciz1 following Ni^{2+}-NTA immobilisation of the extract described in (A).

Figure 17 shows the high salt extracts of samples from the same experiment as that shown in Figure 16. In Figure 17A, which shows samples before binding to the Ni^{2+}-NTA, a similar banding pattern is observed in all lanes to that observed in Figure 16A. However, there is no apparent laddered higher molecular weight Ciz1 protein when transfected with His-Ub (lanes 3 and 4, Figure 17A) as there was in the corresponding samples in Figure 16A. It is important to consider the possibility that these higher molecular weight bands are simply below the limit of detection of the system. Interestingly, there is a marked difference between these samples after binding to the

Ni^{2+}-NTA resin (Fig. 17B) in lanes 3 and 4 when compared to the corresponding samples of the low salt extracts in Figure 16B. In lane 3 of Figure 16B it shows that in the absence of MG132, samples with His-Ub do not appear to bind to the Ni^{2+}-NTA resin, suggesting a dependency on this drug for detection of Ciz1 as mentioned previously. However, in lane 3 of Figure 17B it shows that with the corresponding high salt extract sample, a lot more Ciz1 is bound to the Ni^{2+}-NTA resin than when MG132 is present (lane 4). This suggests that the dependency on MG132 for detection observed in the low salt extract does not apply for the high salt extract; indeed it suggests the exact opposite.

3.2.4 Identifying a possible E3 ligase responsible for Ciz1 ubiquitylation: APC/C^{Cdh1}

The data presented above are consistent with the ubiquitylation of Ciz1. As Ciz1 has been shown to be active in the late G_1 to early S phases, the most obvious candidate for the E3 ligase responsible for Ciz1 ubiquitylation is APC/C^{Cdh1}; which is the principle E3 ligase responsible for the degradation of cyclins during the G_1 phase. Supporting this, Ciz1 contains a putative RXXL destruction box that is utilised by APC/C^{Cdh1} for substrate recognition (section 1.3). The presence of this putative D-box has been identified in multiple species, supporting the theory that this is a functional destruction box (Fig. 18).

As Cdh1 is the component of the APC/C^{Cdh1} complex responsible for binding targets, the following experiments to determine whether this complex is responsible for the ubiquitylation of Ciz1 were performed using Cdh1 alone. In order to test whether Cdh1 can actually bind Ciz1, GST-tagged Cdh1 and Ciz1 were produced. Immobilisation of the GST-Ciz1 or GST-Cdh1 were used for protein interaction assays. For these experiments, the N-terminal fragment of Ciz1 containing the

replication activity, termed N471, was used. A mutant of N471 was also produced where the consensus sequence 'RXXL' for the destruction box was mutated to 'AXXA' using whole plasmid mutagenesis. Success of this procedure was confirmed by DNA sequencing (Eurofins Genomics). Also, agarose gel electrophoresis was performed following DpnI digestion of the wild-type vector to confirm successful amplification of the plasmid.

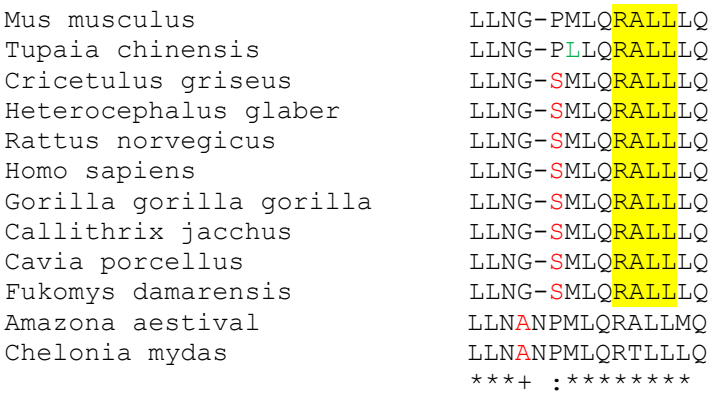

Figure 18: The D-box sequence in Ciz1 is highly conserved in ten species
BLAST searches of the N-terminal region of Ciz1 identified that the RXXL motif was conserved in mammalia. Primary sequence alignments were performed using Clustal (www.ebi.ac.uk).

Following DNA sequencing, plasmids containing a GST-tagged Ciz1 or GST-Cdh1 were transformed into BL-21 *E. coli* cells which were then grown to maximise protein production. The proteins of interest were then purified, followed by cleavage from the GST tag in some cases by 3C protease and protein-protein binding assays were set up.

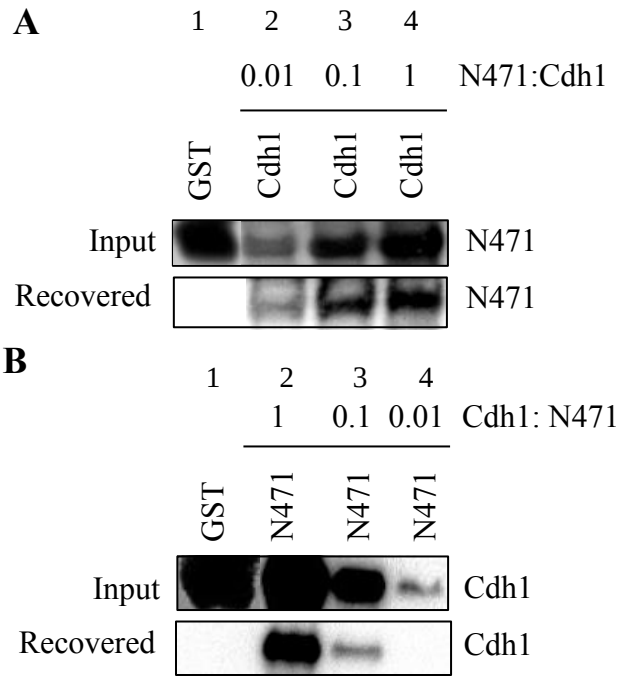

Figure 19: Protein-protein interaction studies between Cdh1 and WT-Ciz1-N471
Proteins were bound for an hour before washing. Samples were taken before (input) and after (recovered) binding, with GST used as a control for non-specific tag interactions. Three volumes of the soluble protein being bound were used. Samples were removed to show protein loads (upper panels). **(A)** GST-Cdh1 was immobilised and increasing amounts of Ciz1 added. Recovered Ciz1 bound to Cdh1 was found for all protein concentrations (lower panel). **(B)** Reactions were performed as for (A) except GST-Ciz1 was immobilised and increasing amounts of Cdh1 added. Recovered Cdh1 bound to Ciz1 was found for all protein concentrations (lower panel).

In an attempt to minimise false- positive and negative results; each experiment was performed in two ways. For example, Cdh1 was bound to immobilised N471 and N471 was bound to immobilised Cdh1 in parallel reciprocal experiments. Results shown in Figures 19A and B show that after binding, proteins of interest were recovered. This suggests that Ciz1 binds to Cdh1 and Cdh1 binds to Ciz1. Increasing volumes of N471 added show that this binding occurs in a concentration dependent manner (lanes 2-4, Fig. 19A). Decreasing volumes of Cdh1 added demonstrate this same phenomenon (lanes 2-4, Fig. 19B).

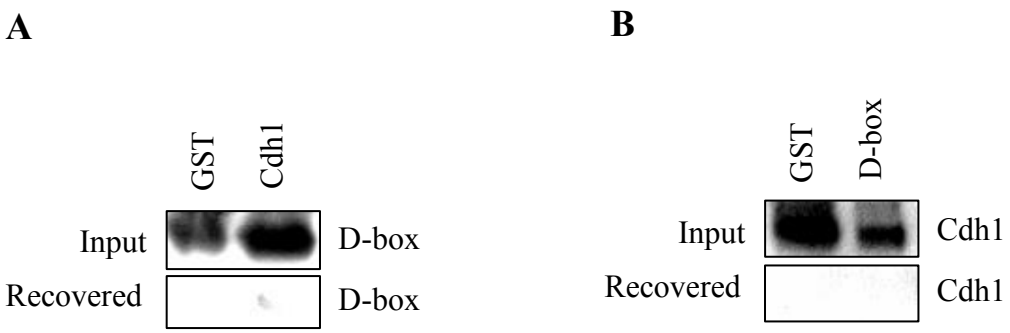

Figure 20: Protein-protein interaction studies between Cdh1 and N471-D-box
Proteins were bound for an hour before washing. Samples were taken before (input) and after (recovered) binding, with GST used as a control. Samples were removed to show protein loads (upper panels). **(A)** GST-Cdh1 was immobilised and Ciz1 was added. Ciz1 was not recovered after binding (lower panel). **(B)** Reactions were performed as for (A) except GST-D-box-Ciz1 was immobilised and Cdh1 added. Cdh1 was not recovered after binding (lower panel).

Having found that the putative destruction box within Ciz1, denoted by the 'RXXL' motif, is highly conserved (Fig. 18) and that results shown in Figure 19 suggest that Ciz1 is a target of the APC/C^{Cdh1} complex; it seems likely that Cdh1 binds to Ciz1 via this putative D-box. In order to investigate whether this is indeed the case, an N471-D-box protein mutant was created by whole plasmid mutagenesis and confirmed by DNA sequencing (Eurofins Genomics) followed by protein production using BL-21 *E. coli* cells as described previously. The experiment was set up in the same manner as that also described previously (Fig. 19). Results show that no binding occurs between Cdh1 and the D-box mutant (Figs. 20A and B).The results in Figures 19 and 20 suggest that Cdh1 and Ciz1 interact and that this interaction is mediated by the putative destruction box; supporting the hypothesis that APC/C^{Cdh1} is a viable candidate for being the E3 ligase responsible for ubiquitylating Ciz1. The fact that no binding occurs when the D-box is mutated is a strong indicator as this sequence is commonly found in substrates of this E3 ligase.

3.2.5 Discussion

One of the major systems used to degrade proteins involved in cell cycle regulation is the ubiquitin proteasome system which uses many proteins such as ubiquitin as a signaling system and E3 ligases to recognize substrates. Previous studies have observed that Ciz1 could be degraded by this system as addition of a proteasomal inhibitor MG132 resulted in recovery of Ciz1 protein levels (Fig. 5) (Copeland, unpublished data). This was also oobserved in this study (section 3.1). A quantitative proteomic survey of *in vivo* ubiquitylation sites by mass spectrometry identified a lysine residue at position 830 in human Ciz1 that was found to form an isopeptide bond with a glycine residue of ubiquitin (Wagner et al., 2011); identifying that Ciz1 is ubiquitylated. The work presented here supports this observation and due to detection of multiple bands detected in the His-ubiquitin pull-down assays suggest that Ciz1 is poly-ubiquitylated.

The use of His-Ub and Ni^{2+}-NTA immobilization to identify ubiquitylated proteins has been widely used (Kirkpatrick et al., 2005). The low salt fraction in these studies showed distinct bands of higher molecular weight than Ciz1 (Fig. 16A), creating a laddering effect in the samples seen previously with other polyubiquitylated proteins (Bloom and Pagano, 2005). Following Ni^{2+}-NTA immobilization, Ciz1 was only recovered in the presence of MG132. This suggests that there is some dependency on MG132 although the prominent laddering present in the absence of the proteasomal inhibitor prior to immobilization suggests otherwise. A small amount of Ciz1 was also recovered in the presence of this chemical in the absence of His-Ub. This is attributed to the fact that Ciz1 has three zinc fingers (Mitsui et al., 1999) which are capable of binding to Ni^{2+} (Hanas et al., 2005). This would also explain why Ciz1 was recovered in all the samples when cells were transfected with GFP-WT-Ciz1. Two dominant

bands were observed in the sample with addition of MG132 in the presence of His-Ub prior to Ni^{2+}-NTA immobilization which could indicate a dependency on MG132 and that the absence of recovered Ciz1 after immobilization when no proteasomal inhibitor is present could simply be due to lower levels of the protein that were undetectable when developing the western blot at the optimum exposure. Longer exposures resulted in the blot quickly becoming completely black such that no individual bands were visible.

In the high salt soluble pools, fewer bands of higher molecular weight were observed prior to Ni^{2+}-NTA immobilization although one such band was observed after immobilization in the sample where no MG132 was added. As with the low salt soluble samples, two distinct bands are observed with the addition of MG132, although only one band is observed in the absence of the chemical. This supports expectations that inhibition of the proteasome should result in increased levels of protein substrates, which in turn supports the theory that Ciz1 is a substrate of the ubiquitin proteasome system. These double bands could also indicate that high levels of Ciz1 protein are mono-ubiquitylated, which could be attributed to a function separate to that of marking for degradation (Hicke, 2001) since the latter requires substrates to be polyubiquitylated. However, after Ni^{2+}-NTA immobilization, a lot more Ciz1 was recovered in the absence of MG132 than in its presence unlike the recovery of the protein in the low salt soluble pool. This could indicate that there is a difference in Ciz1 regulation between separate cell compartments. However, this experiment would need to be repeated to confirm this observation, preferably using a slightly modified method to minimize binding of Ciz1 to the Ni^{2+}-NTA via its zinc fingers.

Considering that Ciz1 is known to function during the late G_1 phase and it has been shown here that Ciz1 is likely a substrate of APC/C^{Cdh1}; it is possible that the results obtained here suggesting that Ciz1 is poly-ubiquitylated are representative of Ciz1 poly-ubiquitylation to differing degrees by APC/C^{Cdh1}.

Having confirmed that Ciz1 is indeed ubiquitylated as suggested by previous experiments (Wagner et al., 2011) and the observation that inhibition of the proteasome resulted in increased protein levels (Fig. 5); identification of the possible E3 ligase responsible for this reaction was investigated. As it was previously observed that Ciz1 contains a destruction box sequence and the fact that Ciz1 is largely active during the G_1 and S phases, APC/C^{Cdh1} was considered as a possible candidate. Results obtained suggest that Cdh1 does bind to Ciz1 and that Ciz1 also binds to Cdh1. Both interactions occur in a concentration dependent manner. These interaction studies suggest that APC/C^{Cdh1} is the E3 ligase responsible for the ubiquitylation of Ciz1. This suggestion is supported by further *in vitro* protein-protein interaction studies between Cdh1 and a mutant form of Ciz1 where the putative destruction box had been mutated. No binding occurred between these two proteins; not only supporting the theory that the E3 ligase is APC/C^{Cdh1}; but also that the putative destruction box identified is also functional. Further experimentation is required to determine whether Ciz1 stability is affected by loss of this D-box *in vivo*.

Results presented here suggest that Ciz1 protein levels are regulated by ubiquitylation mediated by APC/C^{Cdh1} but this requires additional experimentation to confirm this *in vivo*. Experiments using His-Ub suggest that Ciz1 is poly-ubiquitylated; supporting the previous observation made in section 3.1 that inhibition of the 26S proteasome results in increased Ciz1 levels. This suggests that Ciz1 is degraded by the ubiquitin proteasome system. Using *in vitro* protein interaction studies, Cdh1 has been shown to

bind Ciz1, suggesting that Ciz1 ubiquitylation is mediated by Cdh1. This is supported by the evidence provided by further *in vitro* protein interaction studies using Cdh1 and Ciz1 with a mutated putative D-box. These demonstrated that in the absence of the RXXL sequence, binding no longer occurred between Ciz1 and Cdh1. This also suggests that the RXXL sequence, often used by APC/C^{Cdh1} to recognize its substrates, functions as a D-box in Ciz1.

3.3 INVESTIGATION OF A POTENTIAL CDK-PHOSPHORYLATION SITE INVOLVED IN CIZ1 STABILITY

3.3.1 Investigation of Ciz1-N471 as a substrate of cyclin A-CDK2, *in vitro*

The use of *in vitro* kinase assays allows a preliminary view of the relationship between an enzyme and a substrate. Having previously observed that Ciz1 is a substrate of cyclin A-CDK2 (Copeland et al., 2015), *in vitro* kinase assays were performed and phosphorylation status of S331, was determined. A phospo-specific antibody was also raised against this site. Another site, T293, which has already been confirmed to be phosphorylated by cyclin A-CDK2, was used as a positive control. Several concentrations of Ciz1-N471 were used in an attempt to discover the kinetic profiles of the reaction between cyclin A-CDK2 and Ciz1-N471; at the two chosen sites T293 and S331.

Preliminary results shown in Figure 5 (unpublished data, Copeland) as well as the results obtained in this study (section 3.1) suggest that Ciz1 levels increase after phosphorylation. However, it has also been established that phosphorylation of Ciz1 at T144, T192 and T293 inhibits Ciz1 DNA replication function (Copeland et al., 2015). These apparent contradictory observations remain to be fully resolved. This may be due to the S331 site within Ciz1 that is also readily phosphorylated by cyclin A-CDK2 but does not inhibit Ciz1 function although phosphorylation of other sites in Ciz1 in the N-terminal functional domain is inhibited (Copeland et al., 2015).

3.3.2 Localisation of Ciz1 containing the S331A and S331D mutations is unchanged

It has been well documented that mutations of phosphorylation sites within proteins can lead to aberrant sub-cellular localisation causing various disease states (Hung and Link, 2011). Ciz1 has been shown to largely associate with the nuclear matrix (Ainscough et al., 2007). However, considering the fourteen putative CDK phosphorylation sites it is possible that one of the putative phosphorylation sites in Ciz1 can alter sub-cellular localisation when phosphorylated. As it has been indicated that phosphorylation of S331 might have a significant function (Copeland et al., 2015), sub-cellular localisation of Ciz1 was investigated using GFP-WT-Ciz1 to observe normal sub-cellular localisation; GFP-S331A-Ciz1 to observe any potential effects on localisation if the protein is unphosphorylable at S331; and GFP-S331D-Ciz1, a phosphomimetic mutant, to observe whether phosphorylation at this site alters sub-cellular localisation. This initial experiment was performed as it is possible that the mutated Ciz1 protein may not physically be in the right location to be a substrate for cyclin A-CDK2. The GFP-S331A-Ciz1 mutant was created using whole plasmid mutagenesis by PCR followed by DNA sequencing (Eurofins Genomics) to confirm the successful introduction of the mutation.

These experiments were performed by transfecting cells with the GFP-tagged Ciz1 constructs containing the wild-type protein, an unphosphorylated protein and a protein with a phosphomimetic residue. Cells were then fractionated (Fig. 14) (section 3.2.2) followed by western blotting (Fig. 21) and immunofluorescence (Figs. 22-23). The use of these constructs is a viable method of determining Ciz1 localisation as it was previously determined that localisation of GFP-WT-Ciz1 is the same as that of

endogenous Ciz1 (Fig. 15).

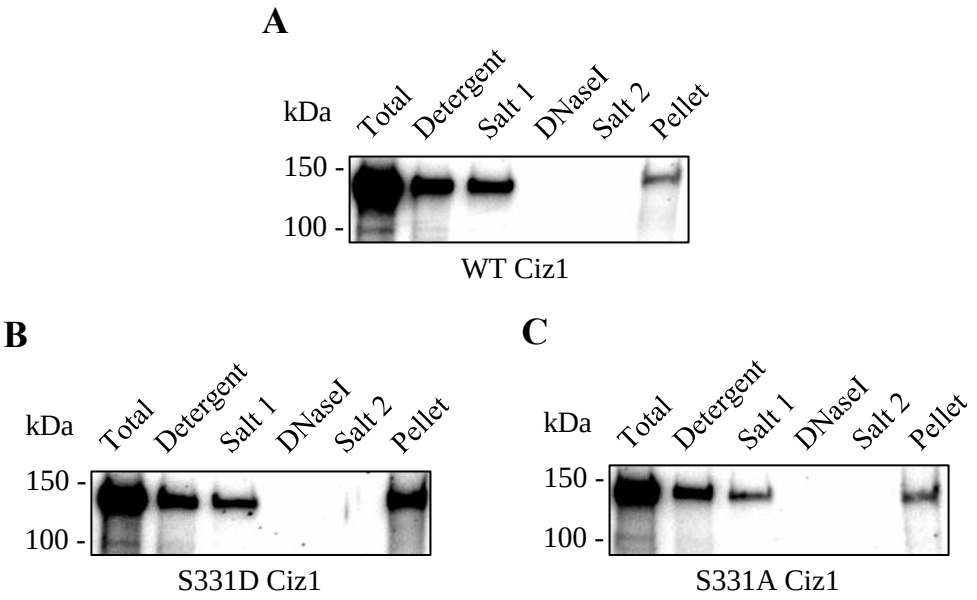

Figure 21: Mutation of S331 does not alter sub-cellular localisation
Cells were fractionated 24 hours after transfection with GFP-tagged Ciz1 constructs containing either the wild type, S331D mutant or S331A mutant. The detergent used was 1% Triton X-100 and the final salt concentration was 0.5M NaCl. Cells were treated with DNaseI for 1 hour. (**A**) Fractionation of cells transfected with WT Ciz1. (**B**) Fractionation of cells transfected with Ciz1 containing the S331D mutation . (**C**) As with (B), except cells are transfected with the S331A mutant.

Fractionation of transfected cells followed by western blotting (Fig. 21) shows that phosphorylation status does not alter the sub-cellular localisation of the Ciz1 protein (Figs. 21A and B): it is largely associated with the nuclear matrix. Sub-cellular localisation of both mutants is the same as that of the wild-type protein and the endogenous protein as seen previously in Figure 15 and by Ainscough et al. (2007). Ciz1 and all mutants tested also associated with the nuclear matrix but a sub-fraction was also found in detergent and high salt soluble pools. Determination of sub-cellular localisation of Ciz1 mutants by fractionation and western blotting is consistent and localisation of the recombinant wild-type protein appears to be the same as that of the endogenous protein (Fig. 15).

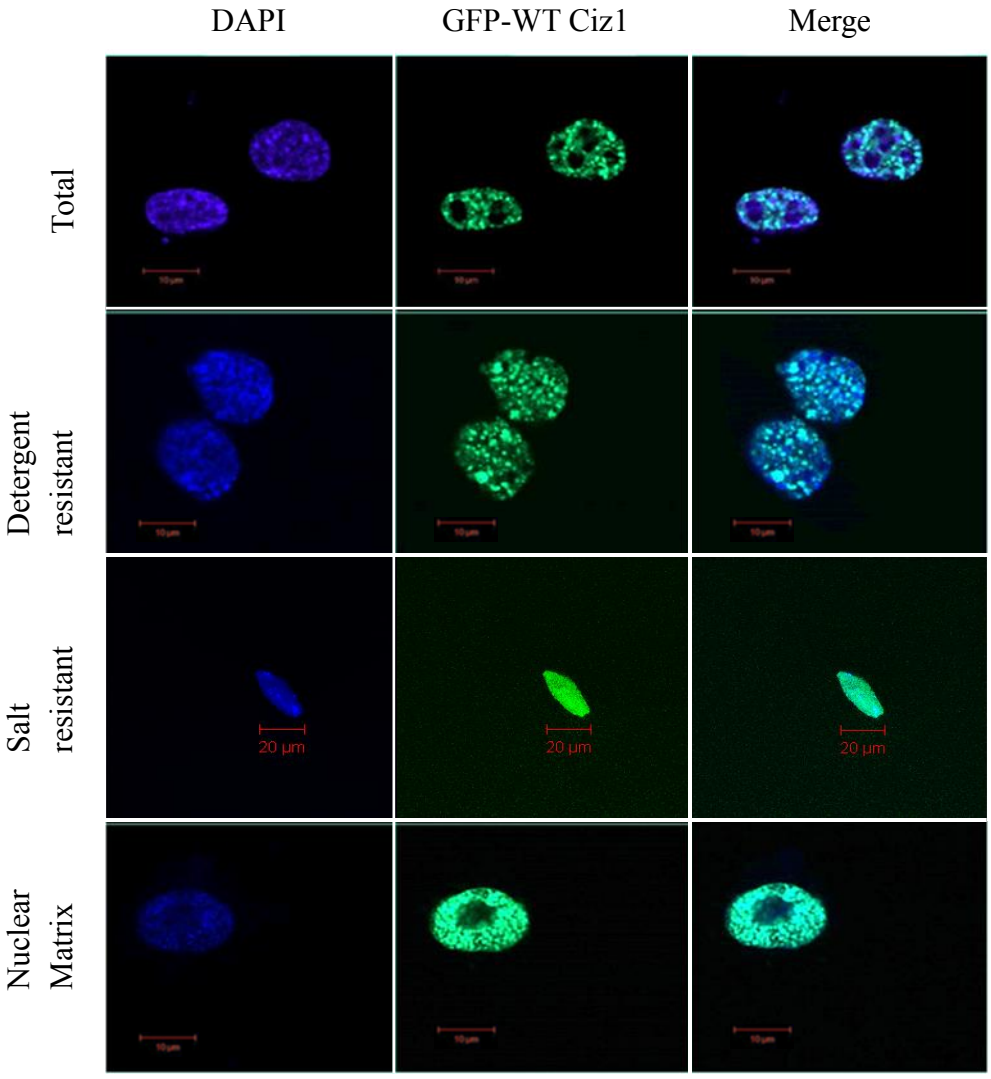

Figure 22: Fractionation of cells reveals WT-Ciz1 is largely associated with the nuclear matrix
Immunofluorescence images showing nuclei transfected with GFP-WT-Ciz1 after undergoing the same fractionation steps as performed for the western blots revealing that WT-Ciz1 is largely found at the nuclear matrix.

In order to further confirm this observation, fractionation of cells after transfection with GFP-WT-Ciz1 followed by immunofluorescence was also performed (Fig. 22), which supported results obtained by western blotting (Fig. 21A).

3.3.3 The anti-pS331 antibody: confirming specificity

Prior to investigation of the phosphorylation status of the S331 site, confirmation that the S331 phospho-specific antibody recognises its intended target only was required.

Having already synthesised the S331A-Ciz1-N471 protein, an *in vitro* kinase assay was performed using this protein and western blots were probed with the anti-pS331 and anti-pT293 antibodies (Fig. 23). The T293 phospho-specific antibody has previously been characterised (Copeland et al., 2015).

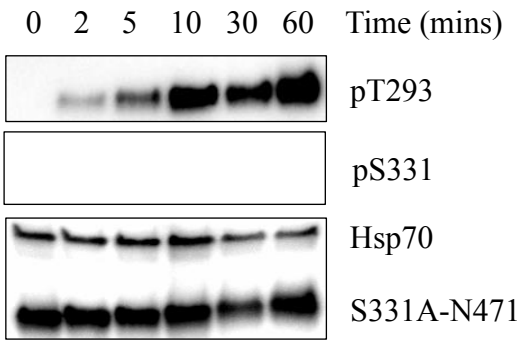

Figure 23: Characterisation of the α-pS331 antibody
Final concentrations of 2μM of S331A-Ciz1-N471 and 5nM cyclin A-CDK2 were used. The anti-pS331 antibody did not detect anything whereas the anti-pT293 antibody did; as expected.

Results obtained for the S331A-Ciz1-N471 protein (Fig. 23) reveal that the anti-pS331 antibody does not recognise this mutated site as expected. Probing with anti-pT293 and anti-N471 confirmed the presence of the protein as well as the fact that the cyclin A-CDK2 did phosphorylate at the T293 site. These results suggest that the anti-pS331 antibody does indeed recognise the required site. Considering that sub-cellular localisation is not altered, it is possible that this mutation might have an effect on protein function rather than localisation. This is supported by the fact that this site is within the C-terminal domain of the full-length protein which is responsible for protein function.

3.3.4 Ciz1-N471 is phosphorylated at sites T293 and S331 by cyclin A-CDK2

Determining the rate of a reaction can be complicated when multiple reactants are involved as it is necessary to measure the concentrations of each one at the same time; and when determining rates of reaction can lead to some complex mathematics.

Having to measure multiple reactants can also increase the margin of error of the entire system. It also complicates determining the correct parameters required for solving the rate of reaction (Schnell and Mendoza, 2004). In order to simplify this, the initial concentration of one of the reactants is much higher than that of the other reactant. This means that as the reaction progresses, the concentration of the reactant in excess changes only minutely compared to the concentration of the other reactant and can therefore be considered as a constant during the first moments of the reaction; thus leaving only one variable left. This condition is known as a pseudo-first order condition, as it appears that the rate of reaction is only dependent on one variable (Malatesta, 2005); making determination of the rate of reaction simpler to determine. For this reason, the following experiments were set up such that the initial substrate concentrations (Ciz1) were in excess. Small samples were removed from the reaction at specific time points to determine phosphorylation levels. These were added to 2x SDS-PAGE loading buffer and boiled immediately after removal in order to inhibit further enzyme activity. The reactions were performed at 37^{o}C.

Since different antibodies were used in these experiments, with unknown binding affinities, conditions were established such that basic rates of phosphorylation could be determined for a range of Ciz1 concentrations. This allowed initial rates to be determined for each site at a range of concentrations and the rates to be plotted against the concentrations. These conditions were established by taking the highest concentration of Ciz1 tested (2µM) and performing the *in vitro* kinase assay. When detecting phosphorylation levels, optimal concentrations of the antibodies were used and the blot was exposed until the upper detection limit of the equipment was reached. This exposure time was then used as the acquisition time for all the other Ciz1 concentrations tested.

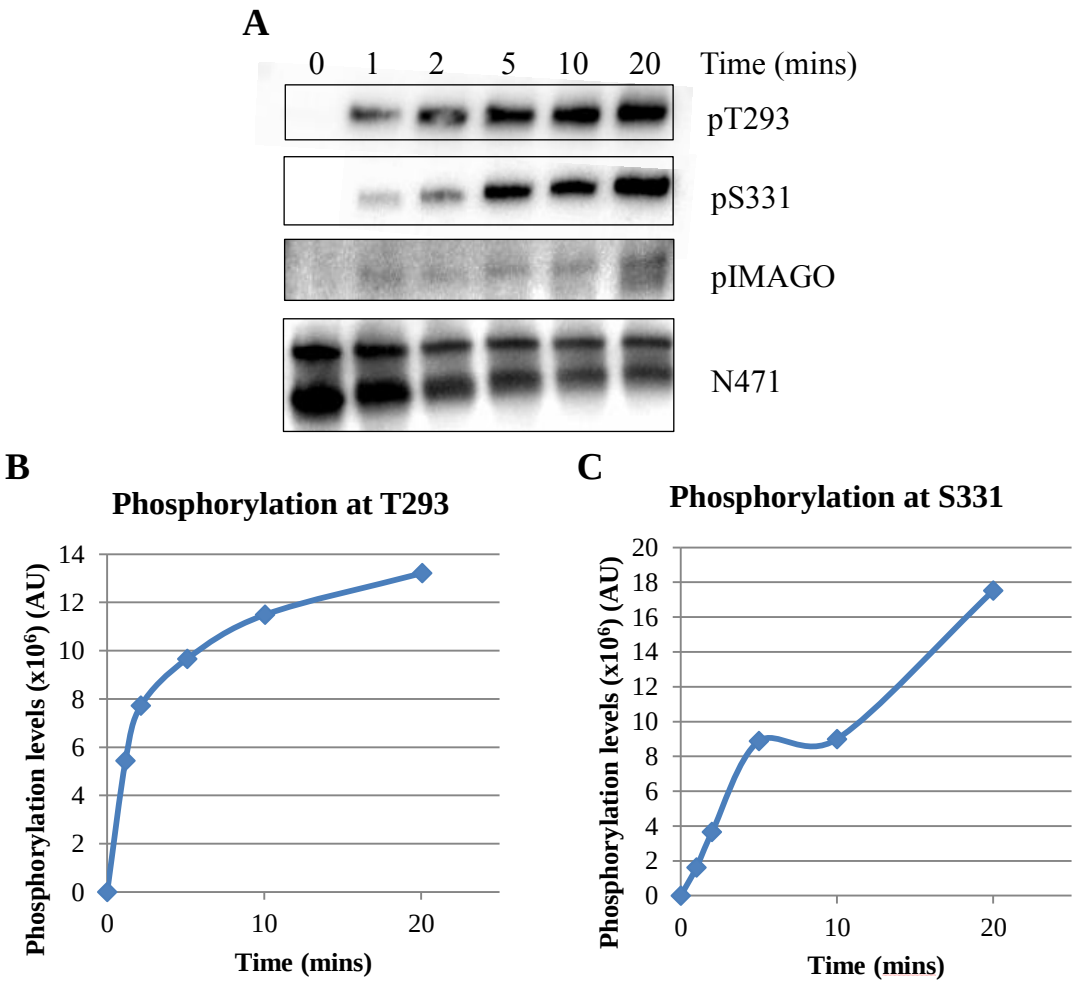

Figure 24: Phosphorylation of T293 and S331 in WT-Ciz1-N471 by cyclin A-CDK2 increases with time

Cyclin A-CDK2 was added at t=0. **(A)** Western blots were produced using anti-pT293, anti-pS331, pIMAGO and anti-Ciz1. The total Ciz1 protein (detected by α-N471) was used as a loading control. **(B)** Phosphorylated protein levels as detected by anti-pT293 were quantified using ImageLab software, signal intensity was plotted against time and shown in a line graph. **(C)** Phosphorylated protein levels as detected by anti-pS331 were quantified and a line graph was produced.

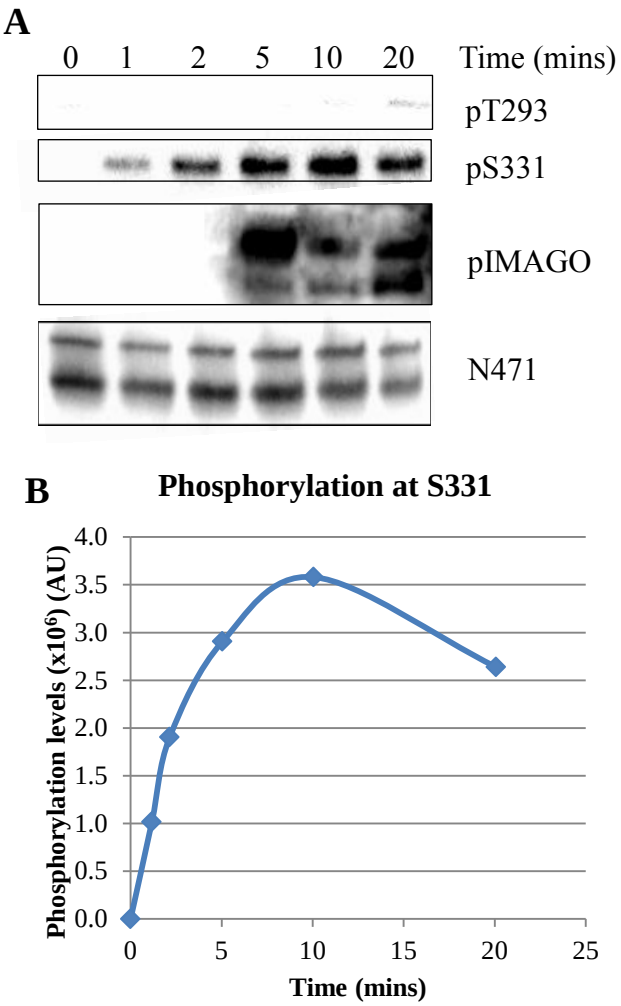

Figure 25: Phosphorylation of S331 in DDD-Ciz1-N471 by cyclin A-CDK2 increases with time

This experiment was performed at 37°C with cyclin A-CDK2 introduced to the system at t=0. Each reaction started with a total volume of 200µl and at each time point, 25µl were removed. Samples were boiled in 2x SDS-PAGE loading buffer for 10 minutes immediately after removal from the reaction. **(A)** Western blots were produced using anti-pT293, anti-pS331, pIMAGO and anti-Ciz1. The total Ciz1 protein (detected by anti-Ciz1) was used as a loading control. **(B)** Phosphorylated protein levels as detected by anti-pS331 were quantified and a graph was produced.

Initial experiments were conducted using the proteins WT-Ciz1-N471 (Fig. 24) and the protein DDD-Ciz1-N471 (Fig. 25) containing phosphomimetic mutations of sites T144, T192 and T293 which were detected using the anti-Ciz1 N471 and anti-Ciz1 pT293 antibodies. As can be observed in Figure 24A and Figure 25A, two bands are detected by the anti-N471 antibody. This is due to the fact that this antibody also recognises Hsp70 that co-purifies with recombinant Ciz1 constructs. Quantifications of phosphorylation levels of Ciz1 at T293 (Fig. 24B) and S331 (Fig. 24C) show that

as Ciz1 is exposed to cyclin A-CDK2, it is continuously phosphorylated. However, a direct comparison between these two sites cannot be performed by using these two graphs as the binding affinities of the two antibodies used are unknown. It is clear in Figure 25A, that the anti-pT293 antibody does not detect anything as expected but that the anti-pS331 antibody does. This shows that phosphorylation at T293 does not prevent consequent phosphorylation of S331. Another phospho-protein detection system, the pIMAGO system (Expedeon) was also tested in order to view total levels of phosphorylated protein.

As can be observed in both Figures 24A and 25A, the pIMAGO detection system (Expedeon) does not seem to be very sensitive to this phosphorylated protein. This system specifically detects phosphorylated molecules. Unlike phospho-specific antibodies, it does not bind to only specific amino acid sequences so is able to detect phosphorylation at any site within a protein. It is clear when using the phospho-specific antibodies that Ciz1 is phosphorylated by cyclin A-CDK2 at both the T293 and the S331 sites. An observation to consider is that at 20 minutes, phosphorylation levels of DDD-N471 at the S331 site appear to have decreased (Fig. 25B), although when comparing pS331 levels and N471 levels, a likely explanation for this occurrence is simply that there is less protein in this sample compared to the samples at the earlier time points.

3.3.5 Determining phosphorylation rate profiles of Ciz1-N471 by cyclin A-CDK2 at T293 and S331

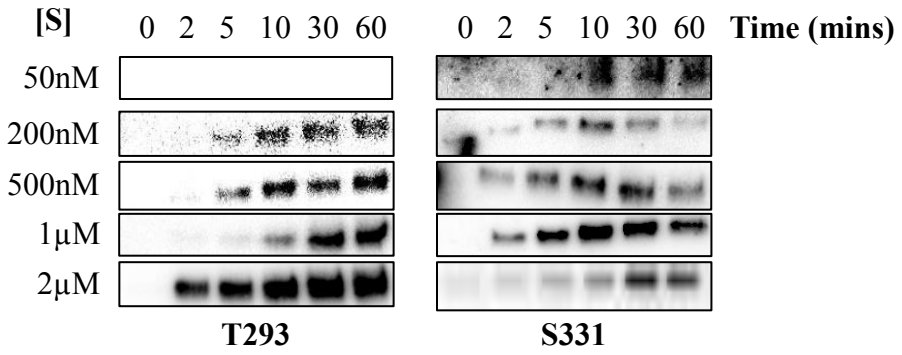

Figure 26: Phosphorylation levels at T293 and S331 using increasing substrate concentrations
For each substrate (WT Ciz1) concentration, *in vitro* kinase assays were performed twice. A concentration of 5nM of cyclin A-CDK2 was used for all assays. Western blots were probed with either anti-pT293 or anti-pS331 as indicated.

As both phospho-specific antibodies have been shown to recognise their specific sites, it was possible to explore whether differences in phosphorylation rates of these two sites could be observed using *in vitro* kinase assays. To construct a graphical representation of the kinetics rate profile of these phosphorylated sites, several kinase assays were performed using various concentrations of WT-Ciz1-N471 ranging between 50nM and 2µM and 5nM of cyclin A-CDK2. Once these assays had been performed, samples were used to produce western blots which were probed with anti-pT293 and anti-pS331 (Fig. 26). Protein levels were quantified and plotted on graphs (Fig. 27).

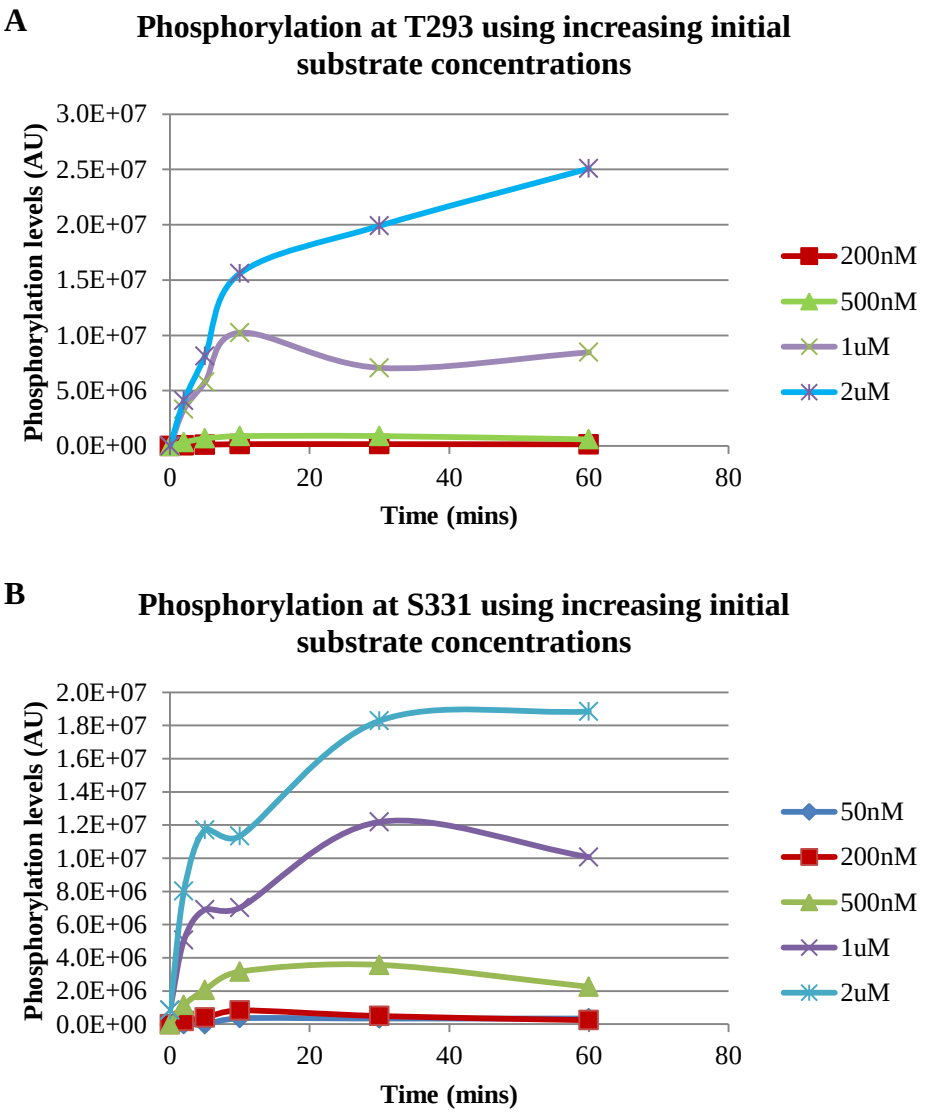

Figure 27: Graphs representing increasing phosphorylation levels as initial substrate concentration increases
These graphs were used to calculate initial velocities for each substrate concentration. (A) Average increases in phosphorylation levels at T293 over time using initial substrate concentrations between 200nM and 2µM. (B) Average increases in phosphorylation levels at S331 over time using initial substrate concentrations between 50nM and 2µM.

Although direct comparisons between the rates of phosphorylation of Ciz1 at these two sites cannot be made due to the unknown binding affinities of the two anitbodies used; it is interesting to note that the S331 phosphomimetic antibody (Fig. 27B) was able to detect low levels of phosphorylation when Ciz1 was present at a concentration of only 50nM whereas nothing was detected by the T293 phospho-specific antibody

(Fig. 27A). It would be interesting to determine binding affinities of these two antibodies as at this stage, it is not possible to determine whether the S331 phospho-specific antibody simply has a stronger binding affinity than its T293 counterpart or whether S331 is more readily phosphorylated by cyclin A-CDK2 than T293. However, taking this into consideration, it is also interesting to note that when Ciz1 is present at a concentration of 2uM, the T293 phospho-specific antibody (Fig. 27A) detects higher levels of phosphorylated protein than the S331 phospho-specific antibody (Fig. 27B). If binding increases in a linear fashion up to 2uM, this suggests that T293 is phosphorylated to a higher level than S331. Further investigation is required to determine whether this is true though, using an alternative method to using those phosphor-specific antibodies such as the use of radiolabelled isotopes.

3.3.6 Discussion

Mutation of a single site within a protein that is sometimes phosphorylated can have drastic effects on function and sub-cellular localisation which can lead to some serious diseases (Hung and Link, 2011, Shin et al., 2002, Gregory et al., 2003). Preliminary work suggests that the S331 site within Ciz1 is phosphorylated at an earlier stage of the cell cycle (late G_1) than the T293 site (S phase) and that Ciz1 is a substrate of cyclin E-CDK2 (Copeland et al., 2015); although this requires more thorough investigation. Since experiments described earlier suggested that APC/C^{Cdh1}, which is active during the late G_1 phase, is a potential E3 ligase responsible for ubiquitylation of Ciz1 and in turn its degradation; S331 was marked as a potential CDK-mediated phosphorylation site that, when phosphorylated, increases protein stability according to results presented in Figure 5 and section 3.1. In order to investigate whether S331 does play a role in protein stability, several experiments were performed designed to determine the effects if this site is mutated.

Prior to investigating whether S331 may be involved in contributing to protein stability, it was confirmed that phosphorylation of this site does not alter sub-cellular localisation. Results show that S331 is phosphorylated by cyclin A-CDK2 (Fig. 24A). Further work is required such as using site directed mutagenesis of individual CDK sites and radiolabelled ATP to probe more precisely the kinetic behaviour of Ciz1 phosphorylation. In addition, cyclin E-CDK2 may play an important role in phosphorylation of the S331 site during the late G_1 phase, conferring a degree of protection from degradation. This could be assessed first using *in vitro* kinase assays to determine whether S331 can be phosphorylated by cyclin E-CDK2 and then using cell based assays by synchronising cell populations and observing the effects on phosphorylation of specific sites within Ciz1 such as S331 if cyclin E-CDK2 is inhibited.

As previously stated, preliminary work suggests that S331 is phosphorylated during the late G_1 phase whereas T293 appears to be phosphorylated later on during the S phase. Since the main cyclin active during the G_1-S phase transition is cyclin E bound to CDK2, it would have been interesting to observe phosphorylation rates of T293 and S331 and compare them with those obtained when using cyclin A-CDK2. Unfortunately, we were unable to purify cyclin E-CDK2 despite several attempts that would have enabled further investigation and comparison of cyclin-CDK2 complex specificities.

As it was demonstrated using *in vitro* means that the S331 site within Ciz1 can be phosphorylated by cyclin A-CDK2, it remains a possibility that this site could contribute to protein stability. As there are several lysine residues situated nearby the S331 site (Fig. 13), it is possible that S331 could contribute to protein stability by influencing ubiquitylation of these sites or by more indirect methods.

Results obtained do not show conclusively that S331 is involved in contributing to protein stability. However, we have clearly demonstrated that S331 is phosphorylated by cyclin A-CDK2 *in vitro* and this provides an additional opportunity to test the role of phosphorylation of this site *in vivo*. In order to do this, further *in vivo* work would need to be performed using both the S331A mutation and the S331 phosphomimetic mutation. However, results do indicate that this function is indeed a viable possibility as mutation of this site does not lead to altered sub-cellular localisation and it is phosphorylated *in vitro* by cyclin A-CDK2.

4. GENERAL DISCUSSION

4.1 CDK-mediated phosphorylation of Ciz1

Many proteins involved in the regulation of the cell cycle are known to be phosphorylated by CDKs. These phosphorylation events have a number of different effects on the altered protein; including contributing to protein stability and marking the protein for degradation, usually by the ubiquitin proteasome system. One such modified protein that is known to be protected from ubiquitin-mediated degradation when phosphorylated, which has been well-documented is Cdc6 (Duursma and Agami, 2005, Mailand and Diffley, 2005). Cdc6 is one of the major proteins involved in preparing for the replication of DNA by being a component of the pre-replication complex. When Cdc6 is phosphorylated by cyclin E-CDK2 at residues serine 54 and serine 74, the protein is no longer targeted by the E3 ligase APC/C^{Cdh1}.

Conversely, phosphorylation of proteins can also act as a mark for degradation. One such protein is $p27^{Kip1}$, a non-specific CDK inhibitor able to inhibit all cyclin-CDK complexes required during the G_1 phase and entry into the S phase. It also has several other functions attributed to it including being involved in cellular differentiation and tumour suppression (Sgambato et al., 2000). The protein $p27^{Kip1}$ has been shown to be phosphorylated by CDK2 at residue threonine 187, marking it for degradation by the E3 ligase SCF^{Skp2} (Tsvetkov et al., 1999, Auld et al., 2007).

Ciz1 has been known to associate with cyclin A-CDK2 and thought to associate with cyclin E-CDK2 for some years now (Copeland et al., 2010b); however, it has only recently been shown that Ciz1 is also a substrate of cyclin A-CDK2 (Copeland et al., 2015). Cyclin A-CDK2 has the ability to phosphorylate Ciz1 at residues threonine 144, threonine 192 and threonine 293. These phosphorylation events do not affect protein stability; instead they block replisome formation and inhibit the initiation of DNA replication. They also prevent cyclin A-CDK2 from binding to the Ciz1 protein.

Interestingly, preliminary work using chemical inhibitors of CDK activity (roscovitine) and the 26S proteasome used to degrade proteins (MG132) suggested that phosphorylation of Ciz1 also increases protein stability (Fig. 5) (Copeland, unpublished data). In order to identify whether this is indeed true and, if so, determine which CDK-mediated phosphorylation site(s) is responsible; experiments were designed using mouse 3T3 fibroblasts transfected with plasmid constructs containing a GFP tag and phosphomimetic mutations of Ciz1. To do this, all putative CDK-mediated phosphorylation sites (fourteen in total) were identified. Experiments were also set up to observe the effects of different concentrations of the chemical inhibitors on endogenous Ciz1 protein as well as the wild type recombinant protein to identify the optimal conditions in which to perform these experiments.

Unfortunately, no significant, reproducible effects were observed on recombinant GFP-Ciz1 protein levels at any of the tested chemical concentrations (Figs. 7-10). However, inhibition of CDK activity did result in decreased endogenous Ciz1 protein levels (Fig. 7) suggesting decreased protein stability as a consequence of the absence of certain phosphorylation events. Protein levels were partially recovered in the presence of the 26S proteasome inhibitor (lane 5, Fig. 7), also suggesting that Ciz1 is degraded by the ubiquitin proteasome system. As preliminary work had also suggested that knockdown of cyclin A by using *α-ccna2* siRNA in a synchronised population of cells had a similar effect on Ciz1 protein levels as addition of the CDK inhibitor roscovitine (Fig. 5A); this method was also tested. However, no significant, reproducible effects were again observed (Figs. 11 and 12). Several possible explanations exist, which could explain why results obtained do not agree with those obtained during the preliminary work. The most likely is a problem encountered in the lab at the time these experiments were performed. During this time, all cells used did

not synchronise very well; with some populations not surviving the process at all and others where only very few cells survived. Cell populations that did not undergo the process of synchronisation did not survive for very long either. One possible reason behind this is that the cells used were coming to the end of their life-span. However, during other experiments performed at a later date, cells seemed to synchronise quite well and survived much longer.

Although the chemical CDK inhibitor roscovitine was shown to reduce endogenous Ciz1 levels, suggesting that Ciz1 stabilisation occurs by phosphorylation; the same effects were not observed for recombinant GFP-Ciz1 at the concentrations tested. A possible explanation for this could be that concentrations of chemical inhibitors used were not in the correct range, likely due to the much higher level of protein expression. This would suggest that protein levels were likely affected but due to the very high Ciz1 protein concentrations, these changes were undetectable. New stock solutions of roscovitine were prepared a number of times during this process so it is unlikely that the cause of these unexpected results was due to the use of old aliquots that were no longer as chemically active.

Cyclin A knockdown experiments were performed both in synchronous and asynchronous populations of cells and no effects on Ciz1 levels were observed. These experiments would need to be repeated as sample sizes used here were very small. However, results presented here suggest that not only does CDK-mediated phosphorylation of Ciz1 inhibit its function in DNA replication (Copeland et al., 2015), but that CDK-mediated phosphorylation also stabilises the protein.

Having encountered an inability to identify the optimal conditions in which to perform experiments using chemical inhibitors of CDK activity (roscovitine) and the 26S

proteasome (MG132), it was therefore not possible to use the fourteen phosphomimetic mutants designed to discover which site(s) within Ciz1, if any, is responsible for increasing protein stability when phosphorylated using the methods originally planned. Using an alternative method; that of cyclin A knockdown by transfection with *α-ccna2* siRNA; also did not yield expected results and so could not be used. Even so, if this second method had worked as expected, it would not have been possible to repeat these experiments many times due to the presence of fourteen mutants and the necessity of synchronising cell populations, which by design requires several days to complete as cells are left for 48 hours after reaching 100% confluency before being released back into the cell cycle.

4.2 Ciz1 is a target of the ubiquitin proteasome system

As preliminary work has suggested that inhibiting the 26S proteasome results in Ciz1 protein levels being increased (Fig. 5) (Copeland, unpublished data), it seems that Ciz1 is also a target of the ubiquitin proteasome system. Results obtained (Figs. 7-10 and 12) do indicate some increase in protein levels with addition of MG132 supporting this. Investigations were therefore performed to identify whether Ciz1 is ubiquitylated or not using plasmids constructs containing ubiquitin and a tag. This was because the *Mus musculus* form of Ciz1 contains 37 lysine residues, which are putative ubiquitylation sites (Pickart, 2001). Due to the large number of sites, it was not feasible to mutate each site individually to investigate which site(s) is ubiquitylated and so a more general method was used to identify ubiquitylation.

Experiments performed were conducted using His-tagged ubiquitin. Results obtained did yield some interesting observations. Using two fractions of cells to detect ubiquitylated Ciz1, pull down assays were performed in order to detect both

endogenous Ciz1 and recombinant Ciz1. It was found that although endogenous Ciz1 appeared to be pulled down when bound to His-Ub, recombinant Ciz1 was pulled down even in the absence of His-Ub. This was explained by the fact that Ciz1 has three zinc fingers in the C-terminal domain (Mitsui et al., 1999) that are able to bind to the Ni^{2+} (Hanas et al., 2005), which forms part of the Ni^{2+}-NTA resin used to immobilise proteins of interest. As a result, later experiments were performed using higher concentrations of imidazole so as to increase the amount of His-Ub complexed with recombinant Ciz1 eluted. This did not improve results however and so it was not possible to perform further experiments using recombinant Ciz1 to detect ubiquitylation status by co-transfecting cells with His-Ub and GFP-Ciz1. However, results obtained using endogenous Ciz1 did suggest that, as expected, Ciz1 is ubiquitylated. At least two bands are observed in the presence of MG132. This is consistent with poly-ubiquitylation (Bloom and Pagano, 2005), although is not definitive. This also shows that inhibition of the 26S proteasome is required to efficiently recover Ciz1 bound by His-Ub.

Interestingly, there appeared to be a slight difference in MG132 dependency between the low and high salt fractions used to detect endogenous Ciz1 (Figs. 16A, B and 17A, B). In the low salt extracts, Ciz1 seemed only to be pulled down when the 26S proteasome was inhibited whereas in the high salt extracts, more Ciz1 was pulled down when the 26S proteasome was not inhibited. Unfortunately, due to the previous problems encountered when using the chemical MG132 and the fact that Ciz1 itself can bind to the Ni^{2+}-NTA resin, it is not clear whether or not this apparent difference on dependency is reproducible at this time. Further work is therefore required to determine this. A possible addition to the protocol used could be the addition of chemical inhibitors of deubiquitylating enzymes (DUB) in an attempt to increase

ubiquitylation levels of proteins; although investigation into these inhibitors is still in the early stages (Ndubaku and Tsui, 2015). Inhibition of deubiquitylating enzymes is possible using N-ethylmaleimide that covalently inactivates the nucleophilic thiol residue of DUBs (Huang et al., 2006, Jacobson et al., 2009).

As results obtained using pull down assays of endogenous Ciz1 protein and His-Ub revealed that Ciz1 is ubiquitylated as expected, an investigation into the E3 ligase(s) responsible for this was performed using *in vitro* protein-protein interaction studies with GST-tagged proteins of interest. Of the two main E3 ligase complexes responsible for targeting proteins involved in cell cycle regulation for degradation, APC/C and SCF (Vodermaier, 2004), the most likely candidate for ubiquitylation of Ciz1 is APC/C due, in part, to the identification of a putative destruction box (D-box) identified within the *Ciz1* sequence. This D-box sequence is a motif found in many targets of the APC/C which is recognised by this E3 ligase (Castro et al., 2005). The APC/C has two main activating proteins that also confer substrate specificity: Cdc20 and Cdh1 which bind to complex in a sequential manner. Cdh1 binds the APC/C towards the end of mitosis and stays there until it is phosphorylated and degraded at the end of the G_1 phase (Li and Zhang, 2009, Kramer et al., 2000). As such, APC/C^{Cdh1} was considered a likely candidate.

Ciz1-N471 was found to bind to immobilised GST-Cdh1 in a concentration dependent manner. Similar results were obtained when Cdh1 was bound to GST-Ciz1-N471 (Fig. 19). These results suggested that APC/C^{Cdh1} is indeed an E3 ligase responsible for the ubiquitylation of Ciz1. As Ciz1 has been observed to have a putative D-box, a mutant of Ciz1-N471 was created such that the 'RXXL' sequence that makes up the D-box was mutated to 'AXXA'. As expected, when the D-box in Ciz1 is mutated, no binding occurs between Ciz1-N471 and Cdh1; indicating that APC/C^{Cdh1} binds to Ciz1 via the

D-box and further supporting the possibility that APC/C^{Cdh1} is an E3 ligase responsible for Ciz1 degradation. Further work will need to be performed to verify these interactions using more in depth protein-protein interaction studies such as protein microarrays where proteins are bound to an immobilised sheet although there are several other methods available as well (Hall et al., 2007, Rao et al., 2014). *In vivo* work would also need to be performed to observe the effects on Ciz1 if, for example, Cdh1 is knocked down. Cdh1 binding to substrates leads to poly-ubiquitylation (Rape et al., 2006) and results presented here suggest that Ciz1 is poly-ubiquitylated. It should also be noted that CDK-mediated phosphorylation of Ciz1 appears to contribute to protein stability; an attribute also found in other substrates of APC/C^{Cdh1} (Mailand and Diffley, 2005, Holt et al., 2008, Lee et al., 2007).

The fact that APC/C^{Cdh1} appears to be able to ubiquitylate Ciz1 and that this E3 ligase is only active until the late G_1 phase implies that Ciz1 protein levels must be tightly regulated during this stage. Considering that the function of Ciz1 is to aid cyclin A-CDK2 with the initiation of DNA replication and the observation that APC/C^{Cdh1} can ubiquitylate Ciz1; this suggests that Ciz1 protein levels are tightly regulated such that DNA replication is not initiated until the checkpoint has been passed when restrictions by APC/C^{Cdh1} are removed, allowing Ciz1 levels to rise until all licensed sites have been fired. In order to prevent re-replication of DNA, cyclin A-CDK2 then phosphorylates Ciz1 (Copeland et al., 2015), blocking interactions between these proteins and inhibiting further rounds of initiation of DNA replication.

As it has been suggested that phosphorylation of Ciz1 could also contribute to protein stabilisation, this could mean that a balance is in place between Ciz1 phosphorylation and APC/C^{Cdh1} degradation. Further work is required to understand exactly how Ciz1

levels are regulated as results obtained suggest that there are multiple levels of control which act according to whichever stage the cell cycle is in.

4.3 The S331 site in Ciz1 is phosphorylated by cyclin A-CDK2

It has previously been established that not only is Ciz1 a binding partner of cyclin A-CDK2 but that it is also a substrate of this enzyme complex. Phosphorylation of Ciz1 at sites T144, T192 and T293 by cyclin A-CDK2 results in a reduced ability to initiate DNA replication by inhibiting replisome formation (Copeland et al., 2015). Preliminary work had suggested that this site, S331, might be involved in protein stability and so the kinase assays would demonstrate whether or not, this site can be phosphorylated by cyclin A-CDK2. A study of the interactions between the S331 site and the cyclin A-CDK2 was performed, after confirmation that phosphorylation of S331 does not alter Ciz1 sub-cellular localisation.

An initial study of the S331 site revealed that mutation of this site, such that the site could no longer be phosphorylated or where it appeared to be in a constant state of phosphorylation, does not lead to altered sub-cellular localisation of the protein (Fig. 21). Mutations of proteins are known to be able to cause aberrant localisation, which can result in serious consequences (Hung and Link, 2011). However, it has also been shown that the absence of the N-terminal domain of Ciz1, which contains the nuclear localisation signal, does not inhibit initiation of DNA replication (Ainscough et al., 2007), suggesting that even if mutation of the S331 site did result in altered sub-cellular localisation, the replicative function of Ciz1 might still be intact.

With the S331 site appearing not to be involved in protein localisation; it is possible that this site does contribute to protein stability. Results obtained from *in vitro* kinase assays revealed that the S331 site is indeed phosphorylated by cyclin A-CDK2 (Fig.

24). Further experiments would need to be performed to assess enzyme kinetics of phosphorylation of Ciz1 between cyclin E-CDK2 and cyclin A-CDK2.

Investigation of phosphorylation rates of the T293 and S331 sites could be useful. As the cyclin E-CDK2 complex is active earlier in the G_1 phase than cyclin A-CDK2, differences in specificity could contribute to stabilisation of Ciz1. Any differences would demonstrate which of these cyclin-CDK complexes preferentially phosphorylate which sites and would give an indication as to when during the cell cycle each site is modified. Unfortunately, attempts at growing BL-21 *E. coli* cultures with plasmid vectors containing cyclin E failed to grow to sufficient levels.

In order to test whether the S331 site could be involved in protein stability, pull down assays were performed using His-Ub and various forms of recombinant Ciz1 to assess ubiquitylation status. If the phosphomimetic mutant (S331D) was not ubiquitylated or was ubiquitylated to a lesser degree, this would have suggested that this site is responsible for protein stability. However, despite using a slightly modified protocol, recombinant Ciz1 was still being pulled down in the absence of His-Ub, attributed to the presence of the zinc fingers within the protein. It was therefore not possible to determine if S331 does a play a role in protein stabilisation. It is a possible function as it has now been demonstrated to be phosphorylated by cyclin A-CDK2.

4.4 A model of Ciz1 function

According to evidence and theories presented in this thesis, also based on published data and preliminary work, the following model of Ciz1 regulation is proposed (Fig. 28). During the G_1 phase, replication complex assembly begins. As cyclin E-CDK2 activity rises, CMG complex assembly begins with DDK activation. This is the phase of the cell cycle where Ciz1 levels are rising correlating with the increase in kinase

activity. Ciz1 protein levels are regulated by phosphorylation events and the UPS. The results presented here are consistent with the APC/C^{Cdh1} complex regulating Ciz1 function via substrate recognition via the destruction box within Ciz1. The balance between Ciz1 protective phosphorylation by CDK2 and Ciz1 ubiquitylation by APC/C^{Cdh1} during the G_1 phase until the cell is ready for entry into the S phase may contribute to genome stability through regulation of Ciz1 protein levels.

Once the cell is ready to enter the S phase, Ciz1 binds to cyclin A-CDK2 and together, this complex promotes the initiation of DNA replication (Copeland et al., 2010b) leading to replisome formation. Ciz1 protein levels are reaching their maximum level at this phase of the cell cycle (Copeland et al., 2015) potentially due to the degradation of the Cdh1 subunit by SCF at the G_1/S phase transition (Kramer et al., 2000). As the cell progresses through the S phase, in order to prevent re-replication of DNA, cyclin A-CDK2 gradually phosphorylates Ciz1 at sites T144, T192 and T293; causing dissociation from the cyclin-CDK complex (Copeland et al., 2015). Ciz1 levels are then maintained throughout the remainder of the cell cycle and fall during early G_1 in the subsequent cell cycle. This cycling of Ciz1 protein levels mirrors the relative CDK activity present in the cell.

Ciz1 protein over-expression has been associated with several types of cancer. The fine tuning of Ciz1 levels by opposing phosphorylations and UPS-mediated degradation could contribute to regulation of Ciz1 function, thereby preventing untimely DNA replication that is associated with replication stress. These mechanisms may contribute to maintenance of genomic stability.

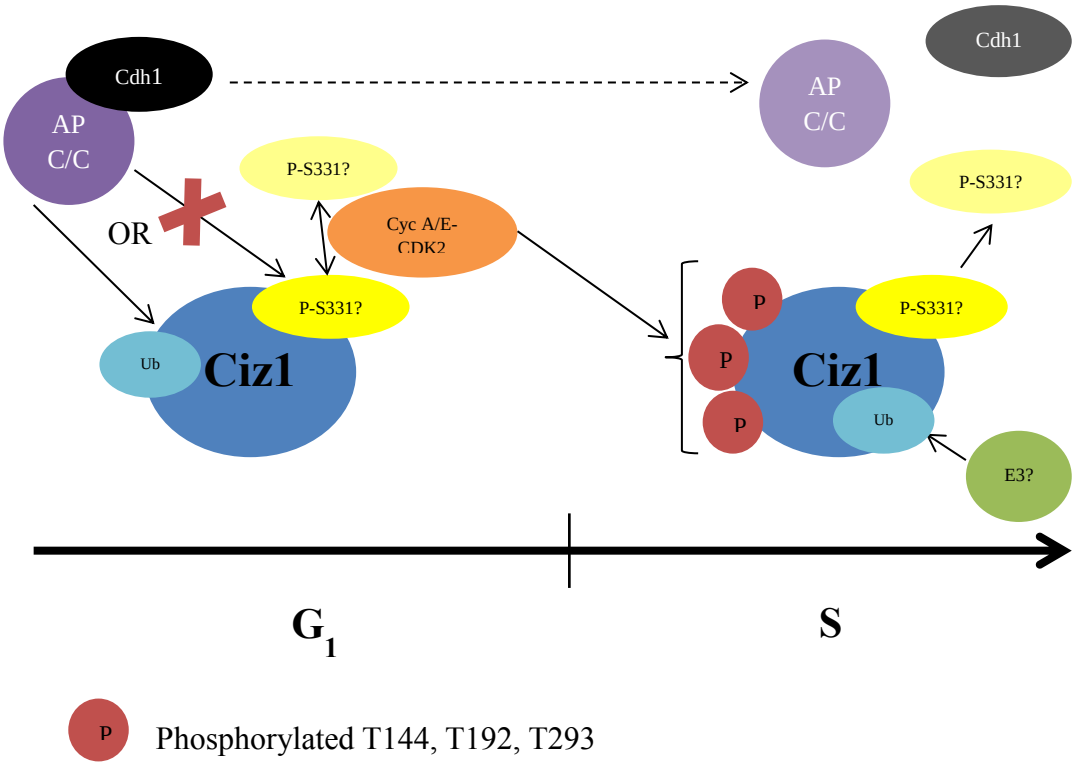

Figure 28: Proposed model for phosphorylation and ubiquitylation events of Ciz1 during the G_1 and S phases
Compiling all evidence obtained from previous studies and in this study, this model is proposed for the events that occur during the G_1 and S phases regarding Ciz1.

4.5 Ciz1 in cancer

Dysregulated Ciz1 has been observed in multiple cancer types (Higgins et al., 2012, Okumura et al., 2011, Wang et al., 2014a). If the model presented here in Figure 28 is correct, albeit incomplete, it is fairly clear how dysregulated Ciz1 could lead to a dysregulated cell cycle and eventually lead to the development of cancer. Control of the initiation of DNA replication is paramount to a healthy cell cycle as the following processes should not be allowed to occur if the previous steps have not been completed or the cell is not in the position to be able to divide in order to produce two healthy daughter cells. Loss of this control can lead to cancer. Considering that Ciz1 is involved in regulating the initiation of DNA replication, understanding how this protein is regulated could lead to the knowledge of how this protein id dysregulated in

cancers and potentially what treatments could be performed such that this dysregulation is reversed or counteracted in such a way that Ciz1 protein levels return to normal and also function normally. This knowledge would also allow a better understanding of whether the dysregulated Ciz1 protein observed in these cancers is a cause or a consequence of this state.

If dysregulated Ciz1 is a cause of cancer, understanding the cause of dysregulation could lead to the identification of a novel therapeutic target. Understanding how Ciz1 is normally regulated is therefore extremely important. If dysregulated Ciz1 is a consequence of cancer, it is possible that treating the consequence could ameliorate the cancer and, together with treatment of the initial cause, lead to a complete response instead of a partial response and could even decrease to probability of recurrence and development of resistance.

Targetting the UPS has lead to some surprising success as the drugs appear to target cancer cells only (Shen et al., 2013). If this therapy were to be administered together with another drug that would also affect Ciz1 protein stability, Ciz1 stability would be regulated from two directions, increasing the chance of having a positive effect and reverting the cell back to its normal state. According to results presented here, if the putative CDK-phosphorylation site(s) responsible for contributing to protein stability can be identified, inhibition of phosphorylation at this site(s) would lead to increased protein degradation, a desired consequence considering that in cancers, Ciz1 is observed to be up-regulated (section 1. 7).

4.6 Future work

Further work is required to determine which sites within Ciz1, if any, contribute to protein stability. The S331 site is a possible candidate for this function but *in vivo*

work using a phosphomimetic mutant and a mutant where phosphorylation is not possible is required in order to determine what the function of phosphorylation at this site is. It would also be interesting to observe if ubiquitylation status of Ciz1 is altered if S331 is mutated. This can be taken further by investigating whether mutation of other putative CDK-mediated phosphorylation sites affects ubiquitylation of Ciz1.

Confirmation of APC/C^{Cdh1} as an E3 ligase responsible for Ciz1 degradation is also required. This can be determined with the use of Cdh1 knock downs and observing effects on Ciz1 protein levels. Further investigation of the putative D-box should be performed *in vivo* as well to demonstrate that this sequence is not only functional *in vitro*.

Investigations into whether Ciz1 is a substrate of cyclin E-CDK2 *in vivo* should also be performed. Synchronised cell experiments would be able to show whether the S331 site is phosphorylated prior to the T293 site and which cyclin-CDK complexes are primarily responsible for these events. *In vitro* kinase assays with cyclin A-CDK2 using higher Ciz1 concentrations and radioisotopes could also be performed to determine if enzyme kinetics occur according to Michaelis-Menten kinetics and if so, determine the K_{cat} and V_{max} values for this reaction.

5. REFERENCES

ADHIKARY, S., MARINONI, F., HOCK, A., HULLEMAN, E., POPOV, N., BEIER, R., BERNARD, S., QUARTO, M., CAPRA, M. & GOETTIG, S. 2005. The ubiquitin ligase HectH9 regulates transcriptional activation by Myc and is essential for tumor cell proliferation. *Cell,* 123**,** 409-421.

AINSCOUGH, J. F. X., RAHMAN, F. A., SERCOMBE, H., SEDO, A., GERLACH, B. & COVERLEY, D. 2007. C-terminal domains deliver the DNA replication factor Ciz1 to the nuclear matrix. *Journal of Cell Science,* 120**,** 115-124.

AKTAS, H., CAI, H. & COOPER, G. M. 1997. Ras links growth factor signaling to the cell cycle machinery via regulation of cyclin D1 and the Cdk inhibitor p27KIP1. *Molecular and cellular biology,* 17**,** 3850-3857.

ALESSI, F., QUARTA, S., SAVIO, M., RIVA, F., ROSSI, L., STIVALA, L. A., SCOVASSI, A. I., MEIJER, L. & PROSPERI, E. 1998. The cyclin-dependent kinase inhibitors olomoucine and roscovitine arrest human fibroblasts in G1 phase by specific inhibition of CDK2 kinase activity. *Experimental cell research,* 245**,** 8-18.

ARIAS, E. E. & WALTER, J. C. 2007. Strength in numbers: preventing rereplication via multiple mechanisms in eukaryotic cells. *Genes & development,* 21**,** 497-518.

AULD, C. A., FERNANDES, K. M. & MORRISON, R. F. 2007. Skp2-mediated p27(Kip1) degradation during S/G(2) phase progession of a adipocyte hyperplasia. *Journal of Cellular Physiology,* 211**,** 101-111.

BACH, S., KNOCKAERT, M., REINHARDT, J., LOZACH, O., SCHMITT, S., BARATTE, B., KOKEN, M., COBURN, S. P., TANG, L., JIANG, T., LIANG, D. C., GALONS, H., DIERICK, J. F., PINNA, L. A., MEGGIO, F., TOTZKE, F., SCHACHTELE, C., LERMAN, A. S., CARNERO, A., WAN, Y. Q., GRAY, N. & MEIJER, L. 2005. Roscovitine targets, protein kinases and pyridoxal kinase. *Journal of Biological Chemistry,* 280**,** 31208-31219.

BAKER, G. L., LANDIS, M. W. & HINDS, P. W. 2005. Multiple functions of D-type cyclins can antagonize pRb-mediated suppression of proliferation. *Cell Cycle,* 4**,** 329-337.

BEDFORD, L., PAINE, S., SHEPPARD, P. W., MAYER, R. J. & ROELOFS, J. 2010. Assembly, structure, and function of the 26S proteasome. *Trends in Cell Biology,* 20**,** 391-401.

BERNDSEN, C. E. & WOLBERGER, C. 2014. New insights into ubiquitin E3 ligase mechanism. *Nature structural & molecular biology,* 21**,** 301-307.

BLOOM, J. & CROSS, F. R. 2007. Multiple levels of cyclin specificity in cell-cycle control. *Nature Reviews Molecular Cell Biology,* 8**,** 149-160.

BLOOM, J. & PAGANO, M. 2005. Experimental tests to definitively determine ubiquitylation of a substrate. *In:* DESHAIES, R. J. (ed.) *Ubiquitin and Protein Degradation, Pt B.*

BLOW, J. J. 2001. Control of chromosomal DNA replication in the early Xenopus embryo. *The EMBO Journal,* 20**,** 3293-3297.

BOCHMAN, M. L. & SCHWACHA, A. 2008. The mcm2-7 complex has in vitro helicase activity. *Molecular Cell,* 31**,** 287-293.

BOCHMAN, M. L. & SCHWACHA, A. 2009. The Mcm Complex: Unwinding the Mechanism of a Replicative Helicase. *Microbiology and Molecular Biology Reviews,* 73**,** 652-683.

BUSCHHORN, B. A. & PETERS, J.-M. 2006. How APC/C orders destruction. *Nature cell biology,* 8**,** 209-211.

CARPENTER, G. & COHEN, S. 1990. Epidermal growth factor. *J Biol Chem,* 265**,** 7709-7712.

CASTRO, A., BERNIS, C., VIGNERON, S., LABBE, J. C. & LORCA, T. 2005. The anaphase-promoting complex: a key factor in the regulation of cell cycle. *Oncogene,* 24**,** 314-325.

CHAU, V., TOBIAS, J. W., BACHMAIR, A., MARRIOTT, D., ECKER, D. J., GONDA, D. K. & VARSHAVSKY, A. 1989. A MULTIUBIQUITIN CHAIN IS CONFINED TO SPECIFIC LYSINE IN A TARGETED SHORT-LIVED PROTEIN. *Science,* 243**,** 1576-1583.

CHEUNG, T. H. & RANDO, T. A. 2013. Molecular regulation of stem cell quiescence. *Nature reviews Molecular cell biology,* 14**,** 329-340.

CHO, R. J., CAMPBELL, M. J., WINZELER, E. A., STEINMETZ, L., CONWAY, A., WODICKA, L., WOLFSBERG, T. G., GABRIELIAN, A. E., LANDSMAN, D. &

LOCKHART, D. J. 1998. A genome-wide transcriptional analysis of the mitotic cell cycle. *Molecular cell,* 2**,** 65-73.

COPELAND, N. A., SERCOMBE, H. E., AINSCOUGH, J. F. X. & COVERLEY, D. 2010. Ciz1 cooperates with cyclin-A-CDK2 to activate mammalian DNA replication in vitro. *Journal of Cell Science,* 123**,** 1108-1115.

COPELAND, N. A., SERCOMBE, H. E., WILSON, R. H. C. & COVERLEY, D. 2015. Cyclin-A-CDK2-mediated phosphorylation of CIZ1 blocks replisome formation and initiation of mammalian DNA replication. *Journal of Cell Science,* 128**,** 1518-1527.

COVERLEY, D., LAMAN, H. & LASKEY, R. A. 2002. Distinct roles for cyclins E and A during DNA replication complex assembly and activation. *Nature Cell Biology,* 4**,** 523-528.

COVERLEY, D., MARR, J. & AINSCOUGH, J. 2005. Ciz1 promotes mammalian DNA replication. *Journal of Cell Science,* 118**,** 101-112.

DAILEY, L., AMBROSETTI, D., MANSUKHANI, A. & BASILICO, C. 2005. Mechanisms underlying differential responses to FGF signaling. *Cytokine & growth factor reviews,* 16**,** 233-247.

DE BOER, L., OAKES, V., BEAMISH, H., GILES, N., STEVENS, F., SOMODEVILLA-TORRES, M., DESOUZA, C. & GABRIELLI, B. 2008. Cyclin A/cdk2 coordinates centrosomal and nuclear mitotic events. *Oncogene,* 27**,** 4261-4268.

DEN HOLLANDER, P. & KUMAR, R. 2006. Dynein light chain 1 contributes to cell cycle progression by increasing cyclin-dependent kinase 2 activity in estrogen-stimulated cells. *Cancer Research,* 66**,** 5941-5949.

DEN HOLLANDER, P., RAYALA, S. K., COVERLEY, D. & KUMAR, R. 2006. Ciz1, a Novel DNA-binding coactivator of the estrogen receptor alpha, confers hypersensitivity to estrogen action. *Cancer Res,* 66**,** 11021-9.

DI FIORE, B., DAVEY, N. E., HAGTING, A., IZAWA, D., MANSFELD, J., GIBSON, T. J. & PINES, J. 2015. The ABBA motif binds APC/C activators and is shared by APC/C substrates and regulators. *Developmental cell,* 32**,** 358-372.

DIFFLEY, J. F. & LABIB, K. 2002. The chromosome replication cycle. *Journal of cell science,* 115**,** 869-872.

DIKIC, I., WAKATSUKI, S. & WALTERS, K. J. 2009. Ubiquitin-binding domains—from structures to functions. *Nature reviews Molecular cell biology,* 10**,** 659-671.

DONZELLI, M. & DRAETTA, G. F. 2003. Regulating mammalian checkpoints through Cdc25 inactivation. *EMBO reports,* 4**,** 671-677.

DUURSMA, A. & AGAMI, R. 2005. p53-Dependent regulation of Cdc6 protein stability controls cellular proliferation. *Molecular and Cellular Biology,* 25**,** 6937-6947.

ELETR, Z. M., HUANG, D. T., DUDA, D. M., SCHULMAN, B. A. & KUHLMAN, B. 2005. E2 conjugating enzymes must disengage from their E1 enzymes before E3-dependent ubiquitin and ubiquitin-like transfer. *Nature structural & molecular biology,* 12**,** 933-934.

EVRIN, C., CLARKE, P., ZECH, J., LURZ, R., SUN, J., UHLE, S., LI, H., STILLMAN, B. & SPECK, C. 2009. A double-hexameric MCM2-7 complex is loaded onto origin DNA during licensing of eukaryotic DNA replication. *Proceedings of the National Academy of Sciences of the United States of America,* 106**,** 20240-20245.

FASANARO, P., CAPOGROSSI, M. C. & MARTELLI, F. 2010. Regulation of the endothelial cell cycle by the ubiquitin-proteasome system. *Cardiovascular research,* 85**,** 272-280.

FOSTER, D. A., YELLEN, P., XU, L. & SAQCENA, M. 2010. Regulation of G1 Cell Cycle Progression: Distinguishing the Restriction Point from a Nutrient-Sensing Cell Growth Checkpoint(s). *Genes & cancer,* 1**,** 1124-31.

FUKUSHIMA, H., OGURA, K., WAN, L., LU, Y., LI, V., GAO, D., LIU, P., LAU, A. W., WU, T., KIRSCHNER, M. W., INUZUKA, H. & WEI, W. 2013. SCF-mediated Cdh1 degradation defines a negative feedback system that coordinates cell-cycle progression. *Cell Rep,* 4**,** 803-16.

GELEY, S., KRAMER, E., GIEFFERS, C., GANNON, J., PETERS, J.-M. & HUNT, T. 2001. Anaphase-promoting complex/cyclosome–dependent proteolysis of human cyclin A starts at the beginning of mitosis and is not subject to the spindle assembly checkpoint. *The Journal of cell biology,* 153**,** 137-148.

GIACINTI, C. & GIORDANO, A. 2006. RB and cell cycle progression. *Oncogene,* 25**,** 5220-5227.

GIORDANO, A., ROSSI, A., ROMANO, G. & BAGELLA, L. 2007. Tumor suppressor pRb2/p130 gene and its derived product Spa310 spacer domain as perspective candidates for cancer therapy. *Journal of cellular physiology,* 213**,** 403-406.

GLICKMAN, M. H. & CIECHANOVER, A. 2002. The ubiquitin-proteasome proteolytic pathway: destruction for the sake of construction. *Physiological reviews,* 82**,** 373-428.

GOODSELL, D. S. 1999. The molecular perspective: the ras oncogene. *The oncologist,* 4**,** 263-264.

GREAVES, E. A., COPELAND, N. A., COVERLEY, D. & AINSCOUGH, J. F. X. 2012. Cancer-associated variant expression and interaction of CIZ1 with cyclin A1 in differentiating male germ cells. *Journal of Cell Science,* 125**,** 2466-2477.

GREGORY, M. A., QI, Y. & HANN, S. R. 2003. Phosphorylation by glycogen synthase kinase-3 controls c-myc proteolysis and subnuclear localization. *Journal of Biological Chemistry,* 278**,** 51606-51612.

GU, X., GREINER, E. R., MISHRA, R., KODALI, R., OSMAND, A., FINKBEINER, S., STEFFAN, J. S., THOMPSON, L. M., WETZEL, R. & YANG, X. W. 2009. Serines 13 and 16 are critical determinants of full-length human mutant huntingtin induced disease pathogenesis in HD mice. *Neuron,* 64**,** 828-840.

HAAS, A. L., WARMS, J., HERSHKO, A. & ROSE, I. A. 1982. Ubiquitin-activating enzyme. Mechanism and role in protein-ubiquitin conjugation. *Journal of Biological Chemistry,* 257**,** 2543-2548.

HAHNTOW, I. N., SCHNELLER, F., OELSNER, M., WEICK, K., RINGSHAUSEN, I., FEND, F., PESCHEL, C. & DECKER, T. 2004. Cyclin-dependent kinase inhibitor Roscovitine induces apoptosis in chronic lymphocytic leukemia cells. *Leukemia,* 18**,** 747-755.

HAKIM, O., JOHN, S., LING, J. Q., BIDDIE, S. C., HOFFMAN, A. R. & HAGER, G. L. 2009. Glucocorticoid Receptor Activation of the Ciz1-Lcn2 Locus by Long Range Interactions. *Journal of Biological Chemistry,* 284**,** 6048-6052.

HALL, D. A., PTACEK, J. & SNYDER, M. 2007. Protein microarray technology. *Mechanisms of Ageing and Development,* 128**,** 161-167.

HANAS, J. S., LARABEE, J. L. & HOCKER, J. R. 2005. *Zinc finger interactions with metals and other small molecules*.

HELLER, R. C., KANG, S., LAM, W. M., CHEN, S., CHAN, C. S. & BELL, S. P. 2011. Eukaryotic origin-dependent DNA replication in vitro reveals sequential action of DDK and S-CDK kinases. *Cell,* 146**,** 80-91.

HERSHKO, A., HELLER, H., EYTAN, E., KAKLIJ, G. & ROSE, I. A. 1984. ROLE OF THE A-AMINO GROUP OF PROTEIN IN UBIQUITIN-MEDIATED PROTEIN BREAKDOWN. *Proceedings of the National Academy of Sciences of the United States of America-Biological Sciences,* 81**,** 7021-7025.

HICKE, L. 2001. Protein regulation by monoubiquitin. *Nature Reviews Molecular Cell Biology,* 2**,** 195-201.

HIGGINS, G., ROPER, K. M., WATSON, I. J., BLACKHALL, F. H., ROM, W. N., PASS, H. I., AINSCOUGH, J. F. X. & COVERLEY, D. 2012. Variant Ciz1 is a circulating biomarker for early-stage lung cancer. *Proceedings of the National Academy of Sciences,* 109**,** E3128–E3135.

HOCHEGGER, H., TAKEDA, S. & HUNT, T. 2008. Cyclin-dependent kinases and cell-cycle transitions: does one fit all? *Nat Rev Mol Cell Biol,* 9**,** 910-916.

HOCHSTRASSER, M. 2009. Origin and function of ubiquitin-like proteins. *Nature,* 458**,** 422-429.

HOLT, L. J., KRUTCHINSKY, A. N. & MORGAN, D. O. 2008. Positive feedback sharpens the anaphase switch. *Nature,* 454**,** 353-357.

HSU, J. Y., REIMANN, J. D., SØRENSEN, C. S., LUKAS, J. & JACKSON, P. K. 2002. E2F-dependent accumulation of hEmi1 regulates S phase entry by inhibiting APCCdh1. *Nature cell biology,* 4**,** 358-366.

HUANG, T. T., NIJMAN, S. M., MIRCHANDANI, K. D., GALARDY, P. J., COHN, M. A., HAAS, W., GYGI, S. P., PLOEGH, H. L., BERNARDS, R. & D'ANDREA, A. D. 2006. Regulation of monoubiquitinated PCNA by DUB autocleavage. *Nature cell biology,* 8**,** 341-347.

HUNG, M.-C. & LINK, W. 2011. Protein localization in disease and therapy. *Journal of Cell Science,* 124**,** 3381-3392.

JACKMAN, M., LINDON, C., NIGG, E. A. & PINES, J. 2003. Active cyclin B1–Cdk1 first appears on centrosomes in prophase. *Nature cell biology,* 5**,** 143-148.

JACKSON, S. & XIONG, Y. 2009. CRL4s: the CUL4-RING E3 ubiquitin ligases. *Trends in biochemical sciences,* 34**,** 562-570.

JACOBSON, A. D., ZHANG, N.-Y., XU, P., HAN, K.-J., NOONE, S., PENG, J. & LIU, C.-W. 2009. The lysine 48 and lysine 63 ubiquitin conjugates are processed differently by the 26 s proteasome. *Journal of Biological Chemistry,* 284**,** 35485-35494.

JEFFREY, P. D., RUSSO, A. A., POLYAK, K., GIBBS, E., HURWITZ, J., MASSAGUE, J. & PAVLETICH, N. P. 1995. Mechanism of CDK activation revealed by the structure of a cyclinA-CDK2 complex. *Nature,* 376**,** 313-320.

JIN, T. C., GUO, F., SEREBRIISKII, I. G., HOWARD, A. & ZHANG, Y. Z. 2007. A 1.55 a resolution X-ray crystal structure of HEF2/ERH and insights into its transcriptional and cell-cycle interaction networks. *Proteins-Structure Function and Bioinformatics,* 68**,** 427-437.

KANG, M.-S., LEE, E. K., SONI, V., LEWIS, T. A., KOEHLER, A. N., SRINIVASAN, V. & KIEFF, E. 2011. Roscovitine inhibits EBNA1 serine 393 phosphorylation, nuclear localization, transcription, and episome maintenance. *Journal of virology,* 85**,** 2859-2868.

KARMAKAR, S., JIN, Y. & NAGAICH, A. K. 2013. Interaction of glucocorticoid receptor (GR) with estrogen receptor (ER) α and activator protein 1 (AP1) in dexamethasone-mediated interference of ERα activity. *Journal of Biological Chemistry,* 288**,** 24020-24034.

KASTAN, M. B., CANMAN, C. E. & LEONARD, C. J. 1995. P53, cell cycle control and apoptosis: implications for cancer. *Cancer and Metastasis reviews,* 14**,** 3-15.

KERSCHER, O., FELBERBAUM, R. & HOCHSTRASSER, M. 2006. Modification of proteins by ubiquitin and ubiquitin-like proteins. *Annu. Rev. Cell Dev. Biol.,* 22**,** 159-180.

KIRKPATRICK, D. S., WELDON, S. F., TSAPRAILIS, G., LIEBLER, D. C. & GANDOLFI, A. J. 2005. Proteomic identification of ubiquitinated proteins from human cells expressing His-tagged ubiquitin. *Proteomics,* 5**,** 2104-2111.

KRAMER, E. R., SCHEURINGER, N., PODTELEJNIKOV, V., MANN, M. & PETERS, J. M. 2000. Mitotic regulation of the APC activator proteins CDC20 and CDH1. *Molecular Biology of the Cell,* 11**,** 1555-1569.

LACEY, K. R., JACKSON, P. K. & STEARNS, T. 1999. Cyclin-dependent kinase control of centrosome duplication. *Proceedings of the National Academy of Sciences,* 96**,** 2817-2822.

LAMIA, K. A., SACHDEVA, U. M., DITACCHIO, L., WILLIAMS, E. C., ALVAREZ, J. G., EGAN, D. F., VASQUEZ, D. S., JUGUILON, H., PANDA, S. & SHAW, R. J. 2009. AMPK regulates the circadian clock by cryptochrome phosphorylation and degradation. *Science,* 326**,** 437-440.

LECKER, S. H., GOLDBERG, A. L. & MITCH, W. E. 2006. Protein degradation by the ubiquitin-proteasome pathway in normal and disease states. *Journal of the American Society of Nephrology,* 17**,** 1807-1819.

LEE, J.-H., KIM, H.-S., LEE, S.-J. & KIM, K.-T. 2007. Stabilization and activation of p53 induced by Cdk5 contributes to neuronal cell death. *Journal of Cell Science,* 120**,** 2259-2271.

LEI, M. & TYE, B. K. 2001. Initiating DNA synthesis: from recruiting to activating the MCM complex. *Journal of Cell Science,* 114**,** 1447-1454.

LEMAN, A. R. & NOGUCHI, E. 2013. The replication fork: understanding the eukaryotic replication machinery and the challenges to genome duplication. *Genes,* 4**,** 1-32.

LI, M. & ZHANG, P. 2009. The function of APC/C-Cdh1 in cell cycle and beyond. *Cell Division,* 4.

LI, W. & YE, Y. 2008. Polyubiquitin chains: functions, structures, and mechanisms. *Cellular and Molecular Life Sciences,* 65**,** 2397-2406.

LIN, A. E. & MAK, T. W. 2007. The role of E3 ligases in autoimmunity and the regulation of autoreactive T cells. *Current opinion in immunology,* 19**,** 665-673.

LIU, E., LI, X., YAN, F., ZHAO, Q. & WU, X. 2004. Cyclin-dependent kinases phosphorylate human Cdt1 and induce its degradation. *Journal of Biological Chemistry,* 279**,** 17283-17288.

ŁUKASIK, A., UNIEWICZ, K. A., KULIS, M. & KOZLOWSKI, P. 2008. Ciz1, a p21Cip1/Waf1-interacting zinc finger protein and DNA replication factor, is a novel molecular partner for human enhancer of rudimentary homolog. *FEBS Journal,* 275**,** 332-340.

LUTZMANN, M. & MECHALI, M. 2008. MCM9 binds Cdt1 and is required for the assembly of prereplication complexes. *Molecular Cell,* 31**,** 190-200.

MAILAND, N. & DIFFLEY, J. F. 2005. CDKs promote DNA replication origin licensing in human cells by protecting Cdc6 from APC/C-dependent proteolysis. *Cell,* 122**,** 915-26.

MALATESTA, F. 2005. The study of bimolecular reactions under non-pseudo-first order conditions. *Biophysical chemistry,* 116**,** 251-256.

MASSAGUÉ, J., BLAIN, S. W. & LO, R. S. 2000. TGFβ signaling in growth control, cancer, and heritable disorders. *Cell,* 103**,** 295-309.

MATSUMOTO, Y., HAYASHI, K. & NISHIDA, E. 1999. Cyclin-dependent kinase 2 (Cdk2) is required for centrosome duplication in mammalian cells. *Current Biology,* 9**,** 429-432.

MATSUOKA, S., BALLIF, B. A., SMOGORZEWSKA, A., MCDONALD, E. R., III, HUROV, K. E., LUO, J., BAKALARSKI, C. E., ZHAO, Z., SOLIMINI, N., LERENTHAL, Y., SHILOH, Y., GYGI, S. P. & ELLEDGE, S. J. 2007. ATM and ATR substrate analysis reveals extensive protein networks responsive to DNA damage. *Science,* 316**,** 1160-1166.

MEIJER, L., BORGNE, A., MULNER, O., CHONG, J. P. J., BLOW, J. J., INAGAKI, N., INAGAKI, M., DELCROS, J. G. & MOULINOUX, J. P. 1997. Biochemical and cellular effects of roscovitine, a potent and selective inhibitor of the cyclin-dependent kinases cdc2, cdk2 and cdk5. *European Journal of Biochemistry,* 243**,** 527-536.

MERTINS, P., QIAO, J., PATEL, J., UDESHI, N., CLAUSER, K., MANI, D., BURGESS, M., GILLETTE, M., JAFFE, J. & CARR, S. 2013. Integrated proteomic analysis of post-translational modifications by serial enrichment. *Nat Methods,* 10**,** 634-7.

MEYERSON, M. & HARLOW, E. 1994. Identification of G1 kinase activity for cdk6, a novel cyclin D partner. *Molecular and cellular biology,* 14**,** 2077-2086.

MITSUI, K., MATSUMOTO, A., OHTSUKA, S., OHTSUBO, M. & YOSHIMURA, A. 1999. Cloning and characterization of a novel p21(CiP1/Waf1)-interacting zinc finger protein, Ciz1. *Biochemical and Biophysical Research Communications,* 264**,** 457-464.

MURRAY, A. W. 2004. Recycling the cell cycle: cyclins revisited. *Cell,* 116**,** 221-234.

NAKAYAMA, K. I. & NAKAYAMA, K. 2006. Ubiquitin ligases: cell-cycle control and cancer. *Nat Rev Cancer,* 6**,** 369-81.

NDUBAKU, C. & TSUI, V. 2015. Inhibiting the Deubiquitinating Enzymes (DUBs) Miniperspective. *Journal of Medicinal Chemistry,* 58**,** 1581-1595.

NGUYEN, V. Q., CO, C. & LI, J. J. 2001. Cyclin-dependent kinases prevent DNA re-replication through multiple mechanisms. *Nature,* 411**,** 1068-1073.

NISHIBE, R., WATANABE, W., UEDA, T., YAMASAKI, N., KOLLER, R., WOLFF, L., HONDA, Z., OHTSUBO, M. & HONDA, H. 2013. CIZ1, a p21Cip1/Waf1-interacting protein, functions as a tumor suppressor in vivo. *FEBS Lett,* 587**,** 1529-35.

NURSE, P. 1990. Universal control mechanism regulating onset of M-phase. *Nature,* 344**,** 503-508.

OBAYA, A. & SEDIVY, J. 2002. Regulation of cyclin-Cdk activity in mammalian cells. *Cellular and Molecular Life Sciences CMLS,* 59**,** 126-142.

OHTSUBO, M., THEODORAS, A. M., SCHUMACHER, J., ROBERTS, J. M. & PAGANO, M. 1995. Human cyclin E, a nuclear protein essential for the G1-to-S phase transition. *Molecular and cellular biology,* 15**,** 2612-2624.

OKUMURA, N., YOSHIDA, H., KITAGISHI, Y., NISHIMURA, Y. & MATSUDA, S. 2011. Alternative splicings on p53, BRCA1 and PTEN genes involved in breast cancer. *Biochem Biophys Res Commun,* 413**,** 395-9.

PARDEE, A. B. 1974. A Restriction Point for Control of Normal Animal Cell Proliferation. *Proceedings of the National Academy of Sciences of the United States of America,* 71**,** 1286-1290.

PETERSEN, B. O., LUKAS, J., SØRENSEN, C. S., BARTEK, J. & HELIN, K. 1999. Phosphorylation of mammalian CDC6 by cyclin A/CDK2 regulates its subcellular localization. *The EMBO Journal,* 18**,** 396-410.

PFLEGER, C. M. & KIRSCHNER, M. W. 2000. The KEN box: an APC recognition signal distinct from the D box targeted by Cdh1. *Genes & development,* 14**,** 655-665.

PICKART, C. M. 2001. Mechanisms underlying ubiquitination. *Annual Review of Biochemistry,* 70**,** 503-533.

PLANCHAIS, S., GLAB, N., TRÉHIN, C., PERENNES, C., BUREAU, J. M., MEIJER, L. & BERGOUNIOUX, C. 1997. Roscovitine, a novel cyclin-dependent kinase inhibitor, characterizes restriction point and G2/M transition in tobacco BY-2 cell suspension. *The Plant Journal,* 12**,** 191-202.

RAHMAN, F., AINSCOUGH, J. F., COPELAND, N. & COVERLEY, D. 2007. Cancer-associated missplicing of exon 4 influences the subnuclear distribution of the DNA replication factor CIZ1. *Hum Mutat,* 28**,** 993-1004.

RAHMAN, F. A., AZIZ, N. & COVERLEY, D. 2010. Differential detection of alternatively spliced variants of Ciz1 in normal and cancer cells using a custom exon-junction microarray. *BMC Cancer,* 10**,** 482.

RAO, V. S., SRINIVAS, K., SUJINI, G. N. & KUMAR, G. N. S. 2014. Protein-protein interaction detection: methods and analysis. *International journal of proteomics,* 2014**,** 147648-147648.

RAPE, M., REDDY, S. K. & KIRSCHNER, M. W. 2006. The processivity of multiubiquitination by the APC determines the order of substrate degradation. *Cell,* 124**,** 89-103.

RIALLAND, M., SOLA, F. & SANTOCANALE, C. 2002. Essential role of human CDT1 in DNA replication and chromatin licensing. *Journal of Cell Science,* 115**,** 1435-1440.

RIZZARDI, L. F. & COOK, J. G. 2013. Flipping the switch from g1 to s phase with e3 ubiquitin ligases. *Genes Cancer,* 3**,** 634-48.

SACCO, E., HASAN, M. M., ALBERGHINA, L. & VANONI, M. 2012. Comparative analysis of the molecular mechanisms controlling the initiation of chromosomal DNA replication in yeast and in mammalian cells. *Biotechnol Adv,* 30**,** 73-98.

SÁNCHEZ, I. & DYNLACHT, B. D. New insights into cyclins, CDKs, and cell cycle control. Seminars in cell & developmental biology, 2005. Elsevier, 311-321.

SATYANARAYANA, A., HILTON, M. B. & KALDIS, P. 2008. p21 Inhibits Cdk1 in the absence of Cdk2 to maintain the G1/S phase DNA damage checkpoint. *Mol Biol Cell,* 19**,** 65-77.

SCHEFFNER, M., NUBER, U. & HUIBREGTSE, J. M. 1995. Protein ubiquitination involving an E1–E2–E3 enzyme ubiquitin thioester cascade. *Nature,* 373**,** 81-83.

SCHNELL, S. & MENDOZA, C. 2004. The condition for pseudo-first-order kinetics in enzymatic reactions is independent of the initial enzyme concentration. *Biophysical chemistry,* 107**,** 165-174.

SCHULMAN, B. A. & HARPER, J. W. 2009. Ubiquitin-like protein activation by E1 enzymes: the apex for downstream signalling pathways. *Nature Reviews Molecular Cell Biology,* 10**,** 319-331.

SGAMBATO, A., CITTADINI, A., FARAGLIA, B. & WEINSTEIN, I. B. 2000. Multiple functions of p27(Kip1) and its alterations in tumor cells: A review. *Journal of Cellular Physiology,* 183**,** 18-27.

SHARMA, K., D'SOUZA, R., TYANOVA, S., SCHAAB, C., WIŚNIEWSKI, J., COX, J. & MANN, M. 2014. Ultradeep human phosphoproteome reveals a distinct regulatory nature of Tyr and Ser/Thr-based signaling. *Cell Rep,* 8**,** 1583-94.

SHEN, M., SCHMITT, S., BUAC, D. & DOU, Q. P. 2013. Targeting the ubiquitin–proteasome system for cancer therapy. *Expert Opin Ther Targets,* 17**,** 1091-1108.

SHERR, C. J. & ROBERTS, J. M. 1999. CDK inhibitors: positive and negative regulators of G(1)-phase progression. *Genes & Development,* 13**,** 1501-1512.

SHIN, I., YAKES, F. M., ROJO, F., SHIN, N.-Y., BAKIN, A. V., BASELGA, J. & ARTEAGA, C. L. 2002. PKB/Akt mediates cell-cycle progression by phosphorylation of p27Kip1 at threonine 157 and modulation of its cellular localization. *Nature medicine,* 8**,** 1145-1152.

SPENCER, S. L., CAPPELL, S. D., TSAI, F.-C., OVERTON, K. W., WANG, C. L. & MEYER, T. 2013. The proliferation-quiescence decision is controlled by a bifurcation in CDK2 activity at mitotic exit. *Cell,* 155**,** 369-383.

STRAUSFELD, U. P., HOWELL, M., DESCOMBES, P., CHEVALIER, S., REMPEL, R. E., ADAMCZEWSKI, J., MALLER, J. L., HUNT, T. & BLOW, J. J. 1996. Both cyclin

A and cyclin E have S-phase promoting (SPF) activity in Xenopus egg extracts. *Journal of Cell Science,* 109**,** 1555-1563.

SUN, Y. 2003. Targeting E3 ubiquitin ligases for cancer therapy. *Cancer biology & therapy,* 2**,** 623-629.

TAKIZAWA, C. G. & MORGAN, D. O. 2000. Control of mitosis by changes in the subcellular location of cyclin-B1–Cdk1 and Cdc25C. *Current opinion in cell biology,* 12**,** 658-665.

TSOU, M.-F. B. & STEARNS, T. 2006. Mechanism limiting centrosome duplication to once per cell cycle. *Nature,* 442**,** 947-951.

TSVETKOV, L. M., YEH, K. H., LEE, S. J., SUN, H. & ZHANG, H. 1999. P27(Kip1) ubiquitination and degradation is regulated by the SCFSkp2 complex through phosphorylated Thr187 in p27. *Current Biology,* 9**,** 661-664.

VAN ZON, W., OGINK, J., TER RIET, B., MEDEMA, R. H., RIELE, H. T. & WOLTHUIS, R. M. F. 2010. The APC/C recruits cyclin B1-Cdk1-Cks in prometaphase before D box recognition to control mitotic exit. *Journal of Cell Biology,* 190**,** 587-602.

VASSILEV, L. T. 2007. MDM2 inhibitors for cancer therapy. *Trends in molecular medicine,* 13**,** 23-31.

VERMEULEN, K., VAN BOCKSTAELE, D. R. & BERNEMAN, Z. N. 2003. The cell cycle: a review of regulation, deregulation and therapeutic targets in cancer. *Cell Proliferation,* 36**,** 131-149.

VISINTIN, R., CRAIG, K., HWANG, E. S., PRINZ, S., TYERS, M. & AMON, A. 1998. The phosphatase Cdc14 triggers mitotic exit by reversal of Cdk-dependent phosphorylation. *Molecular cell,* 2**,** 709-718.

VODERMAIER, H. C. 2004. APC/C and SCF: Controlling each other and the cell cycle. *Current Biology,* 14**,** R787-R796.

WAGA, S. & STILLMAN, B. 1998. The DNA replication fork in eukaryotic cells. *Annual review of biochemistry,* 67**,** 721-751.

WAGNER, S. A., BELI, P., WEINERT, B. T., NIELSEN, M. L., COX, J., MANN, M. & CHOUDHARY, C. 2011. A proteome-wide, quantitative survey of in vivo

ubiquitylation sites reveals widespread regulatory roles. *Molecular & cellular proteomics : MCP,* 10**,** M111.013284-M111.013284.

WALTER, J. & NEWPORT, J. 2000. Initiation of eukaryotic DNA replication: origin unwinding and sequential chromatin association of Cdc45, RPA, and DNA polymerase α. *Molecular cell,* 5**,** 617-627.

WANG, D. Q., WANG, K., YAN, D. W., LIU, J., WANG, B., LI, M. X., WANG, X. W., LIU, J., PENG, Z. H., LI, G. X. & YU, Z. H. 2014a. Ciz1 is a novel predictor of survival in human colon cancer. *Exp Biol Med (Maywood),* 239**,** 862-870.

WANG, Z., LIU, P., INUZUKA, H. & WEI, W. 2014b. Roles of F-box proteins in cancer. *Nat Rev Cancer,* 14**,** 233-47.

WARDER, D. E. & KEHERLY, M. J. 2003. Ciz1, Cip1 interacting zinc finger protein 1 binds the consensus DNA sequence ARYSR(0-2)YYAC. *Journal of Biomedical Science,* 10**,** 406-417.

WEBER, J. D., RABEN, D. M., PHILLIPS, P. J. & BALDASSARE, J. J. 1997. Sustained activation of extracellular-signal-regulated kinase 1 (ERK1) is required for the continued expression of cyclin D1 in G(1) phase. *Biochemical Journal,* 326**,** 61-68.

WELCKER, M. & CLURMAN, B. E. 2008. FBW7 ubiquitin ligase: a tumour suppressor at the crossroads of cell division, growth and differentiation. *Nat Rev Cancer,* 8**,** 83-93.

WOHLSCHLEGEL, J. A., DWYER, B. T., TAKEDA, D. Y. & DUTTA, A. 2001. Mutational Analysis of the Cy Motif from p21 Reveals Sequence Degeneracy and Specificity for Different Cyclin-Dependent Kinases. *Molecular and Cellular Biology,* 21**,** 4868-4874.

YIN, H., LEE, G. I., PARK, H. S., PAYNE, G. A., RODRIGUEZ, J. M., SEBTI, S. M. & HAMILTON, A. D. 2005. Terphenyl-Based Helical Mimetics That Disrupt the p53/HDM2 Interaction. *Angewandte Chemie,* 117**,** 2764-2767.